GTPase activating protein Rap1GAP2 and synaptotagmin-like protein 1 interact and are involved in platelet dense granule secretion

Dissertation
zur Erlangung des Doktorgrades
der Naturwissenschaften

vorgelegt beim Fachbereich
Chemische und Pharmazeutische Wissenschaften
der Johann Wolfgang Goethe - Universität
in Frankfurt am Main

von
Olga Neumüller
aus Balchasch, Kasachstan

Frankfurt 2008
D30

Vom Fachbereich Chemische und Pharmazeutische Wissenschaften der Johann Wolfgang Goethe-Universität als Dissertation angenommen.

Dekan: Prof. Dr. Dieter Steinhilber

Gutachter: Prof. Dr. Theodor Dingermann
PD Dr. Albert P. Smolenski
Prof. Dr. Steve Watson

Datum der Disputation: 25.11.2009

Für meine Eltern.
In Liebe und Dankbarkeit.

TABLE OF CONTENTS

LIST OF ORIGINAL PUBLICATIONS

Publications

Neumüller O., Hoffmeister M., Babica J., Prelle C., Gegenbauer K., Smolenski A.P., (2009). GTPase-activating protein Rap1GAP2 and synaptotagmin-like protein 1 interact and regulate dense granule secretion in platelets. *Blood* 114: 1396-1404.

Hoffmeister M., Riha P., **Neumüller O.,** Danielewski O., Schultess J., Smolenski A.P., (2008). Cyclic nucleotide-dependent protein kinases inhibit binding of 14-3-3 to the GTPase-activating protein Rap1GAP2 in platelets. *J Biol Chem* 283: 2297-2306.

Klatt A.R., Klinger G., **Neumüller O.,** Eidenmüller B., Wagner I., Achenbach T., Aigner T., Bartnik E., (2006). TAK1 downregulation reduces IL-1 beta induced expression of MMP13, MMP1 and TNF-alpha. *Biomed Pharmacother* 60: 55-61.

Contributions to conferences and workshops

Neumüller O., Hoffmeister M., Smolenski A.P., (2007). Rap1GAP2 is a new binding partner of Slp1 in platelets. Poster. CGC Workshop: GEFs and GAPs as therapeutic targets., Utrecht, Netherlands.

Neumüller O., Hoffmeister M., Smolenski A.P., (2007). Rap1GAP2 and Slp1 interact in human platelets. Poster. ELSO Conference, Dresden, Germany.

Neumüller O., Hoffmeister M., Danielewski O., Smolenski A.P., (2007). Rap1GAP2 is a new target of the Rab27- and membrane-binding protein Slp1 in platelets. Poster. Pharmaceutical Sciences World Congress, Amsterdam, Netherlands.

Neumüller O., Hoffmeister M., Danielewski O., Smolenski A.P., (2006). Rap1GAP2 is a new interacting partner of the Rab27-binding protein Slp1 in human platelets. Poster. FEBS Special Meeting on Cellular Signaling, Dubrovnik, Croatia.

ABBREVIATIONS

Ade	Adenine
ADP	Adenosine diphosphate
APS	Ammonium persulfate
ATP	Adenosine triphosphate
BSA	Bovine serum albumin
Ca^{2+}	Calcium ion
$[Ca^{2+}]$	Calcium ion concentration
cAK	cAMP-dependent protein kinase
cAMP	Cyclic adenosine monophosphate
cDNA	Copy DNA
cfu	Colony forming unit
cGK	cGMP-dependent protein kinase
cGMP	Cyclic guanosine monophosphate
Ci	Curies
Cy3/5	Cyanin 3/5
DAG	1,2-Diacylglycerol
DEAE-Dextran	Diethylaminoethyl-Dextran
DMEM	Dulbecco's modified Eagle's medium
DMSO	Dimethylsulfoxide
DNA	Deoxyribonucleic acid
Doc2	Double C2 domain
DTE	Dithioerythreitol
DTT	Dithiothreitol
EDRF	Endothelium-derived relaxing factor
EDTA	Ethylenediamine tetra-acetic acid
EGTA	Ethyleneglycol tetra-acetic acid
e.g.	Latin: exempli gratia; for example
EGFP	Enhanced green fluorescent protein
ELISA	Enzyme-linked immunosorbent assay
Fig.	Figure
FBS	Fetal bovine serum
g	Gram
g	Gravity (= 9.81 m/s^2)
GAL4AD	Gal4 activation domain
GAL4BD	Gal4 binding domain
GAP	GTPase activating protein
GDI	GDP dissociation inhibitor
GDP	Guanosine diphosphate
GDPβS	Guanosine 5`-O-[β-thio] diphosphate
GEF	Guanine nucleotide exchange factor
GFP	Green fluorescent protein
GGT	Geranylgeranyl transferase
gm	Gunmetal
GP	Glycoprotein
GPCR	G protein-coupled receptor

GS	Griscelli syndrome
GSH	Glutathione
GST	Glutathione-S-transferase
GT	Glanzmann`s thrombasthenia
GTP	Guanosine triphosphate
GTPγS	Guanosine 5`-O-[γ-thio] triphosphate
h	Hour
HA	Hemagglutinin
HEPES	4-(2-Hydroxyethyl)-1-piperzineethanesulfonic acid
His	Histidine
HRP	Horseradish peroxidase
5HT	5-Hydroxytryptamine, serotonin
IB	Immunoblot
i.e.	Latin: id est; that is
IF	Immunofluorescence
IgG	Immunoglobulin G
IP	Immunoprecipitation
IP_3	Inositol-1,4,5-trisphosphate
IPTG	Isopropyl-β-D-1-thiogalactopyranoside
kb	Kilobase pairs
kD	Kilodalton
l	Liter
LB	Luria-Bertani medium
Leu	Leucine
LDH	Lactate dehydrogenase
LSM	Laser scanning microscope
M	Molarity
mg	Milligram
MHD	Munc homology domain
min	Minute
mmol	Millimol
ml	Milliliter
Mr, MW	Molecular weight
mRNA	Messenger RNA
Ni-NTA	Nickel-nitrilotriacetic acid agarose
NO	Nitric oxide
NSF	N-ethylmaleimide sensitive factor
OCS	Open canalicular system
OD_{600}	Optical density at 600 nm
P	Phosphate
PAR	Protease-activated receptor
PBS	Phosphate buffered saline
PCR	Polymerase chain reaction
PDE	Phosphodiesterase
PDZ-GEF	Postsynaptic density-95 discs-large and zona occludens protein 1-GEF
PGI_2	Prostaglandin I_2, prostacyclin
PH domain	Pleckstrin homology domain
PIP	Phosphoinositide

PKA/B/C/G	Protein kinase A/B/C/G
PKI	PKA inhibitor
PLC	Phospholipase
PSA	Prostate-specific antigen
P-VASP	phosphorylated VASP
RG1	Rap1GAP1
RG2	Rap1GAP2
RNA	Ribonucleic acid
Rp-8-Br-cAMPS	Rp-8-Bromoadenosine-3`,5`-cyclic monophosphorothioate
rpm	Rotations per minute
RT	Room temperature
sec	Second
SD	Standard deviation
SDS	Sodium dodecyl sulphate
SDS- PAGE	SDS-Polyacrylamide gel elektrophoresis
SHD	Slp homology domain
Slac	Slp homologue lacking C2 domains
Slp	Synaptotagmin-like protein
SNAP	Soluble NSF attachment protein
SNARE	Soluble NSF attachment protein receptor
SNP	Sodium nitroprusside
SPA-1	Signal-induced proliferation-associated protein 1
Sp-5,6-DCl-cBIMPS	Sp-5,6-dichloro-1-β-D-ribofuranosylbenzimidazole-3`,5`-monophosphorothioate
Tab.	Table
TBS-T	Tris buffered saline with Tween® 20
TCA	Trichloroacetic acid
TEMED	N,N,N,N-Tetramethylethylendiamine
T_m	Melting temperature
TPA	12-O-Tetradecanoyl phorbol-13-acetate
Tris	Tris-hydroxymethyl-aminomethane
Trp	Tryptophane
TxA_2	Thromboxane A_2
U	Unit
VAMP	Vesicle-associated membrane protein
VASP	Vasodilatator-stimulated phosphoprotein
VSV	Vesicular stomatitis virus glycoprotein
v/v	Volume per volume
WB	Western blotting
wt	Wild-type
w/v	Weight per volume
X-α-Gal	5-Bromo-4-chloro-3-indolyl-α-D-galactopyranoside

SUMMARY

Platelets are anucleate cells that play a major role in hemostasis and thrombosis in the vasculature. During primary hemostasis platelets adhere to sites of vascular damage and the initial platelet coat is reinforced by additional platelets forming a stable aggregate. At the same time platelets secrete their intracellular granules containing substances that further activate platelets in an autocrine and paracrine fashion and affect local coagulation and endothelial smooth muscle cell function. The small guanine nucleotide binding protein Rap1 regulates the activity of the platelet integrin $\alpha_{IIb}\beta_3$ and thus platelet aggregation. Rap1 activity is controlled by guanine nucleotide exchange factors and GTPase activating proteins. In platelets, Rap1GAP2 is the only GTPase activating protein of Rap1.

In order to identify Rap1GAP2-associated proteins, a genetic two-hybrid screening in yeast was performed and synaptotagmin-like protein 1 (Slp1, also called JFC1) was found as a new putative binding partner of Rap1GAP2. Slp1 is a tandem C2 domain containing protein and is known to bind to Rab27, a small GTPase involved in platelet dense granule secretion. The direct interaction between Rap1GAP2 and Slp1 was confirmed in yeast and in transfected cells. More importantly, Slp1 is expressed in platelets and binding of endogenous Rap1GAP2 and Slp1 was verified in these cells. The Rap1GAP2 and Slp1 interaction sites were mapped by mutational analysis. Rap1GAP2 binds through the -*TKXT*- motif within its C-terminus to the C2A domain of Slp1. Moreover, the Slp1 binding -*TKXT*- motif of Rap1GAP2 was confirmed by complementary approaches using short synthetic Rap1GAP2 peptides. The C2A domain of Slp1 is a phospholipid binding domain and thus mediates binding of Slp1 to the plasma membrane. Phospholipid overlay assays revealed that simultaneous binding of Slp1 via its C2A domain to Rap1GAP2 and to phospholipids can occur. In addition, the interaction between Rap1GAP2 and Slp1 is regulated by cAMP-dependent protein kinase (cAK or PKA), and kinase activation in platelets enhanced binding of endogenous Rap1GAP2 to Slp1. *In-vitro* phosphorylation assays revealed that Slp1 is a substrate of PKA, and serine 111 was identified as phosphorylation site. Since Slp1 is a Rab27 binding protein, a trimeric complex of Slp1, Rab27 and Rap1GAP2 is conceivable. The association of Slp1, Rab27 and Rap1GAP2 was investigated by immunofluorescence and co-immuno-precipitation experiments in both, transfected cells and platelets. By Slp1 affinity chromatography and subsequent mass spectrometric analysis additional Slp1 binding proteins were identified in platelets, and binding of Slp1 to Rab8 was confirmed in pull-down assays. To investigate the functional significance of the interaction between Rap1GAP2 and Slp1, an assay system was established to determine serotonin secretion of streptolysin-O permeabilized platelets. Addition of recombinant Slp1 protein to permeabilized platelets strongly inhibited platelet dense granule secretion, whereas addition of recombinant

Rap1GAP2 protein or synthetic Rap1GAP2 peptide enhanced secretion. Deleting the Slp1 binding -*TKXT*- motif abolished the stimulatory effect of Rap1GAP2 on secretion. Addition of Rap1 to permeabilized platelets had no effect on secretion. These findings indicate that the Rap1GAP2 effect on platelet secretion does not depend on the GTPase activating function of Rap1GAP2, but is rather dependent on the -*TKXT*- mediated interaction of Rap1GAP2 with Slp1. In addition, *in-vitro* GAP assays revealed that Slp1 binding to Rap1GAP2 does not affect the Rap1GAP activity of Rap1GAP2, and adhesion assays excluded a role for the Rap1GAP2/Slp1 interaction in cell adhesion.

Altogether, the results of the present study demonstrate that besides its function in platelet aggregation by controlling the activity of the small guanine nucleotide binding protein Rap1, Rap1GAP2 is involved in platelet dense granule secretion by the new -*TKXT*- mediated interaction with the Rab27 and membrane binding protein Slp1. In addition, the interaction between Rap1GAP2 and Slp1 is embedded into an elaborate network of protein-protein interactions in platelets which appear to be regulated by phosphorylation. Future studies will in particular aim to dissect the molecular details of Rap1GAP2 and Slp1 action in platelet secretion and investigate the potential biochemical and pharmacological value of the unique protein binding -*TKXT*- motif of Rap1GAP2.

1. INTRODUCTION

1.1 Platelets

Platelets, or thrombocytes, are specialized blood cells that play a central role in physiological and pathological processes of hemostasis and thrombosis (Davi and Patrono 2007). Platelets are the smallest (0.5 x 3.0 µm) and most numerous (normal range: 2-3 x 10^8/ml) corpuscular components of the circulating blood (Italiano 2008). They are produced from megakaryocytes in the bone marrow (Hartwig and Italiano 2003). Once released, platelets have a lifespan of about 7-10 days. Degradation of platelets occurs in the reticulo-endothelial system of liver and spleen (Gawaz 1999). Platelets do not have a nucleus and thereby lack genomic DNA (Italiano and Shivdasani 2003). However, they contain megakaryocyte-derived messenger RNA (mRNA) and the translational machinery needed for protein synthesis (reviewed by Davi and Patrono 2007). Moreover, pre-mRNA splicing, a typical nuclear function, has recently been detected in the cytoplasm of these anucleate cells (Denis et al. 2005). Platelets are rich in mitochondria and store three different types of granules, alpha granules, dense granules and lysosomes (Rendu and Brohard-Bohn 2001). In the resting state, platelets are discoid shaped having granules homogenously distributed throughout the platelet body. Upon activation, however, platelets undergo a shape change during which pseudopodia are formed and granules are centralized. Platelets are characterized by a unique membrane network including the dense tubular and the surface-connected open canalicular system. The dense tubular system is the main storage pool for free calcium ions (Jardin et al. 2008). The open canalicular system (OCS) is an elaborate system of membrane tunnels and serves on the one hand as a direct passageway to the bloodstream, into which platelet granule contents can quickly be released, and on the other hand, as a reservoir for platelet plasma membrane and membrane receptors (Gawaz 1999, Italiano 2008). The main platelet plasma membrane receptors are adhesive glycoprotein receptors (e.g. GPIb for von Willebrand factor, GPVI for collagen), several G protein-coupled receptors (GPCRs) (e.g. PAR1 and PAR4 for thrombin, $P2Y_1$ and $P2Y_{12}$ for adenosine diphosphate), and β_1 and β_3 integrin receptors (e.g. $\alpha_2\beta_1$ for collagen, $\alpha_{IIb}\beta_3$ for fibrinogen) (Gachet 2008, Coughlin 2005, Varga-Szabo et al. 2008).

Platelets in primary hemostasis

In circulation, the major physiological function of platelets is to sentinel the integrity of the vascular system and to prevent bleeding/hemorrhage after vascular injury, a process called primary hemostasis (Fig.1.1) (Ruggeri 2002, Davi and Patrono 2007). Under conditions of rapid blood flow the initial platelet tethering at sites of vascular injury involves the interaction

of von Willebrand factor with the platelet glycoprotein complex GPIb-V-IX. Moreover, interaction of collagen with glycoprotein GPVI and integrin $\alpha_2\beta_1$ further promotes platelet adhesion and activation (Varga-Szabo et al. 2008, Ruggeri and Medolicchio 2007). Platelet activation results in platelet shape change, granule secretion and aggregation. Platelet granule secretion leads to the release of granule contents which activate platelets in an autocrine and paracrine fashion, thereby perpetuating the initial platelet response. In addition, more platelets are recruited from the circulation to form a growing platelet aggregate. Platelet aggregation is mediated by binding of fibrinogen to the activated integrin $\alpha_{IIb}\beta_3$ (also called GPIIb-IIIa) leading to cohesion of adjacent platelets (Jackson 2007). The so formed primary hemostatic plug, however, is still fragile and only temporarily arrests bleeding. Therefore, stable clot formation is induced during secondary hemostasis through activation of the plasma coagulation system, resulting in thrombin-mediated conversion of fibrinogen to fibrin (Gawaz 1999, Jurk and Kehrel 2005).

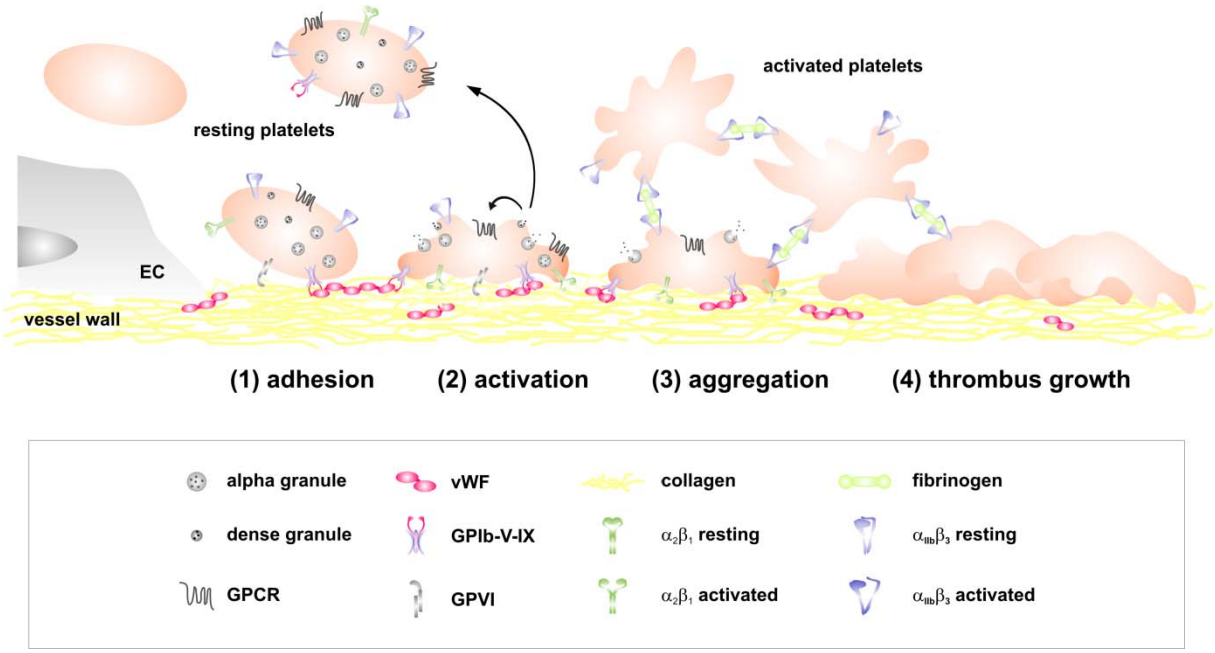

Figure 1.1: Platelets in primary hemostasis.
Primary hemostasis can be classified into different phases ultimately leading to the formation of a primary hemostatic platelet plug. (1) Initial adhesion of resting platelets to sites of vascular damage is mediated through the interaction of immobilized extracellular von Willebrand factor with GPIbα which is part of the GPIb-V-IX complex. The interaction of collagen with GPVI especially induces the activation of adherent platelets. In turn, activated $\alpha_2\beta_1$ integrin binds to collagen, thereby promoting firm platelet adhesion. (2) Platelet activation leads to platelet shape change, granule secretion and aggregation. Activated platelets secrete substances (e.g. adenosine diphosphate) which activate platelets in an autocrine and paracrine fashion operating through G protein-coupled receptors. (3) Platelet aggregation is mediated by binding of fibrinogen to activated $\alpha_{IIb}\beta_3$ integrin leading to cohesion of adjacent platelets. (4) More platelets are recruited and accumulate into a growing platelet thrombus. EC: endothelial cell; GP: glycoprotein; vWF: von Willebrand factor; GPCR: G protein-coupled receptor. Arrows indicate activation. Figure was modified according to Jackson 2007.

Although presented here as separated events, primary and secondary hemostasis are closely linked, e.g. activated platelets accelerate plasma coagulation, and products of the plasma coagulation system, such as thrombin, stimulate platelet aggregation.

1.2 Platelet activation and inhibition

Platelets are rapidly activated by various agonists. Irrespective of collagen as the main non-diffusible platelet agonist, diffusible mediators of platelet activation are α-thrombin, adenosine diphosphate (ADP), and thromboxane A_2 (TxA_2). Platelet activation is counteracted by platelet inhibition. The main platelet inhibitors are nitric oxide (NO, also termed endothelium-derived relaxing factor (EDRF) and prostaglandin I_2 (PGI_2, also termed prostacyclin).

1.1.1 Platelet activators

Diffusible platelet agonists activate platelets through G protein-coupled receptors. Platelet activation via GPCRs involves three major G protein-mediated signaling pathways that are initiated by the activation of the G proteins $G\alpha_q$, $G\alpha_i$ and $G\alpha_{12/13}$ (reviewed by Offermanns 2006). $G\alpha_q$-mediated signaling activates phospholipase Cβ (PLCβ). Activation of PLCβ results in the hydrolysis of phophatidylinositol-4,5-bisphosphate and the formation of the second messengers inositol-1,4,5-trisphosphate (IP_3) and 1,2-diacylglycerol (DAG). IP_3 increases intracellular [Ca^{2+}], whereas DAG activates protein kinase C (PKC). By contrast, activated $G\alpha_i$ inhibits adenylyl cyclase and thus formation of the inhibitory cyclic adenosine monophosphate. Finally, $G\alpha_{13}$, a member of the $G\alpha_{12/13}$ family, activates guanine nucleotide exchange factors of the small GTPase Rho (Hart et al.1998, Fukuhara et al. 2001), leading to the formation of Rho-GTP and rearrangement of the platelet actin cytoskeleton and shape change.

Thrombin

The serine protease α-thrombin is one of the most potent platelet activators. Upon vascular injury exposure of tissue factor to plasma coagulation factors initiates thrombin formation (Daubie et al. 2007). Thrombin is produced on cellular surfaces including that of activated platelets (Heemskerk et al. 2002). Activation of platelets by thrombin is mediated by protease-activated receptors (PARs) (Coughlin 2000). To date four PARs have been described: PAR1, PAR2, PAR3, and PAR4. PARs are activated by proteolytic cleavage of their extracellular N-terminal domain which leads to the generation of a tethered ligand. While PAR1, PAR3, and PAR4 are cleaved and activated by thrombin, PAR2 is activated by trypsin, tryptase and coagulation factors VIIa and Xa (Nystedt et al. 1994, Molino et al. 1997,

Camerer et al. 2000). Human platelets express PAR1 and PAR4 (Kahn et al. 1999). PAR1 is the predominant human platelet thrombin receptor, and couples to $G\alpha_q$, $G\alpha_{12/13}$ and $G\alpha_i$ (reviewed by Coughlin 2005).

In addition to interacting with PARs, α-thrombin binds also to GPIbα, which is part of the GPIb-V-IX complex (Okumara et al. 1978, Andrews et al. 1999). Deletion of the extracellular domain of GPIbα or blockade of the α-thrombin binding site decreased thrombin-induced platelet activation (Brass 2003). However, the precise role of α-thrombin interaction with GPIb-V-IX remains yet to be defined.

Adenosine diphosphate

Adenosine diphosphate is stored in platelet dense granules and is released upon platelet activation. Released ADP activates platelets in an autocrine and paracrine manner. ADP interacts with G protein-coupled receptors of the P2 receptor family: $P2Y_1$ and $P2Y_{12}$. $P2Y_1$ couples to $G\alpha_q$, whereas $P2Y_{12}$ to $G\alpha_i$. Studies using receptor agonists revealed that concomitant activation of both receptors is required for a full response of platelets to ADP (Jin et al. 1998, Jantzen et al. 1999). The $P2Y_{12}$ receptor is irreversibly inhibited by thienopyridines (e.g. ticlopidine, clopidogrel and prasugrel) which are used as antiplatelet drugs (Savi and Herbert 2005, Niitsu et al. 2005). Enzymatic conversion of ADP to the inactive adenosine monophosphate and phosphate by endothelial ecto-ADPase CD39 limits platelet activation by ADP (Atkinson et al. 2006).

Additionally, a third platelet P2 receptor, $P2X_1$, is activated by adenosine triphosphate (ATP). $P2X_1$ is a gated cation channel responsible for a fast calcium influx that contributes to platelet activation (Gachet 2008).

Other platelet activators

Like ADP, thromboxane A_2 functions as a positive feedback mediator during platelet activation. TxA_2 is produced from arachidonic acid by the enzymes cyclooxygenase-1, which is the target of low dose aspirin (Patrono et al. 2005, Patrono and Rocco 2008), and by thromboxane synthase. Because of its short half-life, the action of TxA_2 is locally restricted. TxA_2 operates through its platelet surface receptor TP coupled to $G\alpha_q$ and $G\alpha_{12/13}$ (Murugappan et al. 2004).

Several other substances including epinephrine and serotonin can activate platelets, too. However, in contrast to thrombin, ADP, and TxA_2, they are only weak platelet activators. Serotonin (5-hydroxytryptamine, 5HT) is taken up by platelets, stored in dense granules and released upon platelet activation. It activates platelets in a positive feedback mechanism through interaction with platelet surface receptor 5HT2A which couples to $G\alpha_q$. Moreover,

platelet-derived serotonin causes vasoconstriction (Coppinger and Maguire 2007), and has recently been shown to mediate platelet effects on tissue regeneration (Lesurtel et al. 2006).

1.2.2 Platelet inhibitors

Endothelium-derived nitric oxide and prostaglandin I_2 are the two major inhibitors of platelet activation (Schwarz et al. 2001, Davi and Patrono 2007). Gaseous NO diffuses into platelets and directly activates the soluble guanylyl cyclase to produce cyclic guanosine monophosphate (cGMP). By contrast, PGI_2 acts through a platelet surface receptor, the IP receptor (Norel 2007), which couples to $G\alpha_s$. Activation of $G\alpha_s$ then stimulates adenylyl cyclase to produce cyclic adenosine monophosphate (cAMP). Consequently, a rise in intracellular levels of cGMP and cAMP activates cGMP- and cAMP-dependent protein kinases (cGK/PKG and cAK/PKA). In platelets, PKG and PKA are highly expressed with PKGIβ and PKAIβ and IIβ representing the major isoforms (Schwarz et al. 2001). PKG and PKA phosphorylate substrate proteins leading to the inhibition of platelet activation and aggregation (Schwarz et al. 2001, Münzel et al. 2003, Hofmann et al. 2006). One of the major substrates of PKG and PKA in platelets is the vasodilator-stimulated phosphoprotein (VASP). VASP is phosphorylated at serine 157, serine 239, and threonine 278 by both PKG and PKA (Butt et al. 1994, Reinhard et al. 2001). VASP phosphorylation appears to be involved in the inhibition of agonist-induced activation of integrin $\alpha_{IIb}\beta_3$ and thus platelet adhesion and aggregation (Horstrup et al. 1994, Aszodi et al. 1999, Häuser et al. 1999, Massberg et al. 2004).
cGMP and cAMP are hydrolyzed and thereby inactivated by phosphodiesterases (PDEs). Platelets contain at least three different types of PDEs: PDE2, PDE3, and PDE5 (reviewed by Schwarz et al. 2001, Colman 2004).

1.3 Platelet granule secretion

1.3.1 Platelet granules

Three types of intracellular granules have been described in platelets: alpha granules, dense granules, and lysosomes. Alpha granules are the largest (~ 200-500 nm in diameter) and most abundant platelet granules (~ 80 per platelet) (Reed 2004, Italiano 2008). They store proteins (e.g. von Willebrand factor, fibrinogen) that are important for platelet adhesion, aggregation, and clot formation. Moreover, alpha granules contain various cytokines (e.g. platelet factor 4) and growth factors (e.g. platelet derived growth factor) that contribute to platelet interactions with leukocytes and other cells (Coppinger and Maguire 2007, Sierko and Wojtukiewicz 2007). Platelet dense granules, of which there are ~ 8 per platelet, are 250 nm in size and characterized by virtue of their electron-dense cores. Dense granules contain

small molecules such as ADP, serotonin, calcium, and pyrophosphate (Gawaz 1999, Reed 2004). In particular, the release of dense granule contents allows the recruitment of additional circulating platelets to sites of vascular injury.

Several proteins (e.g. GPIb, $\alpha_{IIb}\beta_3$, P-selectin) that are critical for platelet function are incorporated into the limiting membranes of both alpha and dense granules (King and Reed 2002, Rendu and Brohard-Bohn 2001). Upon platelet granule secretion these proteins become exposed on the platelet surface. The presence of GPIb and $\alpha_{IIb}\beta_3$ facilitates platelet adhesion and aggregation. P-selectin upon engagement of its ligand P-selectin glycoprotein ligand 1 recruits monocytes, neutrophils and lymphocytes, thereby initiating the formation of platelet-leukocyte aggregates (Furie et al. 2001, von Hundelshausen and Weber 2006, Jurk and Kehrel 2008).

Unlike alpha and dense granules, lysosomes are generally considered as degradative compartments (Luzio et al. 2007). However, platelets and some other hematopoietic cells including macrophages and cytotoxic T lymphocytes contain the so-called secretory lysosomes, and lysosome release is stimulated by transient increase in intracellular calcium (Stichcombe and Griffiths 1999, Andrews 2000, Luzio et al. 2007). Platelet lysosomes contain lysosomal enzymes (e.g. β-hexosaminidase, cathepsin D, heparitinase) that might play a role in clot remodeling (Reed 2004).

1.3.2 Molecular mechanisms of platelet granule secretion

Platelet granule secretion is crucial for normal platelet function during primary hemostasis and can be summarized as a process occurring in three steps: (1) platelet activation initiated by a platelet agonist, leading to the increase of intracellular calcium and activation of protein kinase C with subsequent phosphorylation of effector molecules; (2) granule tethering/docking with the target membrane followed by ATP-dependent granule priming; and (3) granule/membrane fusion with release of granule contents into the extracellular environment. Various proteins have been reported to be essential for distinct steps during this process. For example, Rab GTPases and their effectors are widely believed to regulate granule secretion at the tethering/docking step, and membrane proteins of the soluble N-ethylmaleimide sensitive factor attachment protein receptor (SNARE) family in concert with SNARE accessory proteins have been shown to control membrane fusion (Fig.1.2) (Reed et al. 2000, Rendu and Brohard-Bohn 2001, Flaumenhaft 2003, Reed 2004).

Calcium and protein kinase C

Platelet agonists (e.g. collagen, thrombin, ADP) activate platelets through interaction with specific receptors on the platelet plasma membrane. Subsequent phospholipase C - mediated formation of inositol-1,4,5-trisphosphate and 1,2-diacyglycerol leads to an increase

in intracellular calcium and activation of protein kinase C. Both, calcium and PKC are critical determinants of platelet granule secretion, operating in synergy (Walker and Watson 1993, Reed et al. 2000). However, a rise in intracellular calcium is at all times sufficient to induce platelet granule release, and secretion of permeabilized platelets can be stimulated by addition of exogenous calcium ions (Flaumenhaft 2004). The exact mechanism through which an increase in intracellular calcium induces granule secretion is poorly understood. In this regard, specific calcium sensor/effector molecules could play a role. Among them, proteins containing C2 and EF hand domains appear to be likely candidates. The tandem C2 domain containing protein synaptotagmin-I is the most prominent example of a Ca^{2+}-sensor not only in neurons, but also in non-neuronal cells (reviewed by Burgoyne and Morgan 2003, Martens and McMahon 2008). Other C2 domain containing proteins, all of which are implicated in regulated exocytosis, are rabphilin, Doc2, RIM, Munc13, and Slp (Burgoyne and Morgan 2003, Fukuda 2005, Martens and McMahon 2008). EF hand domain containing proteins are e.g. calmodulin and calcyclin. Both proteins are expressed in platelets and have been invoked in secretion (reviewed by Flaumenhaft 2003).

Based on studies using broad spectrum pharmacological inhibitors and activators of protein kinase C, there is evidence suggesting a general role for PKC in platelet activation and in particular, a stimulatory role for this kinase in platelet granule secretion. Inhibitors of PKC block platelet dense granule release (Chung et al. 2000, Rozenvayn and Flaumenhaft 2003, Reed 2004). Phorbol esters such as 12-O-tetradecanoyl phorbol-13-acetate (TPA) activate protein kinase C by mimicking DAG, and stimulation of PKC with TPA in platelets resulted in increased platelet granule release (Rink et al. 1983). Moreover, a purified rat brain PKCα has been shown to augment Ca^{2+}-dependent platelet alpha and dense granule secretion (Yoshioka et al. 2001). PKCs form a family of related serine/threonine kinases that are part of the AGC-type kinase (protein kinase A/protein kinase B/protein kinase C) superfamily. In platelets, isoforms α, β_I, β_{II}, δ, η, θ and ζ are present, and recently, PKCδ has been shown to be required for PAR-mediated platelet dense granule secretion (Murugappan et al. 2004). Activation of PKC results in phosphorylation of downstream effector molecules such as myristoylated alanine-rich C kinase substrate (MARCKS) and Munc-18c (reviewed by Flaumenhaft 2003).

Rab proteins and their effectors

Rab proteins are members of the Ras superfamily of small GTPases and involved in various aspects of intracellular membrane trafficking (Zerial and McBride 2001). To date more than 60 Rab isoforms have been identified in mammals. Some of these are ubiquitously expressed, whereas others are cell-type specific. After synthesis Rab GTPases are soluble. However, post-translational modification by prenylation turns Rab proteins into peripheral

membrane proteins. Attachment of geranylgeranyl group(s) to cysteine residue(s) which is carried out by Rab geranylgeranyl transferase (RabGGT) allows Rab proteins to associate with membranes. Like other small GTPases, Rab GTPases are molecular switches alternating between an active guanine-nucleotide triphopshate (GTP)-bound form and an inactive guanine nucleotide diphosphate (GDP)-bound form. This GTP/GDP cycle is controlled by guanine nucleotide exchange factors (GEFs) and GTPase activating proteins (GAPs). So far, only few Rab GEFs and GAPs have been identified. In the active GTP-bound form Rab proteins are membrane-associated and interact with specific effector molecules. In contrast, GDP-bound Rab proteins are removed from the membrane and are kept cytosolic by means of the Rab GDP dissociation inhibitor (RabGDI) (reviewed by Behnia and Munro 2005, Ali and Seabra 2005).

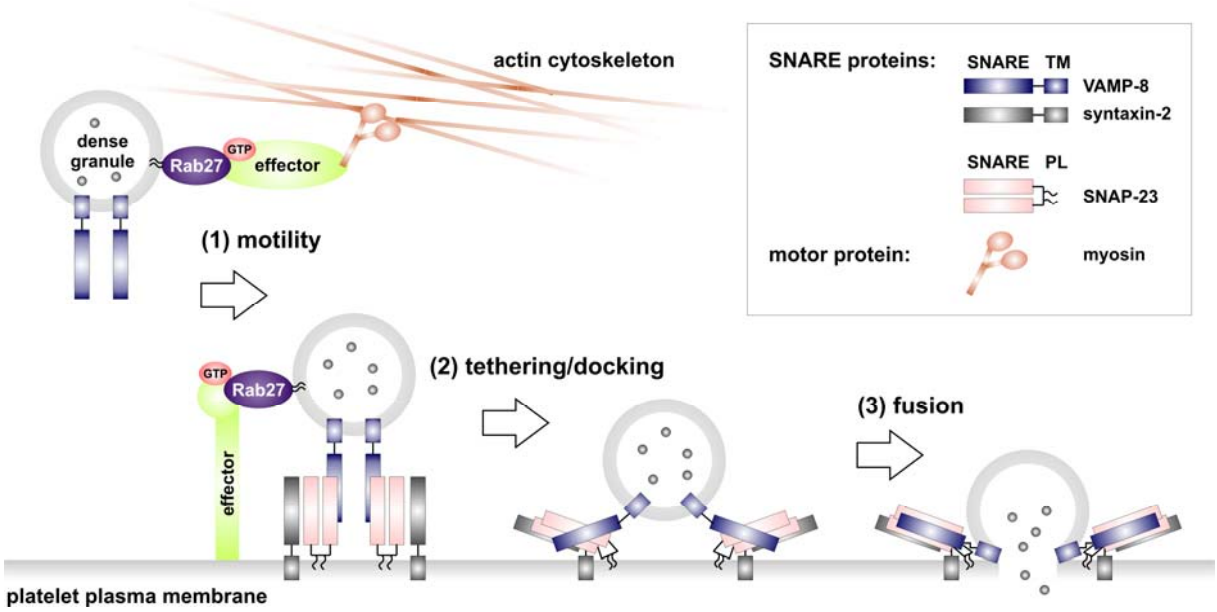

Figure 1.2: Platelet dense granule secretion requires Rab27 and SNARE proteins.
Dense granules in platelets are loaded with small molecules (e.g. ADP, serotonin) that are released on platelet activation. Platelet dense granule release requires the small GTPase Rab27 and the SNARE proteins VAMP-8, syntaxin-2 and SNAP-23. GTP-Rab27 is dense granule-associated and through engagement of effector proteins regulates granule motility (1) and granule tethering/docking to the plasma membrane (2). Rab27 effector proteins interact with motor proteins (e.g. myosin) and/or plasma membrane components (e.g. phospholipids). Once a dense granule is docked, membrane fusion is mediated by SNARE proteins. VAMP-8 is a vesicle-associated (v)-SNARE, and syntaxin-2 and SNAP-23 are target/plasma membrane-associated (t)-SNAREs. SNARE proteins are characterized by SNARE motifs. VAMP-8 and syntaxin-2 each possess a single SNARE motif, whereas SNAP-23 contains two SNARE motifs separated by a palmitoylated linker. Assembly of the SNARE motifs into a tight four α-helix bundle, the so-called SNARE core complex, drives fusion of the two lipid bilayers and hence delivery of dense granule contents into the extracellular environment. GTP: guanine nucleotide triphosphate; SNARE: soluble NSF attachment protein receptor; TM: transmembrane domain; PL: palmitoylated linker.

First evidence that Rab proteins and in particular Rab27 are involved in platelet granule secretion came from studies of *gunmetal (gm)* mice. The naturally occurring *gunmetal* mice

have a mutation in the *RGGTA* gene encoding the α-subunit of the Rab geranylgeranyl transferase which results in a reduction of RabGGT activity to approximately 20 % of wild-type (Detter et al. 2000). In consequence, Rab27 and other Rab proteins in platelets remain unprenylated and thus cytosolic (Detter et al. 2000). Mice with *gm* mutation exhibit abnormalities in platelet alpha and dense granules, thrombocytopenia, and prolonged bleeding (Seabra et al. 2002). Additional evidence that Rab proteins play a critical role in platelet secretion was obtained from studies with Rab GDP dissociation inhibitor. When introduced into permeabilized platelets, RabGDI extracted Rab GTPases from membranes and inhibited Ca^{2+}-induced alpha granule secretion (Shirakawa et al. 2000). The same study by Shirakawa et al. 2000 demonstrated that Rab4 blocked platelet alpha granule but failed to affect secretion from dense granules. These data suggest that the regulatory mechanisms governing alpha and dense granule secretion in platelets are distinct, and Rab4 is required for alpha but not dense granule release. Conversely, incubation of permeabilized platelets with Rab27 inhibited platelet dense granule secretion, and this inhibition could be rescued by addition of Munc13-4 (Shirakawa et al. 2004). Rab27 is expressed in two isoforms, Rab27a and Rab27b, that share 71 % identity at the amino acid level (Pereira-Leal and Seabra 2001). Both, Rab27a and Rab27b are present in platelets and localize predominantly to membranes of platelet dense granules (Barral et al. 2002). Much recent interest has focused on Rab27a because it is the first Rab protein closely associated with human disease (Seabra et al. 2002). In humans, defects in the *RAB27A* gene cause Griscelli syndrome (GS), a rare autosomal disorder which is characterized by hypopigmentation and loss of cytotoxic killing activity. At cellular level, the disease reflects dysfunction in melanosome transport in melanocytes and lytic granule release in cytotoxic T lymphocytes. The corresponding mouse model for GS is designated *ashen* and exhibits a loss-of-function mutation in *RAB27A*. Interestingly, the issue of platelet dysfunction in *ashen* mice has been a matter of debate. Despite the fact that platelet functional defects are not observed in patients with GS, a platelet phenotype has been reported for *ashen* mice (Wilson et al. 2000). Subsequent analysis, however, revealed that the platelet defect seen by Wilson and his co-workers is due to a mutation in a second gene, *Slc35d3*, which encodes an orphan putative sugar nucleotide transporter (Chintala et al. 2007). Consistent with studies of GS in humans, normal platelet function in the presence of *RAB27A* loss-of-function mutation has been described in *ashen* by Barral et al. 2002, suggesting that presence of Rab27b in platelets compensates for the loss of Rab27a. Deletion of *RAB27B* in mice, however, resulted in a bleeding phenotype, albeit the bleeding tendency was more severe in double *RAB27A/B* knockout animals (Tolmachova et al. 2007). Both, Rab27a and Rab27b have been demonstrated to participate in platelet dense granule release with a distinct and probably non-redundant role for Rab27b in dense granule formation (Tolmachova et al. 2007). Conversely, the morphology and

secretion of platelet alpha granules were not affected, consistent with only minor association of Rab27a and Rab27b with alpha granule membranes (Tolmachova et al. 2007, Barral et al. 2002). Rab27 regulates platelet dense granule secretion, operating upstream of SNARE proteins and thus upstream of the membrane fusion event. Rab27 is thought to exert its function by promoting granule motility and/or granule tethering/docking to the plasma membrane (Fig.1.2) (Seabra and Coudrier 2004, Fukuda 2006). Therefore, Rab27 needs to interact with effector molecules, and Munc13-4 was identified as the first Rab27-binding protein in platelets (Shirakawa et al. 2004). To date three groups of Rab27 effectors have been described (Fig.1.3): Slp (synaptotagmin-like proteins), Slac2 (Slp homologue lacking C2 domains), and Munc13-4. Slp and Slac2 family members are defined by a conserved N-terminal synaptotagmin-like protein homology domain (SHD) that binds to Rab GTPases and in particular Rab27 (Fukuda 2005). In addition, Slps contain two tandem C2 domains at their C-termini that are homologous to the C2A and C2B domains of synaptotagmins. In contrast,

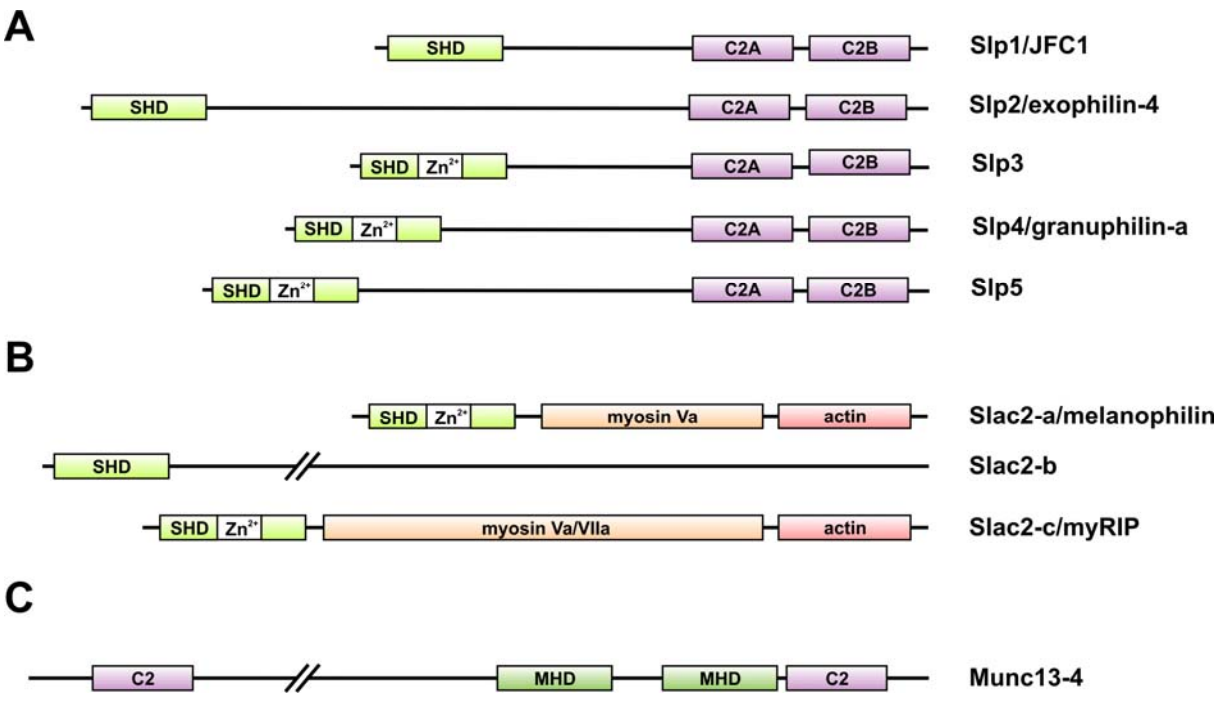

Figure 1.3: Domain structures of putative Rab27 effector proteins.
Three groups of Rab27 binding proteins are known: Slp (synaptotagmin-like proteins), Slac2 (Slp homologue lacking C2 domains) and Munc13-4. **A:** There are five Slp family members (Slp1, 2, 3, 4, and 5). All of them contain an N-terminal Slp homology domain (SHD), which mediates binding to Rab27, and two C-terminal tandem C2A and C2B domains. The Slp homology domain of Slp3, Slp4 and Slp5 is separated by a zinc finger motif (Zn^{2+}). Besides Rab27, Slp1 binds to Rab8 and Slp4 binds to Rab3 and Rab8. **B:** There are three Slac2 family members (Slac2-a, -b and -c). All of them contain the N-terminal Slp homology domain (SHD), which binds to Rab27, but lack tandem C2 domains. Instead, Slac2-a and Slac2-c possess myosin and actin binding domains. Slac2-a binds to myosin Va and Slac2-c binds to myosin Va and VIIa.. **C:** Munc13-4 contains two separate C2 domains and two Munc13 homology domains (MHD). Munc13-4 is a Rab27 binding protein, however, the Rab27 binding site in Munc13-4 is yet unknown. Figure was modified according to Fukuda 2005.

Slac2 proteins lack such domains. In mammals, there are five synaptotagmin-like proteins: Slp1/JFC1, Slp2/exophilin-4, Slp3, Slp4/granuphilin-a, and Slp5. Several studies implicate Slps in the regulation of membrane trafficking in different secretory cells (reviewed by Martens and McMahon 2008).

SNAREs and SNARE accessory proteins

Membrane fusion in platelets depends on SNAREs and is a process whereby two separate lipid bilayers (e.g. granule and OCS/plasma membrane) merge to become one. SNARE proteins are membrane-associated, and on the basis of their localization can be divided into vesicle (v)-SNAREs and target membrane (t)-SNAREs. Prior to granule/membrane fusion, a ternary core complex of SNARE proteins is formed in *trans* on opposing membranes, bringing the granule and plasma membranes into close apposition. Then, upon fusion a *cis* SNARE complex is formed in which all of the contributing SNARE proteins are localized to the same membrane. This *cis* complex is subsequently disassembled by the AAA-ATPase NSF (N-ethylmaleimide sensitive factor) and α-SNAP (soluble NSF attachment protein) (Jahn and Scheller 2006). In platelets, t-SNAREs syntaxin-2, -4, -7, -11 (Lemons et al. 1997, Chen et al. 2000a, Chen et al. 2000b), and SNAP-23, -25, -29 are present (Flaumenhaft et al. 1999, Reed et al. 1999, Polgar et al. 2003). Platelets also contain the v-SNAREs VAMP-2, VAMP-3, VAMP-7, and VAMP-8 (Flaumenhaft et al. 1999, Polgar et al. 2002, Schraw et al. 2003, Ren et al. 2007). Experiments using permeabilized platelets strongly suggest a role for SNARE proteins in platelet granule release (reviewed by Flaumenhaft 2003). However, despite the consensus on t-SNAREs, it was long time unclear which v-SNARE(s) are involved. Recent studies with transgenic mice demonstrated a redundancy of v-SNAREs in platelets, with VAMP-8 as the primary v-SNARE for platelet granule secretion (Ren et al. 2007). Thus, platelet dense granule release requires syntaxin-2, SNAP-23 and VAMP-8 (Fig.1.2), whereas platelet alpha granule and lysosome secretion are mediated by syntaxin-4 and syntaxin-2, SNAP-23 and VAMP-8 (Lemons et al. 1999, Flaumenhaft et al. 1999, Chen et al. 2000a, Chen et al. 2000b, Ren et al. 2007).

In addition, SNARE accessory proteins such NSF, α-SNAP and Munc-18c have been shown to serve as important modulators of SNARE function in platelets. By means of inhibitory peptides and antibodies a role for NSF in platelet dense, alpha and lysosomal granule release could be assigned (Chen et al. 2000a, Lemons et al. 2000, Polgar et al. 1999). Upon inhibition of NSF, SNARE proteins are sequestered in *cis* complexes and are unavailable to interact with SNARE proteins on opposing membranes. α-SNAP binds and activates NSF (Clary et al. 1990). In platelets, wild-type α-SNAP stimulated Ca^{2+}-induced granule secretion, whereas a dominant-negative mutant of α-SNAP and anti-α-SNAP antibodies inhibited granule release (Chen et al. 2000). Moreover, the Sec1/Munc18 homologue Munc-18c (also

known as platelet Sec1 protein) was identified in platelets (Reed et al. 1999). Munc-18c binds to syntaxin-4, and is phosphorylated by PKC upon platelet activation (Reed et al. 1999, Houng et al. 2003). Phosphorylation of Munc-18c decreases binding to syntaxin-4, suggesting that activation-induced dissociation of the Munc-18c/syntaxin-4 complex might contribute to platelet granule secretion. Accordingly, peptides mimicking Munc-18c binding sites augmented Ca^{2+}-induced dense granule release from permeabilized platelets, and similarly, antibodies that inhibit Munc-18c/syntaxin-4 complex formation promoted platelet granule secretion (Houng et al. 2003).

Taken together, platelet granule secretion is essential to hemostasis and is a process mediated by an elaborate protein machinery regulating distinct steps of granule motility, granule tethering/docking and granule/membrane fusion. Yet, the organization of this protein network in platelets is not well understood. Undoubted is the role for SNARE proteins in membrane fusion, and it is clear that small GTPases such as Rab GTPases by engagement of effector molecules are involved as well. Apart from extensive work that has been done on SNAREs, only little is known about Rab proteins and their effectors. So far, Rab4 and Rab27 have been shown to play a role in platelet granule secretion. However, Rab effector proteins have not yet been identified, except for Munc13-4. Moreover, the issue of how agonist-induced platelet activation elicits platelet granule release is obscure. It is evident that elevation of intracellular calcium and activation of protein kinase C play a crucial role. However, the exact signaling mechanism remains to be established.

1.4 Platelet aggregation

The accumulation of platelets into a hemostatic plug is based on the formation of multiple platelet-platelet interactions (platelet aggregation). The major receptor mediating platelet aggregation is integrin $\alpha_{IIb}\beta_3$ (also known as GPIIb-IIIa), which is the most abundant receptor on the platelet surface (Fullard 2004, Varga-Szabo et al. 2008). In humans, lack or dysfunction of $\alpha_{IIb}\beta_3$ cause the bleeding disorder Glanzmann`s thrombasthenia (GT) (Nurden and Nurden 2008). Mice lacking the β_3 integrin resemble the phenotype of GT with absent platelet aggregation and reduced uptake of fibrinogen into platelets (Hodivala-Dilke et al. 1999, Fullard 2004). Integrin $\alpha_{IIb}\beta_3$ binds various ligands including von Willebrand factor, fibrinogen and fibronectin, all of which contain the classical integrin recognition sequence arginine-glycine-aspartic acid (Jackson 2007, Varga-Szabo et al. 2008). In resting platelets, $\alpha_{IIb}\beta_3$ is in a low affinity or inactive state, in which it is not able to bind to its ligands. Agonist-induced platelet activation, however, induces intracellular signaling processes that activate $\alpha_{IIb}\beta_3$ by converting it into an active high affinity conformation (inside-out signaling and change in affinity). In addition, $\alpha_{IIb}\beta_3$ lateral mobility and clustering within the platelet plasma

membrane (change in avidity) supports ligand binding to $\alpha_{IIb}\beta_3$ and thus platelet aggregation (Shattil et al. 2004, Ginsberg et al. 2005).

The exact signaling mechanisms linking agonist-induced platelet activation and activation of platelet integrins (e.g. $\alpha_{IIb}\beta_3$) have been extensively studied, but are yet not fully understood. Recently, Rap1 has been suggested to be an important intermediate (Bos et al. 2001, Shattil et al. 2004, Stork and Dillon 2005). Rap1 is a member of the Ras superfamily of small nucleotide binding proteins and has been implicated to be involved in various aspects of cell adhesion (Bos et al. 2001, Bos et al. 2003, Bos 2005). Rap1 has two isoforms, Rap1a and Rap1b, that share 95 % sequence identity at the amino acid level (Scrima et al. 2008). Rap1b is the predominant isoform in platelets (Klinz et al. 1992). Like other small guanine nucleotide binding proteins, Rap1 exists in an inactive GDP-bound form and is activated, when guanine nucleotide diphosphate is exchanged for guanine nucleotide triphosphate. Replacement of GDP for GTP is stimulated by guanine nucleotide exchange factors, whereas GTPase activating proteins promote the hydrolysis of bound GTP to GDP and thus Rap1 inactivation (Fig.1.4) (Bos et al. 2007).

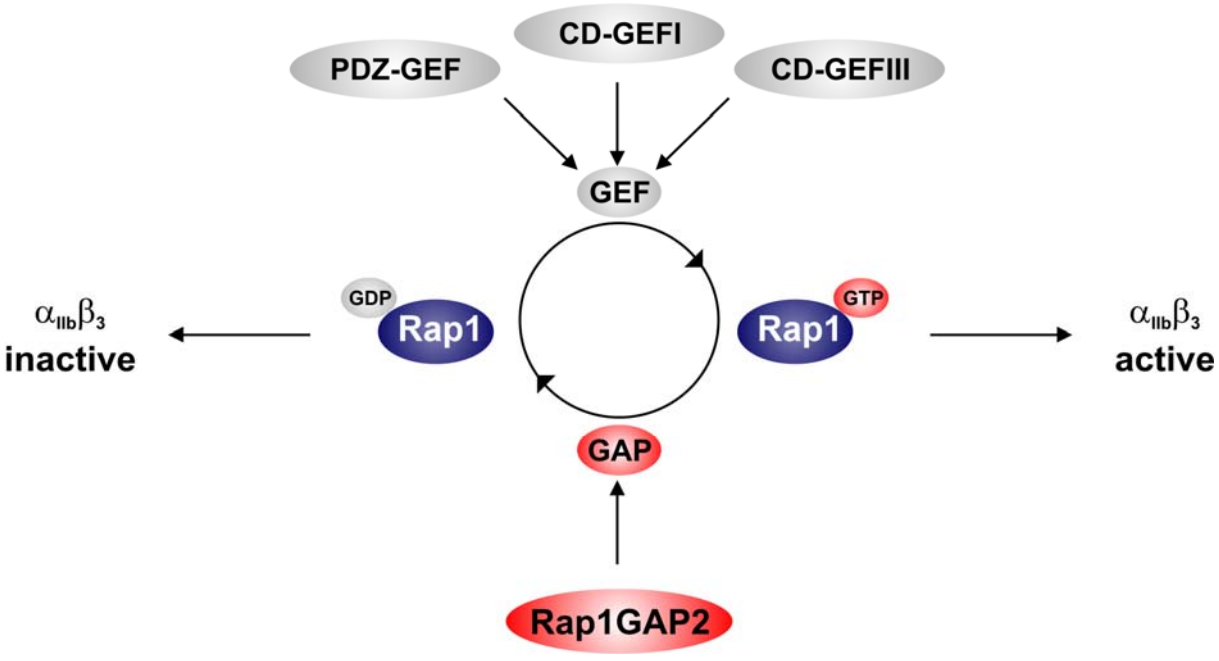

Figure 1.4: Regulation of Rap1 in platelets.
The small guanine nucleotide binding protein Rap1 regulates the activity of the platelet integrin $\alpha_{IIb}\beta_3$, which is required for fibrinogen binding and thus platelet aggregation. Rap1 cycles between an inactive GDP- and an active GTP-bound form. This GDP/GTP cycle is regulated by guanine nucleotide exchange factors (GEFs) and GTPase-activating proteins (GAPs). In platelets, PDZ-GEF1, CalDAG-GEFI and III, and Rap1GAP2 are present. PDZ-GEF: postsynaptic density-95 discs-large and zona occludens protein 1-GEF; CD-GEF: CalDAG-GEF (where cal stands for calcium and DAG for 1,2-diacylglycerol); GDP: guanine nucleotide diphosphate; GTP: guanine nucleotide triphosphate.

In murine megakaryocytes, overexpression of the constitutively active Rap1 mutant augmented agonist-induced binding of fibrinogen to integrin $\alpha_{IIb}\beta_3$ (Bertoni et al. 2002). Moreover, deficiency of Rap1 in mouse platelets resulted in abnormal platelet function and a severe hemostatic defect caused by reduced agonist-induced $\alpha_{IIb}\beta_3$ activation and thus platelet aggregation (Chrzanowska-Wodnicka et al. 2005).

Rap1 becomes rapidly activated on platelet activation with various agonists (Franke et al. 1997, Franke et al. 2000, Woulfe et al. 2002). Rap1 activation is mediated by Rap1-specific GEFs, of which PDZ-GEF1 and CalDAG-GEFI and III are expressed in platelets (Schultess et al. 2005). In particular, CalDAG-GEFI and III are likely candidates to integrate agonist-induced formation of second messengers into the activation of Rap1. Both, CalDAG-GEFI and III, are activated by calcium and 1,2-diacylglycerol (Bos et al. 2007). Recently, platelets from mice lacking CalDAG-GEFI have been demonstrated to have decreased agonist-induced activation of Rap1 and $\alpha_{IIb}\beta_3$, and thus impaired aggregation and thrombus formation (Crittenden et al. 2004). Conversely, platelet inhibition by NO and PGI_2, leading to the activation of cGMP- and cAMP-dependent protein kinases, blocks agonist-induced formation of Rap1-GTP (Franke et al. 1997, Danielewski et al. 2005). Rap1 is phosphorylated by both, PKG and PKA, in platelets (Siess et al. 1990, Miura et al. 1992, Siess and Grünberg 1993, Danielewski 2005). However, the effect of this phosphorylation is currently unknown. The slow kinetics of Rap1 phosphorylation does not correlate with the fast inhibition of the protein, suggesting that Rap1 phosphorylation *per se* is not responsible for the fast inactivation of Rap1. Alternatively, phosphorylation and activation of a Rap1-specific GAP could play a role in this process. Two major groups of Rap1-specific GAPs have so far been described. The first group includes SPA-1 (signal-induced proliferation-associated protein 1) and E6TP1α (SPAR/SPAL), whereas the second group consists of Rap1GAP1 and the recently identified Rap1GAP2 (Bos et al. 2001, Stork and Dillon 2005, Schultess et al. 2005). In platelets, only Rap1GAP2 is present (Schultess et al. 2005). Rap1GAP2 contains a conserved catalytic GAP domain, a dimerization domain, an N-terminal 14-3-3 binding site and a large C-terminal region of so far unknown function (Fig.1.5) (Daumke et al. 2004, Schultess et al. 2005, Hoffmeister et al. 2008). Platelet activation results in phosphorylation of Rap1GAP2 on serine 9, binding of 14-3-3 and inhibition of GAP function (Hoffmeister et al. 2008). Conversely, phosphorylation of Rap1GAP2 by PKG and PKA at serine 7 inhibits 14-3-3 binding to Rap1GAP2 (Schultess et al. 2005, Hoffmeister et al. 2008). The release of 14-3-3 protein from Rap1GAP2 might contribute to the inhibition of platelet aggregation initiated by NO and PGI_2.

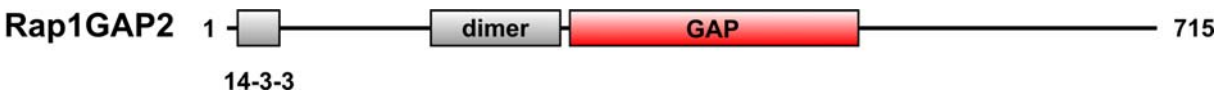

Figure 1.5: Rap1GAP2 is a multidomain protein.
Rap1GAP2 is a modular protein composed of a central catalytic GAP domain (GAP), a dimerization domain (dimer) and an N-terminal 14-3-3 binding site. The C-terminal part of Rap1GAP2 is predicted to have low structural organization and is so far of unknown function.

1.5 Aims of the present study

Rap1GAP2 was identified in our laboratory as the first and so far only known GTPase activating protein of Rap1 in human platelets (Schultess et al. 2005). Since no other Rap1 specific GAPs are available, tight regulation of Rap1GAP2 is probably required. In addition to the central catalytic GAP domain, Rap1GAP2 contains large N- and C-terminal regions of unknown function. It was hypothesized that these regions could be involved in protein-protein interactions. Subsequently, a genetic screening in yeast was performed in order to identify Rap1GAP2-associated proteins. Apart from 14-3-3 (Hoffmeister et al. 2008), synaptotagmin-like protein 1 (Slp1, also called JFC1) was found as a new putative interaction partner of Rap1GAP2.

Based on the results of the yeast-two-hybrid screening, the specific aims of the present study were to

(1) verify binding of Slp1 and Rap1GAP2,

(2) map the interaction site(s) involved in binding of Slp1 and Rap1GAP2,

(3) investigate complex formation by Slp1, Rap1GAP2, Rab27 and other proteins,

(4) determine the function of Slp1/Rap1GAP2 interaction.

The investigations were carried out in both, mammalian cells and human platelets. In particular, in order to define the functional significance of the interaction between Slp1 and Rap1GAP2, both, cellular and platelet models were established and applied.

2. MATERIALS AND METHODS

2.1 Materials

2.1.1 Plasmids and cDNAs

pGBKT7	Clontech Takara Bio, Saint-Germain-en-Laye, France
pACT2	Clontech Takara Bio, Saint-Germain-en-Laye, France
pGEX-4T-3	GE Healthcare, Freiburg, Germany
pET28	Novagen, Darmstadt, Germany
pcDNA^{TM}4/TO	Invitrogen, Karlsruhe, Germany
pcDNA3.1^{TM}/myc-His	Invitrogen, Karlsruhe, Germany
pCMV-3Tag-3	Stratagene, La Jolla, USA
pRluc-N3	BioSignal, Montreal, Canada

Full-length Slp1 cDNA, clone IRATp970G0456D6, was obtained from RZPD (Deutsches Ressourcenzentrum für Genomforschung GmbH, Berlin, Germany).

2.1.2 Constructs and primers

All constructs and primers that were provided or generated and used in this work are listed in the appendix. Primers were purchased from MWG Biotech AG, Martinsried, Germany.

2.1.3 Yeast and bacteria strains, cell lines

Saccharomyces cerevisiae AH109	Clontech Takara Bio, Saint-Germain-en-Laye, France
Escherichia coli strain TOP10	Invitrogen, Karlsruhe, Germany
Escherichia coli strain XL-10 Gold^{TM}	Invitrogen, Karlsruhe, Germany
Escherichia coli strain BL21 Star^{TM} (DE3)	Invitrogen, Karlsruhe, Germany
COS-1 cells African green monkey kidney cells	DSMZ, Braunschweig, Germany
HeLa cells Human epithelial cervixcarcinoma cells	Dr. M. Innocenti, IBCII, Frankfurt, Germany
LNCaP cells Human prostate carcinoma cells	DSMZ, Braunschweig, Germany

2.1.4 Antibodies

Primary antibodies

Antigen	Species (clone)	IB	IP	IF	Generated by
Protein-specific antibodies					
Rap1GAP2	rabbit	1:500	-	-	A. Smolenski
Slp1	rabbit	1:2000	-	-	ImmunoGlobe
Rap1	rabbit	1:500	-	-	Santa Cruz
Rab27a	mouse (1G7)	1:2000	1:50	-	Abnova
Rab8a	mouse (3G1)	1:2000	-	-	Abnova
P-VASP	mouse (16C2)	1:5000	-	-	A. Smolenski
LDH	goat	1:5000	-	-	Chemicon
Tag-specific antibodies					
FLAG	mouse (M2)	1:10000	1:100	-	Sigma
c-Myc	mouse (9E10) rabbit	1:2000 1:100	1:50 -	1:250 -	Santa Cruz
HA	mouse (16B12)	1:2000	-	-	Covance
VSV	mouse (P5D4)	1:5000	1:200	1:250	Sigma
T7	mouse	1:10000	-	-	Novagen
GFP	mouse (7.1 & 13.1)	1:1000	1:100	-	Roche
His_6	mouse	1:5000	-	-	Novagen
GST	mouse (GST-2)	1:10000	-	-	Sigma

.

Secondary antibodies

Horseradish peroxidase-coupled donkey anti-goat IgG, goat anti-rabbit IgG and goat anti-mouse IgG were purchased from Dianova, Hamburg, Germany and used as secondary antibodies for immunoblot analysis in dilutions 1:10000. Cy3- and Cy5-labelled secondary antibodies were obtained from Jackson Immunoresearch, West Grove, USA and used for immunofluorescence analysis in dilutions 1:250.

2.1.5 Enzymes and purified proteins

Pfu DNA Polymerase	Stratagene, La Jolla, USA Fermentas, St. Leon-Rot, Germany
Quick T4 DNA Ligase	New England Biolabs, Beverly, USA
Restriction enzymes	New England Biolabs, Beverly, USA Fermentas, St. Leon-Rot, Germany
Human thrombin	Sigma, Taufkirchen, Germany
Human fibronectin	Calbiochem, Darmstadt, Germany
Creatine phosphokinase	Sigma, Taufkirchen, Germany
Streptolysin-O	Prof. Dr. S. Bhakdi, Mainz, Germany
Catalytic subunit of PKA	Dr. E. Butt-Dörje, Würzburg, Germany

2.1.6 Standards and kits

GeneRuler DNA Ladder Mix	Fermentas, St. Leon-Rot, Germany
Unstained Protein MW Marker	Fermentas, St. Leon-Rot, Germany
QIAquick Gel Extraction Kit	Qiagen, Hilden, Germany
NucleoSpin® Plasmid MiniPrep Kit	Macherey-Nagel, Düren, Germany
NucleoBond® PC500 MaxiPrep Kit	Macherey-Nagel, Düren, Germany
ECL™ WB detection kit	Amersham Biosciences, Freiburg, Germany
Immobilon™ WB detection kit	Millipore, Billerica, USA
Renilla Luciferase Assay System	Promega, Mannheim, Germany
Active® PSA ELISA Kit	Diagnostic Systems Laboratories, Sinsheim, Germany

2.1.7 Chemicals and special reagents

Metafectene™	Biontex, Martinsried, Germany
DEAE-Dextran	Sigma, Taufkirchen , Germany
Chloroquine	Sigma, Taufkirchen, Germany
6α-fluorotestosterone	Biomol, Hamburg,Germany
ADP	Sigma, Taufkirchen, Germany
Forskolin	Sigma, Taufkirchen, Germany

Prostaglandin I_2 (PGI_2)	Biozol, Eching, Germany
Sp-5,6-DCI-cBiMPS	Biolog, Bremen, Germany
Rp-8-Br-cAMPS	Biolog, Bremen, Germany
ortho-Phthalaldehyde	Sigma, Taufkirchen, Germany
Serotonin creatinine sulfate	Sigma, Taufkirchen, Germany
Creatine phosphate	Fluka, Buchs, Switzerland
Protein A/G Plus Agarose	Santa Cruz Biotechnology, Santa Cruz, USA
GSH Sepharose™ 4B	GE Healthcare, Freiburg, Germany
Ni-NTA	Qiagen, Hilden, Germany
Bio Rad Protein Assay	Bio-Rad, München, Germany
Albumine bovine fraction V	Sigma, Taufkirchen, Germany
Albumin bovine fraction V, fatty acid-free	Serva Electrophoresis, Heidelberg, Germany

Rap1GAP2 wild-type peptide with the sequence HNSMEVTKTTFSPPV (amino acids 518-532 of Rap1GAP2a) and Rap1GAP2ΔEVTKTT peptide with the sequence GISHNSMFSPP VVAA (amino acids 515-535 of Rap1GAP2a lacking amino acids 522-527) were obtained from Schafer-N, Copenhagen, Denmark. All chemicals and reagents for yeast culture and transformation were obtained from Clontech Takara Bio, Saint-Germain-en-Laye, France and Sigma, Taufkirchen, Germany, except for x-α-Gal which was purchased from Glycosynth, Warrington, UK. All cell culture media and solutions were purchased from PAA Laboratories, Pasching, Austria. Other chemicals and reagents not listed above were obtained from Sigma, Taufkirchen, Germany, Applichem, Darmstadt, Germany, Merck, Darmstadt, Germany and Roth, Karlsruhe, Germany.

2.1.8 Buffers, solutions and gels

1x TAE Buffer
40 mM Tris
20 mM Acetic acid
1 mM EDTA pH 8.0

TBS	TBS-T
10 mM Tris-HCl pH 7.6	TBS pH 7.6
150 mM NaCl	+ 0.1 % (v/v) Tween® 20

1x SDS Electrophoresis Loading Buffer
0.01 M Tris-HCl pH 8.0
1 mM EDTA

1 % (w/v) SDS (electrophoresis grade)
5 % (v/v) β-Mercaptoethanol
10 % (v/v) Glycerine
0.05 % (w/v) Bromophenol blue

1x SDS Electrophoresis Running Buffer
25 mM Tris
112 mM Glycine
0.1 % (w/v) SDS

Transfer Buffer
25 mM Tris-NaOH pH 8.3
150 mM Glycine
10 % (v/v) Methanol

Ponceau S Staining Solution
1 % (w/v) Ponceau S
15 % (w/v) Trichloroacetic acid

Hot Coomassie Staining Solution
Phast Gel™ Blue R (Coomassie R 350 stain)
GE Healthcare, Freiburg, Germany

LB Medium (Luria-Bertani Medium)
1 % (w/v) Tryptone
0.5 % (w/v) Yeast extract
1 % (w/v) NaCl

Synthetic drop-out (SD) agar medium
-Trp/-Leu/-His/-Ade:
4.67 % (w/v) minimal SD agar base
0.06 % (w/v) -Trp/-Leu/-His/-Ade DO supplement
For SD/-Trp/-Leu/-His/-Ade supplemented with x-α-Gal, 40 mg/l of x-α-Gal were added.

X-α-Gal stock solution
5-bromo-4-chloro-3-indolyl-α-D-galactopyranoside (x-α-Gal) was dissolved in N,N-Dimethylformamide to a final concentration of 20 mg/ml and stored in the dark at -20°C.

Polyacrylamide gels

	Resolving gel			*Stacking gel*
[ml]	**9 %**	**10 %**	**12 %**	**4%**
H_2O	27.725	26.025	22.725	11.38
Acrylamide 30 %	15	16.7	20	2.7
3 M Tris-HCl pH 8.9	6.25	6.25	6.25	-
0.5 M Tris-HCl pH 6.7	-	-	-	5
SDS 10 %	0.5	0.5	0.5	0.5
TEMED	0.025	0.025	0.025	0.02
APS 10 %	0.5	0.5	0.5	0.4

.

2.1.9 Consumables

Protran® nitrocellulose transfer membrane Pore size 0.45 µm	Whatman, Dassel, Germany
Fuji Medical X-ray film Super RX	Fujifilm, Tokyo, Japan
PD-10 desalting columns	GE Healthcare, Freiburg, Germany
Amicon® Ultra centrifugal filter devices 3K / 10K / 50K / 100K	Millipore, Billerica, USA

All cell culture dishes and flasks were purchased from Greiner, Frickenhausen, Germany. All other plastic consumables were from Greiner, Frickenhausen, Germany and Sarstedt, Nuembrecht, Germany.

2.1.10 Equipment

PCR:

GeneAmp® PCR system 9700	Applied Biosystems, Foster City, USA
Eppendorf Mastercycler	Eppendorf, Hamburg, Germany

Agarose gel analysis:

Gel Doc 2000 with Quantity One software	Bio Rad, München, Germany

Immunflourescence analysis:

Zeiss LSM 510 confocal laser scanning microscope with Plan-Apochromat 63x/1.4 oil DIC objective lens and LSM 510 Meta software	Carl Zeiss, Göttingen, Germany

Centrifuges:

Eppendorf centrifuge 5415D	Eppendorf, Hamburg, Germany
Eppendorf centrifuge 5417R	Eppendorf, Hamburg, Germany
Eppendorf centrifuge 5810R	Eppendorf, Hamburg, Germany
Avanti^{TM} J-30I centrifuge	Beckman Coulter, Krefeld, Germany

Photometric analysis:

Eppendorf BioPhotometer	Eppendorf, Hamburg, Germany
Wallac Victor^3 1420 Multilabel Counter	Perkin Elmer, Fremont, USA

2.2 Molecular biological methods

2.2.1 Agarose gel electrophoresis

DNA fragments were separated by electrophoresis on 1 % agarose gels according to their size. Gels were prepared using standard agarose and 1x TAE running buffer. For DNA visualization, 1 µg/ml ethidium bromide was added. Before loading, samples were mixed with 6x DNA loading buffer (Fermentas, St- Leon-Rot, Germany). Gels were run at 100 V 20 min in 1x TAE buffer and finally examined under UV (Gel Doc 2000, Quantity One).

2.2.2 Cloning of PCR products

DNA fragments were amplified by polymerase chain reaction (PCR) using thermostable proofreading DNA polymerase *Pfu* (Stratagene; Fermentas). Primers for cloning were designed with overhangs in their 5` regions containing the appropriate sites for restriction enzymes. All primers that were used can be found in the appendix. Unless otherwise specified, a standard hot start PCR protocol was applied in which the polymerase was added after the initial denaturation step.

Reaction mixture:

Component	*Final concentration*	*Volume for 50 µl of reaction mixture*
dH2O	-	variable
10x Pfu buffer	1x	5 µl
10 mM dNTPs	0.2 mM each	1 µl
Forward primer 10 µM	0.1 µM	1 µl
Reverse primer 10 µM	0.1 µM	1 µl
Template DNA	100 ng	variable
Pfu DNA polymerase 2.5 U/µl	2.5 U	1 µl

Cycling conditions:

Step	*Temperature*	*Time*	
Initial denaturation	95°C	3 min	
Hot start	80°C	1 min	*Pfu* DNA polymerase was added.
Denaturation	95°C	20 sec	25 - 30 cycles
Annealing	variable[A]	20 sec	
Extension	72°C	variable[B]	
Final Extension	72°C	20 min	
Cool down	12°C	unlimited	

[A] usually primer T_m - 5°C, as standard was used 55°C; [B] n [min] = size of insert [kb] x 1.5 plus increments of 1 sec per cycle.

The amplified DNA was separated by agarose gel electrophoresis and analysed under UV. For further processing, DNA of appropriate size was cut out and extracted using QIAquick Gel Extraction Kit according to manufacturer`s instructions. For directional cloning into the plasmid vector, the purified fragment (insert) and the vector were digested with the appropriate restriction enzymes. Then, purified and digested insert and vector were ligated at a molar ratio of insert:vector of 3:1 using Quick T4 DNA Ligase according to manufacturer`s instructions. Ligation products were transformed into ultra-competent *Escherichia coli* Top10 cells and grown overnight on LB-agar plates containing the appropriate antibiotic at 37°C. On the next day, transformed colonies were picked and grown in LB with antibiotic overnight at 37°C under vigorous shaking. The plasmid DNA was purified using NucleoSpin® Plasmid MiniPrep Kit according to manufacturer`s instructions. The presence of the amplified cloned fragment was confirmed by (i) digesting with restriction enzymes and analysis of the

restricted DNA by agarose gel electrophoresis and (ii) by DNA sequencing (MWG Biotech, Martinsried, Germany).

2.2.3 *In-vitro* mutagenesis

To create a mutation (truncation, deletion or point mutation) of any given DNA sequence, site-directed *in-vitro* mutagenesis was performed. For this purpose, target wild-type DNA was amplified by PCR using mutagenic primer pairs (see appendix, list of primers for mutagenesis) and *Pfu* DNA polymerase. The PCR product was digested with *DpnI* (Fermentas, St. Leon-Rot, Germany) for 1 h at 37°C. *DpnI* specifically cleaves methylated and thereby bacterially generated DNA used as template. *DpnI*-resistant DNA was transformed into *Escherichia coli* XL-10 Gold^{TM} by KCM method. In brief, to prepare competent *Escherichia coli* XL-10 Gold^{TM}, cells were grown in LB medium without antibiotic to an OD_{600} of 0.3 to 0.6 at 37°C under vigorous shaking. After short centrifugation, the bacterial pellet was resuspended in ice-cold TSB (LB medium with 10 % (v/v) polyethylene glycol, 5 % (v/v) DMSO, 20 mM Mg_2SO_4). Then, 80 µl of dH_2O, 20 µl of 5x KCM buffer (0.5 M KCl, 0.15 M $CaCl_2$, 0.25 M $MgCl_2$), 5 µl of *DpnI*-digested PCR product and 100 µl of competent *Escherichia coli* XL-10 Gold^{TM} were mixed and incubated on ice for 20 min, followed by further incubation for 10 min at RT. Then, 800 µl of LB medium were added and cells were shaken for 1 h at 37°C. Prior to plating on selective LB-agar with antibiotic, cells were centrifuged at 8000 rpm for 1 min. The supernatant was removed and cells were resuspended in 100 µl of LB medium. Cells were plated and grown overnight at 37°C. The desired mutation was verified by DNA sequencing (MWG Biotech, Martinsried, Germany).

2.3 Cell biological methods

2.3.1 Cell culture and transfection

COS-1 and HeLa cells were cultured in Dulbecco`s modified Eagle`s medium (DMEM) with 4500 mg/l glucose and L-glutamine. LNCaP cells were cultured in RPMI 1640 medium with L-glutamine. All media were supplemented with 10% fetal bovine serum (FBS) and 1% penicillin/streptomycin (PAA Laboratories, Pasching, Austria). Cells were kept at 37°C and ambient air containing 5 % CO_2. For cell splitting, trypsin-EDTA (1x) solution (PAA Laboratories, Pasching, Austria) was used. In brief, one 10 cm dish of confluent cells was washed once with 10 ml of PBS to remove residual medium and cell debris. Then, 2 ml of trypsin-EDTA were added and cells were incubated for up to 10 min at 37°C 5 % CO_2. In order to inactivate trypsin, the detached cells were mixed with a surplus of DMEM and then collected. An appropriate split ratio was calculated (generally 1:10 to 1:20) and cells were replated. The newly seeded cells were left undisturbed for at least 12 to 24 h.

Transient transfections of COS-1 cells were performed with DEAE-dextran. For this purpose, 6 x 10^5 cells counted with CASY cell counter (Innovatis, Bielefeld, Germany) were seeded per 10 cm dish. On the following day, cells were washed with PBS, and 8 to 10 µg of expression plasmids were applied in 5.7 ml of serum-free DMEM mixed with 300 µl of DEAE-dextran (1 mg/ml stock) and 12 µl of chloroquine (100 mM stock). After incubation for 3 h, the transfection mixture was removed and cells were cultured in DMEM with 10 % FBS for 24 to 48 h prior to use. HeLa and LNCaP cells were transiently transfected using Metafectene™ according to manufacturer`s instructions.

2.3.2 Platelet preparation

Washed platelets were obtained by sequential centrifugation. In brief, 20.8 ml freshly drawn venous blood from healthy volunteers who gave their informed consent according to the declaration of Helsinki was collected into 4.2 ml of prewarmed ACD buffer (85 mM sodium citrat, 65 mM citric acid, 100 mM glucose) and centrifuged at 200 *g* for 15 min without brake. Platelet rich plasma was removed and platelets were pelleted at 600 *g* for 15 min. The platelet pellet was then resuspended in prewarmed resuspension buffer (145 mM NaCl, 5 mM KCl, 1 mM $MgCl_2$, 10 mM HEPES, 10 mM glucose, pH 7.4) to a final concentration of approximately 1-3 x 10^8 platelets/ml counted with CASY cell counter (Innovatis, Bielefeld, Germany). The platelet suspension was incubated at 37°C for 30 min prior to use.

2.3.3. Cell lysis

Adherent COS-1 or HeLa cells were washed three times with ice-cold PBS and detached by scraping with a rubber policeman. Washed platelets or washed COS-1 or HeLa cells were lysed 10 min on ice with lysis buffer (50 mM Tris-HCl pH 7.5, 1% (v/v) Triton X-100, 150 mM NaCl, 5 mM $MgCl_2$), containing phosphatase inhibitors (1 mM Na_3VO_4, 50 mM NaF, 5 mM $Na_4P_2O_7$) and protease inhibitors (2 µg/µl aprotinin, 1 µg/µl leupeptin, 0.1 mM phenylmethylsylfonyl fluoride). In order to remove insoluble material, cell lysates were centrifuged at 14000 *g* 4°C for 20 min and cleared supernatants were collected for co-immunoprecipitation and pull-down experiments.

2.3.4 Immunofluorescence microscopy

HeLa cells were grown on glass coverslips (Falcon® culture slides, Becton Dickinson, USA) and transfected with expression vectors for EGFP-tagged Rab27a, VSV-tagged Rap1GAP2 and myc-tagged Slp1. 24 h post-transfection, cells were fixed with 3.7 % paraformaldehyde in PBS for 15 min on ice, washed with PBS and permeabilized with 0.2 % (v/v) Triton X-100 in PBS for 10 min at RT. To detect VSV-tagged Rap1GAP2 and myc-tagged Slp1, primary tag-specific antibodies, diluted with 1 % (w/v) BSA in PBS, were added and incubated for 1 h

at 37°C, followed by incubation with Cy5-conjugated anti-mouse IgG and Cy3-conjugated anti-rabbit IgG as secondary antibodies. After further washing with PBS and water, samples were mounted in GEL/Mount™ (Biomeda, Foster City, CA). Staining was observed using Zeiss LSM 510 confocal laser scanning microscope (Carl Zeiss, Göttingen, Germany).

2.4 Protein biochemical methods

2.4.1 Yeast transformation

Saccharomyces cerevisiae strain AH109 was retransformed with Rap1GAP2-Gal4BD and two positive clones of Slp1-Gal4AD (clone 27 and clone 87) obtained from the yeast-two-hybrid screening with full-length Rap1GAP2a as bait and a human adult brain cDNA library as prey (Hoffmeister et al. 2008). Transformation was carried out by lithium acetate/single stranded DNA/polyethylene glycol method according to Agatep and Gietz 1998. To select for co-transformants, transformed yeasts were grown on synthetic dropout (SD) agar medium lacking tryptophane and leucine (SD/-Trp/-Leu) at 30°C for two days. Grown colonies were transferred on agar plates containing SD medium without tryptophane, leucine, histidine and adenine (SD/-Trp/-Leu/-His/-Ade) and SD/-Trp/-Leu/-His/-Ade supplemented with 5-bromo-4-chloro-3-indoxyl-α-D-galactopyranoside (x-α-Gal). After two days, yeasts were analyzed for survival and α-galactosidase activity or blue coloration, respectively.

2.4.2 Expression and purification of GST fusion proteins

To produce recombinant glutathione-S-transferase (GST) fusion protein of Slp1, full-size cDNA of Slp1 was subcloned into EcoRI and XhoI sites of the prokaryotic expression vector pGEX-4T-3. For GST-14-3-3β protein production, full-size cDNA of 14-3-3β was subcloned in pGEX-4T-3 as described in Hoffmeister et al. 2008. *Escherichia coli* strain BL21 (DE3) was transformed with 50 ng of the appropriate plasmid by heat shock and a starter culture of 25 ml LB medium with 100 µg/ml ampicillin (LB/ampicillin) was grown overnight at 37°C. On the next day, the confluent culture was diluted 20 times with LB/ampicillin (500 ml total) and grown to an OD_{600} of 0.9 at 37°C under vigorous shaking. Protein expression was induced with 0.1 mM isopropyl-β-D-1-thiogalactopyranoside (IPTG) and bacteria were grown overnight at 16°C. On the following day, cells were harvested by centrifugation at 5500 rpm 4°C for 10 min in a Beckman JA-10 rotor (Avanti™ J-30I centrifuge, Beckman Coulter). The bacterial pellet was resuspended in 5 ml of ice-cold lysis buffer (50 mM HEPES pH 7.5, 150 mM NaCl, 1 mM EDTA, 5 % (v/v) glycerol, 0.1 % (v/v) Nonidet P40), containing the complete protease inhibitor cocktail (Roche, Mannheim, Germany). Bacterial walls were disrupted by sonication for 10 sec three times each. To obtain clear bacterial lysate, the bacterial cell

suspension was centrifuged at 16000 rpm 4°C for 30 min in a Beckman JA-30.50 rotor (Avanti^{TM} J-30 centrifuge, Beckman Coulter). Meanwhile, glutathione (GSH) sepharose beads were prepared by washing of 250 µl of GSH sepharose twice with ice-cold PBS and once with lysis buffer. Beads were centrifuged in a swinging bucket rotor at 500 *g* 4°C for 5 min (Eppendorf Centrifuge 5810R). The prewashed beads were incubated with clear bacterial lysate for 1 h at 4°C under gentle rotation, centrifuged and washed extensively three times with ice-cold lysis buffer, three times with PBS containing 0.1 % (v/v) Triton X-100, and three times with PBS. Washed beads were resuspended in 250 µl of PBS supplemented with 5 % (v/v) glycerol, aliquoted, frozen and stored at -20°C. Alternatively, in order to obtain free GST-Slp1 protein, beads were incubated with 2.5 ml of elution buffer (50 mM Tris-HCl pH 8.0, 10 mM glutathione) overnight at 4°C, followed by buffer exchange and protein concentration using Amicon® Ultra 50K centrifugal filter devices.

2.4.3 Expression and purification of His_6-tagged proteins

For recombinant hexa-histidine (His_6)-tagged protein production in *Escherichia coli*, full-size cDNA of Slp1 and the coding sequence of amino acids 1-167 of Rap1b were subcloned into the prokaryotic expression vector pET28. The plasmids were transformed into *Escherichia coli* BL21 and a starter culture of 10 ml LB medium with 30 µg/ml kanamycin (LB/kanamycin) was grown overnight at 37°C. On the next day, the confluent culture was diluted 50 times with LB/kanamycin (500 ml total) and grown to an OD_{600} of 0.6 at 37 °C under vigorous shaking. Protein expression was induced with 0.4 mM IPTG and bacteria were grown for 3 h at 37°C. Cells were harvested, as mentioned in *2.4.2,* and lysed in 5 ml of ice-cold lysis buffer (50 mM NaH_2PO_4-NaOH pH 8.0, 300 mM NaCl) containing protease inhibitors, followed by sonication. Clear bacterial lysate was obtained by centrifugation as described in *2.4.2*. To purify His_6-tagged proteins from the lysate, nickel-nitrilotriacetic acid-agarose (Ni-NTA) was used. His_6-tagged Slp1 was purified in batch mode, whereas His_6-tagged Rap1b was purified via HisTrap HP column (GE Healthcare) using an ÄKTA-system (J. Babica, IBCII, Frankfurt, Germany). For batch purification of His_6-Slp1, 1 ml Ni-NTA suspension was prewashed with ice-cold lysis buffer and subsequently incubated with clear bacterial lysate for 1 h at 4°C on a rotator. Once bound with protein, the resin was centrifuged at 4000 rpm 4°C for 2 min in a swinging bucket rotor (Eppendorf Centrifuge 5810R). The spent lysate was poured off. Washing was performed by resuspension of Ni-NTA in wash buffer (50 mM NaH_2PO_4-NaOH pH 8.0, 300 mM NaCl, 20 mM imidazole) and subsequent centrifugation. The bound His_6-Slp1 protein was eluted sequentially four times with 250 µl of elution buffer (50 mM NaH_2PO_4-NaOH pH 8.0, 300 mM NaCl, 250 mM imidazole). The eluted protein was then collected and combined. Imidazole-containing elution buffer was exchanged by PBS by

using PD-10 desalting columns according to manufacturer`s instructions, followed by concentration of protein with Amicon® Ultra centrifugal filter devices.

Recombinant His_6-tagged Rap1GAP2 wild-type and Rap1GAP2Δ522-527 mutant were affinity purified from COS-1 cells. Briefly, one hundred 10 cm dishes of COS-1 cells were transiently transfected with the appropriate plasmids. 48 h post-transfection, cells were lysed with lysis buffer (50 mM NaH_2PO_4-NaOH pH 8.0, 300 mM NaCl, 1% (v/v) Triton X-100) containing protease inhibitors, and His_6-tagged proteins were affinity purified using Ni-NTA agarose, as described before for His_6-Slp1 batch purification. The purity of all proteins was examined by SDS-PAGE followed by Coomassie Brilliant Blue staining. The concentration was determined by Bradford method (Bio-Rad) and from intensities of the bands in Coomassie Brilliant Blue-stained gels using BSA as standard.

2.4.4 SDS-PAGE and immunoblotting

SDS polyacrylamide gel electrophoresis was used to electrophoretically separate proteins according to their molecular weight and was carried out in vertical gels using Mighty Small II unit (GE Healthcare) and buffers listed under *2.1.8*. Separated proteins were either stained with Coomassie Brilliant Blue or electrophoretically transferred from the gel to a nitrocellulose membrane using the semi-dry transfer unit Fastblot B44 (Whatman Biometra, Göttingen, Germany). Prior to immunoblotting, protein transfer was confirmed by staining the nitrocellulose membrane with Ponceau S staining solution. After short destaining with TBS-T, the membrane was blocked in 5 % (w/v) BSA/TBS-T for 1 h at RT, followed by further incubation with the primary antibody, diluted in 5 % (w/v) BSA/TBS-T, for 1 h at RT or 4°C overnight. After subsequent three rinses with TBS-T, the membrane was incubated with HRP-coupled secondary antibody for 1 h at RT and again washed three times with TBS-T. To detect the HRP signal, two different ECL solutions were used: the ECL™ WB detection reagent from Amersham Biosciences showed good results for strong signals, whereas Immobilon™ WB detection reagent from Millipore proved to be better for weak HRP signals

2.4.5 Immunoprecipitation and pull-down assays

Proteins were immunoprecipitated from 500 µl of lysate by addition of 5 µl of ANTI-FLAG M2 affinity gel (Sigma, Taufkirchen, Germany) or other protein- or tag-specific antibody at 4°C for 4 h or overnight. In case of immunoprecipitation with protein- or tag-specific antibodies, 7 µl of protein A/G plus agarose (Santa Cruz Biotechnology) were added to precipitate the immunocomplex. In pull-down experiments, 1 µl or 5 µl of GSH sepharose, saturated with GST, GST-Slp1 or GST-14-3-3β, respectively, were added to platelet or cellular lysate and incubated at 4°C for 4 h or overnight. After incubation, beads were washed three times with lysis buffer before adding 15 µl of 3x SDS electrophoresis loading buffer and boiling for 5

min. Bound proteins were separated by SDS-PAGE, transferred to a nitrocellulose membrane and visualized by immunoblotting using specific antibodies.

2.4.6 Antibody production

To detect Slp1, a polyclonal antibody against Slp1 was produced using full-length recombinant glutathione-S-transferase-tagged Slp1 purified from *Escherichia coli* BL21 as antigen. Immunization of rabbits and subsequent purification were performed by ImmunoGlobe Antikörpertechnik (Himmelstadt, Germany).

2.4.7 Phospholipid binding assay (PIPStrip)

PIP Strips™ (Echelon Biosciences, Salt Lake City, USA) spotted with 100 pmol of various lipids were blocked with 3 % (w/v) fatty-acid free BSA/TBS-T and incubated with 0.5 µg/ml purified recombinant proteins in TBS-T for 3 h at RT. The membranes were washed three times with TBS-T, incubated with either anti-GST antibody or anti-His_6 antibody in 3 % (w/v) fatty-acid free BSA/TBS-T for 1 h at RT, washed three times with TBS-T and incubated with HRP-coupled goat anti-mouse IgG diluted 1:20000 in 3 % (w/v) fatty-acid free BSA/TBS-T for 1 h at RT. After washing with TBS-T, bound proteins were detected using ECL™ WB detection reagent (Amersham Biosciences).

2.4.8 Peptide binding assay (PepSpot)

Synthetic peptides with either wild-type Rap1GAP2 sequence HNSMEVTKTTFSPP (amino acids 518-531 of Rap1GAP2a) or with one amino acid mutated to alanine or single threonines phosphorylated were synthesized on cellulose membrane (ImmunoGlobe Antikörpertechnik) and incubated with 1 µg/ml of purified recombinant GST-Slp1 in 5 % (w/v) BSA/TBS-T for 3 h at RT. Bound GST-Slp1 was visualized by immunoblotting using anti-GST antibody.

2.4.9 *In-vitro* phosphorylation

COS-1 cells were transiently transfected with myc-tagged wild-type Slp1 and mutants of Slp1 having serine-to-alanine mutations of serine 117 and serine 311. 48 h post-transfection, cells were lysed in lysis buffer, as described in *2.3.3*, and proteins were immunoprecipitated with anti-myc antibody (9E10) and protein A/G plus sepharose. Precipitated proteins were washed and transferred into 20 µl of kinase buffer (30 mM Tris-HCl pH 7.5, 0.1 mM EGTA, 2 mM $MgCl_2$) supplemented with 0.1 % (v/v) β-mercaptoethanol and without or with the catalytic subunit of PKA at a final concentration of 20 ng/µl. In parallel, 50 µl of cold ATP (200 nM stock) and 1 µl of γ-[^{32}P] ATP (10 µCi/µl, obtained from Hartmann Analytic,

Braunschweig, Germany) were carefully mixed, and 5 µl of this mixture were used to start the phosphorylation reaction. Proteins were phosphorylated for 10 min at 30°C. The reaction was stopped by addition of 12.5 µl of 3x SDS electrophoresis loading buffer and boiling for 5 min. Samples were subjected to SDS-PAGE and transferred to a nitrocellulose membrane. ^{32}P incorporation was detected by autoradiography. Slp1 expression was analyzed by immunoblotting using anti-myc antibody.

2.4.10 Affinity chromatography

Affinity chromatography was performed using 1 ml HiTrap™ NHS-activated HP columns (GE Healthcare, Freiburg, Germany) and a peristaltic pump P-1 (Pharmacia). As ligand up to 8 mg/ml of purified recombinant His_6-tagged Slp1 protein in coupling buffer (0.2 M $NaHCO_3$, 0.5 M NaCl, pH 8.3) were covalently coupled to the NHS-activated sepharose according to manufacturer`s instructions. As negative control, HiTrap™ NHS-activated HP column without ligand was prepared and treated identically. As source for interacting proteins, lysate of washed human platelets prepared from 100 ml freshly drawn venous blood was used. Prior to administration onto the column, platelet lysate was adjusted to the composition of the binding buffer (50 mM Tris pH 7.5, 150 mM NaCl) by buffer exchange using PD10 desalting columns. Lysate was filtered through a 0.45 µm filter and applied onto the column with a flow rate of 0.2 ml/min according to manufacturer`s instructions. After washing with 20 ml of binding buffer, bound proteins were eluted with 3 ml of elution buffer (0.1 M glycine pH 3.0) and collected in 6 fractions to 500 µl. Each fraction was concentrated with Amicon® Ultra-4 10K centrifugal filter devices, mixed with 3x SDS electrophoresis loading buffer, boiled and separated by SDS-PAGE followed by Coomassie Brilliant Blue staining. Protein bands of different molecular weight ranging from 16 to 100 kD were finally excised and analyzed by tryptic digest and mass spectrometry (Dr. Guiliano Elia, Conway Institute for Biomolecular and Biomedical Research, Dublin, Ireland).

2.5 Other methods

2.5.1 *In-vitro* GAP assay

For GTP loading, 25 µM His_6-Rap1b was incubated with 125 nM [^{32}P]GTP (800 Ci/mmol, 10 µM/µl, obtained from Hartmann Analytic, Braunschweig, Germany) in the presence of 25 µM GTP, 10 mM EDTA, 1 mM DTE, and 30 mM Tris-HCl pH 7.5 for 1 h at RT. The exchange reaction was stopped by adding 20 mM of $MgCl_2$. The non-incorporated nucleotides were removed by gel filtration using NAP-5 columns (GE Healthcare). FLAG-tagged Slp1 and Rap1GAP2 proteins were purified from transfected HeLa cells using ANTI-FLAG M2 affinity gel (Sigma). Precipitated proteins were incubated with purified [^{32}P] GTP-loaded His_6-Rap1b

in a buffer containing 30 mM Tris-HCl pH 7.5, 5 mM $MgCl_2$ and 1 mM DTE in 50 µl aliquots at 25°C. After different time points, 5 µl aliquots were removed and mixed with 395 µl of ice-cold 5 % (w/v) charcoal suspension in 20 mM phosphoric acid. After centrifugation at 12000 rpm 4°C for 10 min, 200 µl of supernatants were removed, mixed with 2 ml of scintillation fluid and counted (TRI-CARB 2900 TR liquid scintillation analyzer plus QuantaSmart™ software, Perkin Elmer, Fremont, USA).

2.5.2 Cell adhesion assay

96 well plates were coated overnight at 4°C with 20 µg/ml fibronectin in PBS, washed with PBS, and blocked for 1 h at RT with 0.5 % (w/v) BSA in PBS. After washing, 50 µl of DMEM containing 10% (v/v) FBS were added per well. HeLa cells were transiently transfected with pRluc-N3 (BioSignal Packard), either alone or in combination with Rap1GAP2-FLAG or Rap1GAP2-FLAG and Slp1-myc. Cells were washed, detached with 0.05 % (w/v) EDTA in PBS, spun down, resuspended in DMEM containing 10 % (v/v) FBS, counted using Neubauer counting chamber and finally diluted to a concentration of 2 x 10^5 cells/ml. 50 µl of cell suspension were added per well of the previously prepared 96 well plate. After a short spinning down for 1 min at 10 *g*, cells were allowed to adhere for 50 min at 37°C. Non-adherent cells were removed by washing with prewarmed 0.5 % (w/v) BSA in PBS. Adherent cells were lysed and subjected to luciferase assay using *Renilla* luciferase assay system according to manufacturer`s instructions (Promega, Mannheim, Germany). Expression levels of transfected constructs were examined by immunoblotting. Numbers of bound cells were calculated and corrected for transfection efficiency by measuring luciferase activity of total input cells.

2.5.3 Prostate-specific antigen secretion assay

LNCaP cells were cultured as described in *2.3.1*. Prior to transfection, cells were seeded in six well plates at 3 x 10^5 cells/ml and left undisturbed for 12-24 h. Cells were transiently transfected with 2 µg of the indicated expression plasmids with Metafectene™ according to manufacturer`s instructions. 12 h post-transfection, medium was replaced with fresh RPMI 1640 containing 100 nM 6α-fluorotestosterone or DMSO as control. Cells were incubated for additional 36 h at 37°C in 5 % CO_2. Then, cell medium was collected and stored at -20°C before analysis. The concentration of secreted prostate-specific antigen (PSA) in the medium was measured using PSA ELISA kit as described by the manufacturer (Diagnostic Systems Laboratories, Sinsheim, Germany). Cells were washed with PBS, trypsinized, counted and diluted to a concentration of 2 x 10^5 cells/ml. For protein expression analysis, cells were lysed in hot 3x SDS electrophoresis loading buffer and boiled for 5 min. Proteins were

separated by SDS-PAGE, transferred onto a nitrocellulose membrane and subjected to immunoblotting using tag-specific antibodies.

2.5.4 Serotonin secretion of intact platelets

Serotonin (5-hydroxytryptamine, 5HT) forms a fluorophore with *ortho*-phthalaldehyde, which was detected by measuring the fluorescence emission at 475 nm using Wallac Victor 1420 Multilabel Counter according to Holmsen and Dangelmaier 1989. To inhibit serotonin reuptake during secretion, 4 µM of fluoxetine hydrochloride, a selective serotonin reuptake inhibitor, were added to 300 µl of platelet suspension (approximately 1-3 x 10^8 platelets/ml, counted with CASY cell counter, Innovatis, Bielefeld, Germany). To induce serotonin secretion, washed platelets were either treated with thrombin at different concentrations for 5 min at 37°C, or pretreated with 10 µM of forskolin for 20 min or 1 µM of sodium nitroprusside (SNP) for 5 min at 37°C, followed by thrombin treatment as indicated. The secretion reaction was stopped by addition of 30 µl of ice-cold 50 mM EDTA pH 7.4. Samples were mixed, centrifuged (except for the totals) and put on ice. For protein precipitation, 270 µl of supernatants and totals were transferred to Eppendorf tubes containing 60 µl of ice-cold 6 M trichloroacetic acid (TCA), vortexed and centrifuged. 250 µl aliquots of these TCA extracts were added to 1 ml of *ortho*-phthalaldehyde reagent (0.5 % (w/v) *ortho*-phthalaldehyde in ethanol mixed with 10 volumes of 8 N HCl), boiled for 10 min and cooled on ice. Samples and totals were transferred into 15 ml Falcon tubes and washed twice with chloroform by vigorous vortexing 10 sec each. Fluorescence emission of the upper phase was measured as described above. For assay validation, serotonin creatinine sulphate, dissolved to 1 mM in 1 N HCl, was used as standard. Working solutions ranging from 0 to 5 µM were prepared in dH_2O and processed as described above, starting with TCA protein precipitation. Blank values were subtracted from all readings.

2.5.5 Serotonin secretion of permeabilized platelets

Freshly obtained washed platelets (1 x 10^8 platelets/ml, counted with CASY cell counter, Innovatis, Bielefeld, Germany) were resuspended in 70 µl of prewarmed buffer A (50 mM HEPES-KOH pH 7.4, 78 mM KCl, 4 mM $MgCl_2$, 2 mM EGTA, 0.2 mM $CaCl_2$, 5 mM DTT), containing 4 mg/ml BSA, 5 mM ATP, 8 mM creatine phosphate, 50 µg/ml creatine phosphokinase. Platelets were permeabilized using 0.6 µg/ml streptolysin-O in buffer A containing 4 mg/ml BSA at 30°C for 5 min. Then, permeabilized platelets were placed on ice and incubated with proteins or peptides to be tested for additional 40 min, followed by further incubation at 30°C for 5 min. Finally, platelets were stimulated with either 10 µl of prewarmed buffer A, where the free calcium ion concentration was calculated to approximately 20 nM, or 10 µl of prewarmed stimulation buffer (50 mM HEPES-KOH pH 7.4, 78 mM KCl, 4 mM

$MgCl_2$, 2mM EGTA, 20 mM $CaCl_2$), which results in 20 µM of free calcium, at 30°C for 1 min. In case of guanosine 5`-O-[γ-thio] triphosphate (GTPγS)-induced secretion of dense granules, platelets were stimulated with 100 µM of GTPγS at 30°C for 5 min. The reaction was stopped by addition of 200 µl of 2-fold concentrated ice-cold stop buffer (100 mM HEPES-KOH pH 7.4, 156 mM KCl, 8 mM $MgCl_2$, 18 mM EGTA, 0.4 mM $CaCl_2$) and incubation on ice for 5 min. Then, platelets were removed (except for totals) by centrifugation at 4°C 5000 *g* for 5 min, and released serotonin in the supernatant was measured as described in *2.5.4*. In all cases, the secretion levels of serotonin were expressed as percentage of total serotonin stored in platelet dense granules. Permeabilization was monitored by immunoblotting of platelet total lysates and supernatants using anti-LDH antibody.

2.5.6 Statistical analysis

Shown data represent means ± SD of at least three independent experiments performed in triplicate. The statistical significance of the means was analyzed by Student`s *t* test using SigmaPlot 8.0. *P*-values are expressed as follows * $p < 0.05$, ** $p < 0.01$, *** $p < 0.001$ and considered as statistically significant. All experiments (e.g. co-immunoprecipitation and pull-down assays) were conducted at least three times.

3. RESULTS

3.1 Verification of Slp1 as new interaction partner of Rap1GAP2

3.1.1 Slp1 is a new binding partner of Rap1GAP2

To identify Rap1GAP2-associated proteins, a genetic two-hybrid screening in yeast was performed (O. Danielewski and A. Smolenski, IBCII, Frankfurt, Germany). Full-length wild-type Rap1GAP2a, the predominant splice isoform of Rap1GAP2 in platelets, was subcloned into the pGBKT7 vector, generating a fusion protein between Rap1GAP2 and the DNA binding domain (BD) of the yeast transcription factor Gal4, and was used as bait (1. hybrid). Likewise, a human adult brain cDNA library was constructed into the pACT2 prey vector to generate fusions of the various proteins encoded by the library cDNAs and the Gal4 transcriptional activation domain (AD) (2. hybrid). The bait vector and 3.5 x 10^6 cfu of the library were introduced into the yeast reporter strain AH109 and a high-stringency screening was carried out as described by the manufacturer. Yeasts were grown on synthetic dropout (SD) media and selected by proliferation (nutritional selection for *TRP, LEU, HIS3* and *ADE2*). Among the 112 positive library clones that were found to interact in the screening, two clones were identified as synaptotagmin-like protein 1 (Slp1, also called JFC1) (clones 27 and 87, accession numbers NP_116261 or BC035725).

To confirm the two-hybrid interaction between Rap1GAP2 and Slp1, Rap1GAP2-Gal4BD and Gal4BD as negative control were co-transformed together with the prey plasmids of clone 27 and clone 87 into AH109, and yeasts were assayed for growth and α-galactosidase activity (Fig.3.1). After initial selection for co-transformants on SD/-Trp/-Leu agar plates, yeasts were transferred on SD/-Trp/-Leu/-His/-Ade agar to select for co-transformants that host a positive two-hybrid interaction of Rap1GAP2 and Slp1. If Rap1GAP2 and Slp1 interact, the Gal4BD was brought into proximity to Gal4AD. Subsequently, the Gal4 transcription factor was reconstituted and activated the transcription of the reporter genes *HIS3, ADE2 and MEL1*. *HIS3* and *ADE2* encode the amino acids histidine and adenine, thereby enabling yeasts to produce and survive in absence of these amino acids. These yeasts were selected by growth on SD/-Trp/-Leu/-His/-Ade agar plates (Fig.3.1, *left panel*). In contrast, the gene product of *MEL1* is α-galactosidase. α-Galactosidase cleaves x-α-Gal, yielding α-D-galactose and 5-bromo-4-chloro-3-hydroxyindole which in turn is oxidized into the blue pigment 5,5'-dibromo-4,4'-dichloro-indigo. To select for α-galactosidase activity, transformed yeasts were grown on SD/-Trp/-Leu/-His/-Ade agar plates supplemented with x-α-Gal. If Rap1GAP2 and Slp1 interact, yeast colonies turned blue (Fig.3.1, *right panel*). In contrast, yeasts transformed with the empty bait vector pGBKT7 (Gal4BD) and prey vector pACT2 of Slp1 clone 27 did not survive on SD/-Trp/-Leu/-His/-Ade agar plates, indicating that absence of Rap1GAP2 as

binding partner of Slp1 results in physically separated Gal4BD and Gal4AD. In conclusion, yeast-two-hybrid screening revealed Slp1 as a new putative interaction partner of Rap1GAP2 and the interaction between Rap1GAP2 and Slp1 was confirmed by yeast retransformation and x-α-Gal staining.

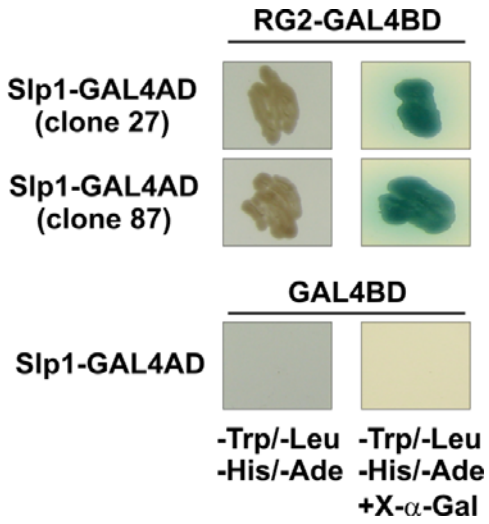

Figure 3.1: Rap1GAP2 and Slp1 associate in yeast. AH109 yeasts were co-transformed with Rap1GAP2-Gal4BD (RG2-Gal4BD) and Slp1-Gal4AD clone 27 and clone 87, respectively. As negative control, Slp1-Gal4AD clone 27 was co-transformed with empty vector pGBKT7 expressing Gal4BD. Transformed yeasts were analyzed for growth on SD/-Trp/-Leu/-His/-Ade agar plates (*left panel*) and x-α-galactosidase activity on SD/-Trp/-Leu/-His/-Ade supplemented with x-α-Gal (*right panel*).

3.1.2 Rap1GAP2 and Slp1 interact in transfected mammalian cells

To confirm the Rap1GAP2/Slp1 interaction outside the yeast-two-hybrid system, pull-down assays were performed. For this purpose, HeLa cells were transiently transfected with FLAG-tagged Rap1GAP2. 24 h post-transfection, cells were lysed, and lysates were subjected to pull-down assays using equal amounts of purified recombinant full-length Slp1 fused to GST and GST as control. The precipitates were analyzed for the presence of bound FLAG-tagged Rap1GAP2 by immunoblot using anti-FLAG antibody. As shown in Fig.3.2A, GST-Slp1 was clearly able to pull down transfected Rap1GAP2 from cell lysates, whereas GST alone did not. To verify that Rap1GAP2 and Slp1 interact also in intact mammalian cells, co-immunoprecipitation experiments were performed. HeLa cells were transfected with FLAG-tagged Rap1GAP2 and myc-tagged Slp1 either alone or in combination. On the next day, cells were lysed, and Rap1GAP2 was immunoprecipitated with anti-FLAG antibody. The precipitates were analyzed for the presence of bound myc-tagged Slp1 by immunoblotting using anti-myc antibody. As shown in Fig.3.2B, Slp1 was only present in precipitates from cells overexpressing both, Slp1 and Rap1GAP2. This result was further confirmed in a reverse co-immunoprecipitation experiment using anti-myc antibody (Fig.3.2C). All experiments were also carried out using transfected COS-1 cells, yielding the same results (data not shown).

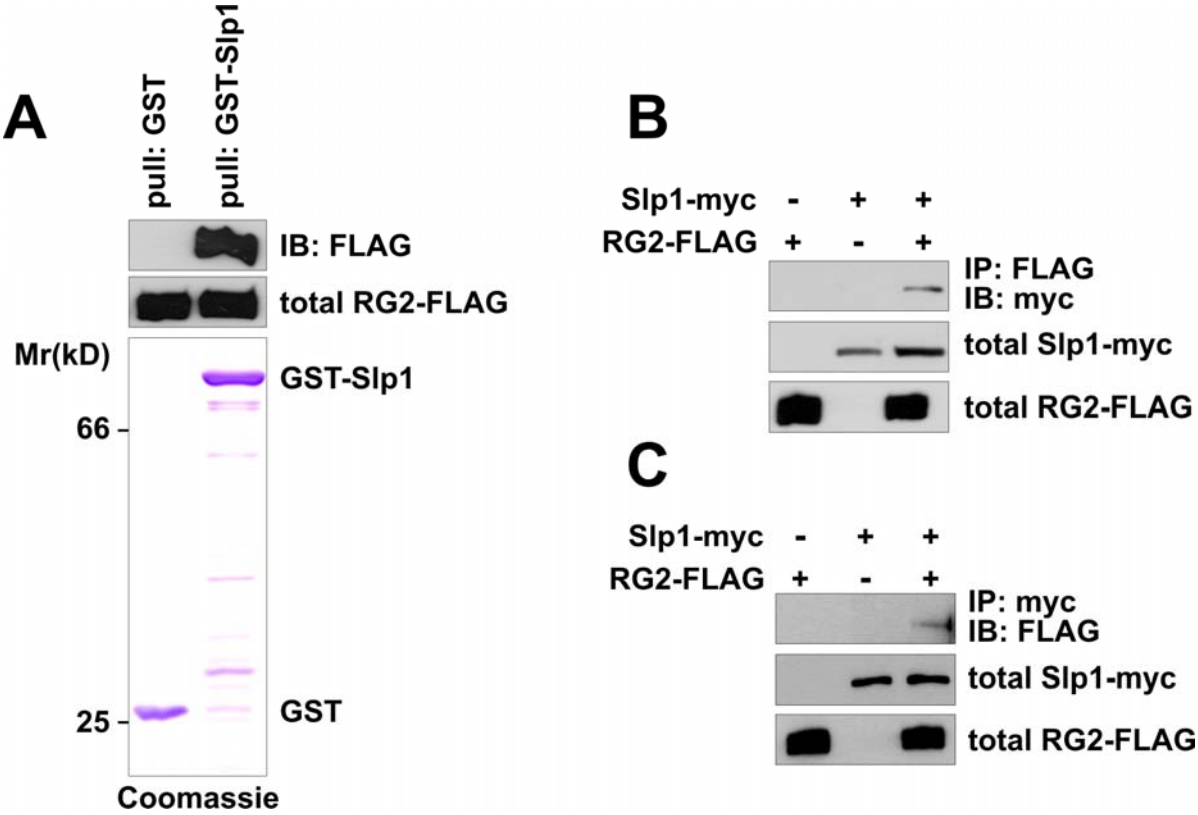

Figure 3.2: Rap1GAP2 interacts with Slp1 in transfected HeLa cells.
A: Pull-down of transfected Rap1GAP2 with GST-Slp1. HeLa cells were transiently transfected with FLAG-tagged Rap1GAP2 (RG2-FLAG). Equal amounts of GST as control and GST-Slp1 coupled to GSH sepharose beads were used for precipitation (*lower panel*). Bound Rap1GAP2 protein was visualized by immunoblot using anti-FLAG antibody (*upper panel*). The *middle panel* shows expression levels of Rap1GAP2 (total RG2-FLAG, 2% input). The broad band of Rap1GAP2 is probably due to extensive post-translational modifications.
B and **C:** Co-immunoprecipitation of transfected Rap1GAP2 and Slp1. HeLa cells were transiently transfected with FLAG-tagged Rap1GAP2, myc-tagged Slp1 or FLAG-tagged Rap1GAP2 together with myc-tagged Slp1. After cell lysis, Rap1GAP2 was immunoprecipitated with anti-FLAG antibody (B) and Slp1 with anti-myc antibody (C), respectively. The precipitates were analyzed for the presence of bound Slp1 (B, *upper panel*) or bound Rap1GAP2 (C, *upper panel*) by immunoblot using tag-specific antibodies. The *two lower panels* show expression levels of Slp1 (total Slp1-myc, 2% input) and Rap1GAP2 (total RG2-FLAG, 2% input).

Taken together, the interaction between Rap1GAP2 and Slp1 was confirmed by pull-down assays and co-immunoprecipitation experiments in transfected mammalian cells.

To investigate whether Slp1 also binds to other RapGAPs, Rap1GAP1 was tested. Rap1GAP1 is the closest relative of Rap1GAP2 with about 50 % overall identity at amino acid level (Schultess et al. 2005). HeLa cells were transiently transfected with HA-tagged Rap1GAP1, which was kindly provided by Prof. Dr. J. Bos, Utrecht, Netherlands. 24 h post-transfection, cells were lysed, and lysates were subjected to GST-Slp1 pull-down assays. As shown in Fig.3.3, no binding of GST-Slp1 to Rap1GAP1 was observed. The same result was also obtained in co-immunoprecipitation experiments using transfected HeLa cells (data not shown). In conclusion, Slp1 does not bind to Rap1GAP1, indicating that the interaction between Slp1 and Rap1GAP2 is specific.

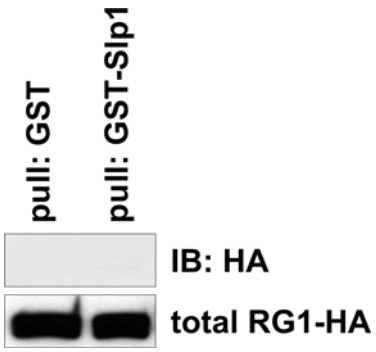

Figure 3.3: Rap1GAP1 does not bind to Slp1.
HeLa cells were transiently transfected with HA-tagged Rap1GAP1 (RG1-HA). Cells were lysed, and lysates were subjected to pull-down assays using equal amounts of GST as negative control and GST-Slp1. The precipitates were analyzed for the presence of bound Rap1GAP1 by immunoblot using anti-HA antibody (*upper panel*). The *lower panel* shows expression levels of Rap1GAP1 (total RG1-HA, 2% input).

3.1.3 Slp1 is expressed and binds to Rap1GAP2 in human platelets

Rap1GAP2 is the only GTPase activating protein of Rap1 expressed in human platelets (Schultess et al. 2005). To asses the interaction between Rap1GAP2 and Slp1 in a more physiological context, pull-down assays using human platelet lysate were performed. Washed human platelets were lysed as described under Materials and Methods (*2.3.3*), and platelet lysates were subjected to pull-down assays using equal amounts of GST and GST-Slp1. The precipitates were analyzed for the presence of endogenous Rap1GAP2 by immunoblot using anti-Rap1GAP2 antibody. As shown in Fig.3.4A, only GST-Slp1, but not GST, bound to endogenous Rap1GAP2 protein. So far, it was unknown if Slp1 is expressed in platelets. Endogenous expression of Slp1 in platelets, however, is a prerequisite for the association of both proteins, Rap1GAP2 and Slp1, at endogenous level and determines the physiological relevance of the Rap1GAP2/Slp1 interaction for platelet function. To check if Slp1 is present in platelets, a polyclonal antibody against full-length human Slp1 was generated (IBCII, ImmunoGlobe Antikörpertechnik). The antibody specifically recognized the 66 kD Slp1 protein in HeLa cells transfected with myc-tagged Slp1, but not in mock-transfected cells (Fig.3.4B). Importantly, the antibody recognized a band of similar molecular weight in human platelet lysate, suggesting that Slp1 is endogenously expressed in human platelets (Fig.3.4C). Unfortunately, neither this newly generated anti-Slp1 antibody nor our anti-Rap1GAP2 antibody were able to immunoprecipitate their antigens efficiently from human platelet lysates. Therefore, in order to obtain conclusive evidence that endogenous Rap1GAP2 and Slp1 interact, an alternative precipitation approach was developed and applied as described in Hoffmeister et al. 2008.

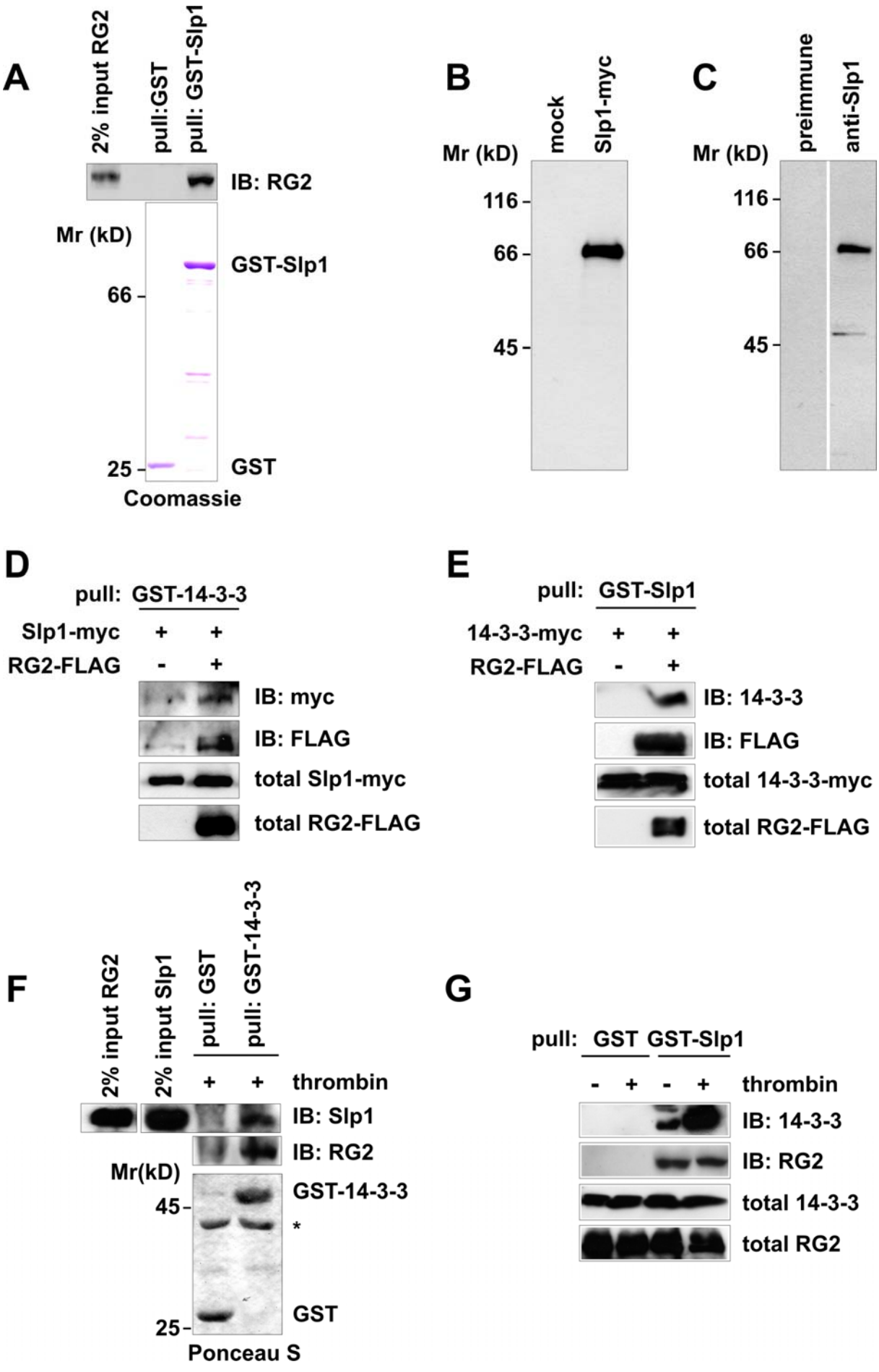
A
2% input RG2
pull:GST
pull: GST-Slp1
IB: RG2
Mr (kD)
GST-Slp1
66
25
GST
Coomassie
B
mock
Slp1-myc
Mr (kD)
116
66
45
C
preimmune
anti-Slp1
Mr (kD)
116
66
45
D
pull: GST-14-3-3
Slp1-myc + +
RG2-FLAG - +
IB: myc
IB: FLAG
total Slp1-myc
total RG2-FLAG
E
pull: GST-Slp1
14-3-3-myc + +
RG2-FLAG - +
IB: 14-3-3
IB: FLAG
total 14-3-3-myc
total RG2-FLAG
F
2% input RG2
2% input Slp1
pull: GST
pull: GST-14-3-3
+ + thrombin
IB: Slp1
IB: RG2
Mr(kD)
GST-14-3-3
45
*
25
GST
Ponceau S
G
pull: GST GST-Slp1
- + - + thrombin
IB: 14-3-3
IB: RG2
total 14-3-3
total RG2

Figure 3.4: Endogenous Rap1GAP2 and Slp1 interact in human platelets.
A: Pull-down of endogenous Rap1GAP2 with GST-Slp1. Equal amounts of GST as control and GST-Slp1 coupled to GSH sepharose beads were incubated with human platelet lysate. Bound endogenous Rap1GAP2 protein was visualized with anti-Rap1GAP2 antibody (RG2, *upper panel*). Expression level of Rap1GAP2 is shown as 2% input of total Rap1GAP2.
B: Anti-Slp1 antibody recognizes the 66 kD Slp1 protein in transfected HeLa cells. HeLa cells were transiently transfected with empty vector pcDNA3.1/mycHis (mock) or myc-tagged Slp1 (Slp1-myc). Cells were lysed, and lysates were analyzed by immunoblot using anti-Slp1 antibody.
C: Slp1 is expressed in human platelets. Washed human platelets were lysed, and lysates were analyzed by immunoblot using preimmune serum and anti-Slp1 antibody, respectively.
D: Pull-down of transfected Rap1GAP2 and Slp1 with GST-14-3-3β. COS-1 cells were transiently transfected with myc-tagged Slp1 and without or with FLAG-tagged Rap1GAP2 (RG2-FLAG). Cells were lysed, and GST fusion protein of 14-3-3β was used to precipitate Rap1GAP2 and indirectly Slp1 bound to Rap1GAP2. Precipitated Slp1 was detected by immunoblot using anti-myc antibody (*top panel*). Precipitation of Rap1GAP2 was controlled by immunoblot with anti-FLAG antibody (*second panel from top*). In parallel, total cell lysates were analyzed for the expression of Slp1 (total Slp1-myc, 2% input) and Rap1GAP2 (total RG2-FLAG, 2% input).
E: Pull-down of transfected Rap1GAP2 and 14-3-3β with GST-Slp1. COS-1 cells were transiently transfected with myc-tagged 14-3-3β and without or with FLAG-tagged Rap1GAP2 (RG2-FLAG). Cells were lysed, and GST fusion protein of Slp1 was used to precipitate Rap1GAP2 and indirectly 14-3-3β bound to Rap1GAP2. Precipitated 14-3-3β was detected by immunoblot using anti-14-3-3 antibody (*top panel*), and precipitated Rap1GAP2 using anti-FLAG antibody (*second panel from top*). The *two lower panels* show expression levels of 14-3-3β (total 14-3-3-myc, 2% input) and Rap1GAP2 (total RG2-FLAG, 2% input).
F: Pull-down of endogenous Rap1GAP2 and Slp1 from human platelets. Washed human platelets were treated with 0.1 U/ml thrombin for 1 min at 37°C. Platelets were lysed, and lysates were subjected to pull-down assays using equal amounts of GST as control and GST-14-3-3β. The precipitates were analyzed for the presence of endogenous Rap1GAP2 (RG2) and Slp1 using specific anti-Rap1GAP2 and anti-Slp1 antibodies (*first and second panel from top*). Expression levels of Rap1GAP2 and Slp1 are shown as 2% input of total protein amounts. The *lower panel* shows the amounts of GST and GST-14-3-3β used for precipitation. Unspecific band is marked with asterisk (*).
G: Pull-down of endogenous Rap1GAP2 and 14-3-3 from human platelets. Washed human platelets were treated with 0.1 U/ml thrombin for 1 min at 37°C as indicated. Platelets were lysed, and lysates were subjected to pull-down assays using equal amounts of GST as control and GST-Slp1. The precipitates were analyzed for the presence of endogenous 14-3-3 and Rap1GAP2 (RG2) by immunoblot with anti-14-3-3 and anti-Rap1GAP2 antibodies (*first and second panel from top*). The *two lower panels* show expression levels of 14-3-3 (total 14-3-3, 2% input) and Rap1GAP2 (total RG2, 2% input).

To this end, a second Rap1GAP2 binding partner, 14-3-3, was expressed and purified as GST fusion protein from *Escherichia coli* BL21 and used to precipitate sufficient amounts of endogenous Rap1GAP2. Binding of 14-3-3 proteins to Rap1GAP2 was discovered and characterized in our group. We could show that 14-3-3 proteins bind to Rap1GAP2 at phosphorylated serine 9 within the N-terminus of Rap1GAP2. Moreover, platelet activation by ADP and thrombin enhances serine 9 phosphorylation and thereby increases 14-3-3 binding to endogenous Rap1GAP2 (Hoffmeister et al. 2008). To exclude the possibility that 14-3-3 and Slp1, designated Rip2 in Hoffmeister et al. 2008, interact directly with each other, control experiments in COS-1 cells were performed. To mimic the endogenous situation in platelets, COS-1 cells were transiently transfected with myc-tagged Slp1 and FLAG-tagged Rap1GAP2. As control, cells were transfected with myc-tagged Slp1 only. After two days, cells were lysed, and GST-14-3-3 was used to pull down Rap1GAP2 and indirectly Slp1 that was associated with Rap1GAP2 in cells overexpressing both proteins. The precipitates were analyzed for the presence of FLAG-tagged Rap1GAP2 and myc-tagged Slp1 by immunoblot using tag-specific antibodies. As shown in Fig.3.4D, GST-14-3-3 precipitated Slp1 only in

presence of Rap1GAP2, demonstrating that 14-3-3 could not bind to Slp1 by itself. This result could further be confirmed in a reverse experiment using COS-1 cells transfected with myc-tagged 14-3-3 and with or without FLAG-tagged Rap1GAP2. Purified recombinant GST-Slp1 was used to pull down Rap1GAP2 and indirectly 14-3-3 associated with Rap1GAP2. As expected, precipitated 14-3-3 was only detected in precipitates from cells overexpressing both, Rap1GAP2 and 14-3-3 (Fig.3.4E). To show that Rap1GAP2 and Slp1 interact at endogenous level in human platelets, purified recombinant GST-14-3-3 was used to pull down endogenous Rap1GAP2 from platelet lysate. To induce serine 9 phosphorylation and thereby enhance binding of GST-14-3-3 to Rap1GAP2, platelets were treated with thrombin. As shown in Fig.3.4F, GST-14-3-3 was clearly able to pull down endogenous Rap1GAP2 and Slp1 bound to Rap1GAP2 from human platelets. In a reverse experiment, GST-Slp1 was used to pull down endogenous Rap1GAP2 from platelet lysate. As shown in Fig.3.4G, GST-Slp1 was able to co-precipitate endogenous 14-3-3 via Rap1GAP2, whereas GST alone did not bind Rap1GAP2 or 14-3-3. Thrombin treatment of platelets resulted in increased binding of 14-3-3 to Rap1GAP2 at endogenous level (Fig.3.4G, *top panel*). Taken together, these experiments confirm that the interaction between Rap1GAP2 and Slp1 is direct and show that both proteins interact at endogenous level in human platelets.

Slp1 is a member of the synaptotagmin-like protein (Slp) family, and to date, five distinct isoforms (Slp1-5) have been reported in mammals (Fukuda 2005). Database search (http://plateletweb.bioapps.biozentrum.uni-wuerzburg.de) revealed that among those, Slp4 is expressed in platelets, too. To test if Rap1GAP2 binds to Slp4 or other Slp isoforms (Slp2, Slp3 and Slp5), co-immunoprecipitation experiments were performed. No interaction between Rap1GAP2 and Slp2, Slp3, Slp4, and Slp5 was detected (data not shown).

3.2 Characterization of the Rap1GAP2/Slp1 interaction

3.2.1 The C2A domain of Slp1 is sufficient for binding to Rap1GAP2

Slp1 is composed of an N-terminal Rab27 binding domain (SHD) and two tandem C2 domains, C2A and C2B, at the C-terminus (Fukuda and Mikoshiba 2001, McAdara Berkowitz et al. 2001). From the yeast-two-hybrid screening the binding site for Rap1GAP2 within Slp1 was assumed to be located within the two C2 domains of Slp1. Both Slp1 clones that were found to interact with Rap1GAP2 in yeast matched the C-terminal part of Slp1 containing the two tandem C2 domains (amino acids 293-549 of Slp1). Therefore, to determine the binding site for Rap1GAP2 within Slp1, mutants composed of C2A, C2B or C2AB domain of Slp1 fused to GST were expressed and purified from *Escherichia coli* BL21 and used in pull-down assays (Fig.3.5A). In brief, HeLa cells were transfected with FLAG-tagged Rap1GAP2. After

cell lysis, equal amounts of GST as negative control, GST-C2A, GST-C2B, and GST-C2AB were used to precipitate transfected Rap1GAP2. The precipitates were analyzed for the presence of FLAG-tagged Rap1GAP2 by immunoblot using anti-FLAG antibody. As shown in Fig.3.5B, GST did not bind to Rap1GAP2. No binding was detected between GST-C2B and Rap1GAP2. In contrast, GST-C2A and GST-C2AB were able to pull down transfected Rap1GAP2 from HeLa cell lysates, indicating that the C2A domain is required and sufficient for binding of Slp1 to Rap1GAP2.

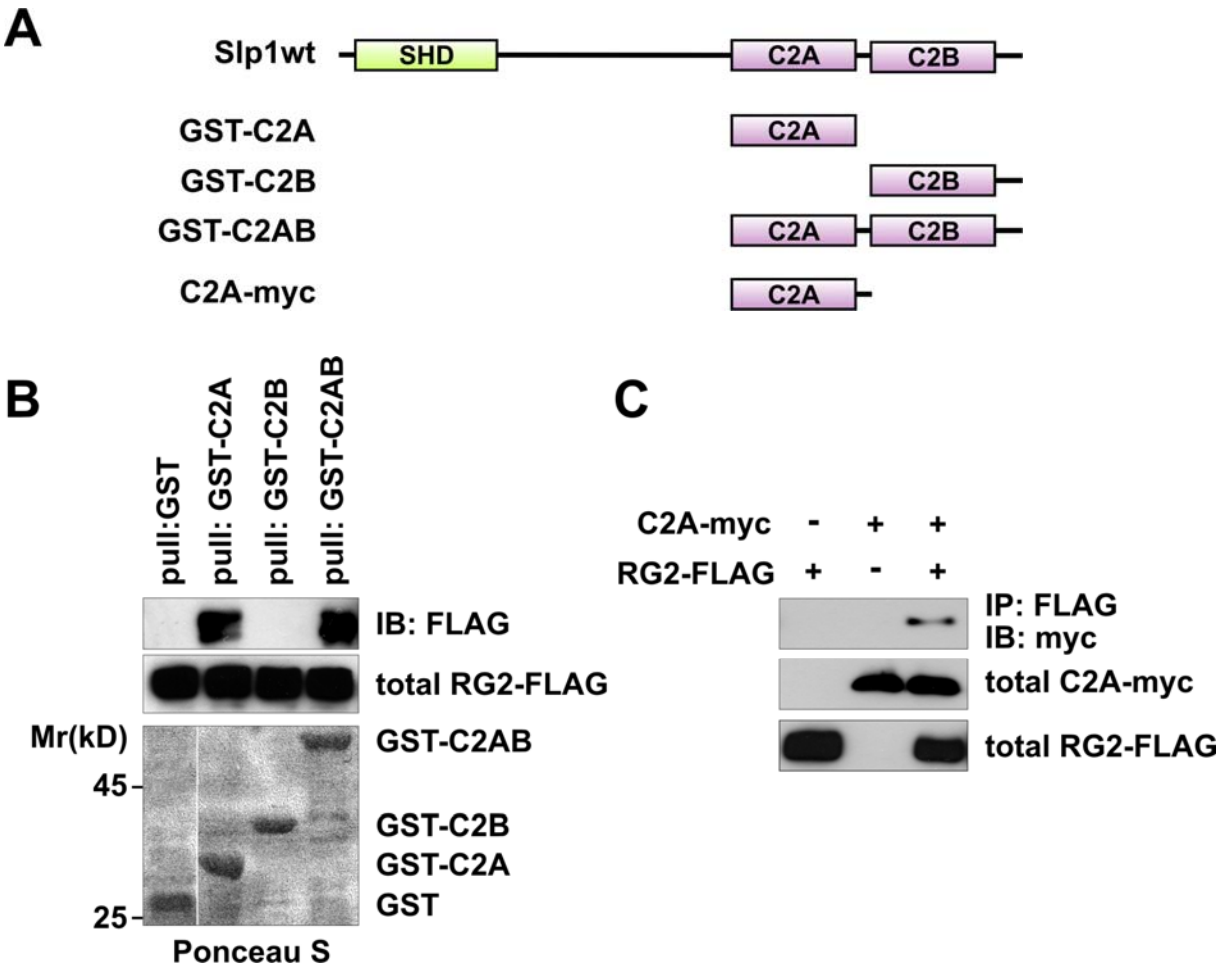

Figure 3.5: The C2A domain of Slp1 is sufficient for binding of Slp1 to Rap1GAP2.
A: Schematic representation of Slp1 mutants. GST fusion proteins of C2A (amino acids 292-393 of Slp1), C2B (amino acids 433-580 of Slp1) and C2AB (amino acids 292-580 of Slp1) were used in pull-down assays. Myc-tagged C2A (amino acids 292-432 of Slp1) was used in co-immunoprecipitation experiments.
B: Pull-down of transfected Rap1GAP2 with GST-Slp1 mutants. Lysates of HeLa cells overexpressing FLAG-tagged Rap1GAP2 (RG2-FLAG) were subjected to pull-down experiments using equal amounts of GST as control and GST fusion proteins of C2A, C2B and C2AB. The precipitates were analyzed for the presence of bound Rap1GAP2 by immunoblot with anti-FLAG antibody (*upper panel*). The *middle panel* shows expression levels of Rap1GAP2 (total RG2-FLAG, 2% input), and the *lower panel* GST and GST fusion proteins of Slp1 used for precipitation.
C: Co-immunoprecipitation of transfected Rap1GAP2 and Slp1-C2A. HeLa cells were transiently transfected with FLAG-tagged Rap1GAP2, myc-tagged C2A domain of Slp1 or FLAG-tagged Rap1GAP2 together with myc-tagged C2A. After cell lysis, Rap1GAP2 was immunoprecipitated with anti-FLAG antibody. Precipitated C2A was detected by immunoblot using anti-myc antibody (*upper panel*). The *two lower panels* show expression levels of C2A (total C2A-myc, 2% input) and Rap1GAP2 (total RG2-FLAG, 2% input).

This result was further confirmed in intact mammalian cells. In co-immunoprecipitation experiments using HeLa cells overexpressing FLAG-tagged Rap1GAP2 and myc-tagged C2A domain of Slp1, C2A was co-immunoprecipitated together with Rap1GAP2 using anti-FLAG antibody (Fig.3.5C).
Binding activities of some C2 domains are modulated by calcium ions (Lemmon 2008). However, the Rap1GAP2/Slp1 interaction was not affected by calcium depletion in pull-down assays (data not shown).

3.2.2 Binding of Rap1GAP2 does not affect lipid binding of Slp1

It has previously been reported that Slp1 binds via its C2A domain to phosphoinositides *in-vitro,* showing preference for PtdIns(3,4,5)P_3 over PtdIns(3)P, PtdIns(3,4)P_2, and PtdIns(4,5)P_2 (McAdara Berkowitz et al. 2001, Catz et al. 2002). In transfected mammalian cells the C2A domain of Slp1 has been shown to localize exclusively to the plasma membrane, suggesting that the C2A domain of Slp1 is responsible for the specific membrane association of the full-length Slp1 protein (Catz et al. 2002). This finding was confirmed in live imaging experiments of HeLa cells transfected with DsRed-tagged Slp1 C2A domain (Fig.3.6A). Moreover, in the present work the C2A domain of Slp1 has been demonstrated to serve as protein-protein interaction domain and to mediate binding of Slp1 to Rap1GAP2. These two observations raise the question whether Rap1GAP2 binding to the C2A domain of Slp1 could affect the lipid binding ability of Slp1 via C2A and thus targeting of Slp1 to the plasma membrane and its plasma membrane association. To answer this question, phospholipid binding assays were performed. To first test and compare the lipid binding ability of full-length Slp1 and the C2A domain of Slp1, purified recombinant GST-C2A and GST-Slp1 were used to probe nitrocellulose membranes spotted with various biologically active phospholipids (PIPs) as indicated (Fig.3.6B). GST-tagged PH domain of PLCδ1 was used as positive control (Echelon Biosciences), and GST was used as negative control. As shown in Fig.3.6C, both controls yielded expected results. PLCδ1 PH domain bound to PtdIns(4,5)P_2, whereas GST did not bind to any phospholipid. Importantly, GST-C2A and GST-Slp1 were able to bind to phospholipids, exhibiting a similar phosholipid binding pattern. The slight variations in binding intensities could be due to unintended variations in protein concentrations applied onto the membranes. Interestingly, both, GST-C2A and GST-Slp1 bound preferentially to phosphatidic acid (PA) followed by phosphatidylinositol-monophosphates PtdIns(3)P, PtdIns(4)P, PtdIns(5)P and phosphatidylinositolbisphosphates PtdIns(4,5)P_2 and PtdIns(3,4)P_2. Binding to PtdIns(3,5)P_2 and PtdIns(3,4,5)P_3 was apparent, but rather weak. To investigate next if binding of Rap1GAP2 to the C2A domain of Slp1 could affect phospholipid binding ability of Slp1, membranes were incubated with GST-Slp1 either alone or together with purified recombinant His_6-tagged Rap1GAP2. To evaluate whether

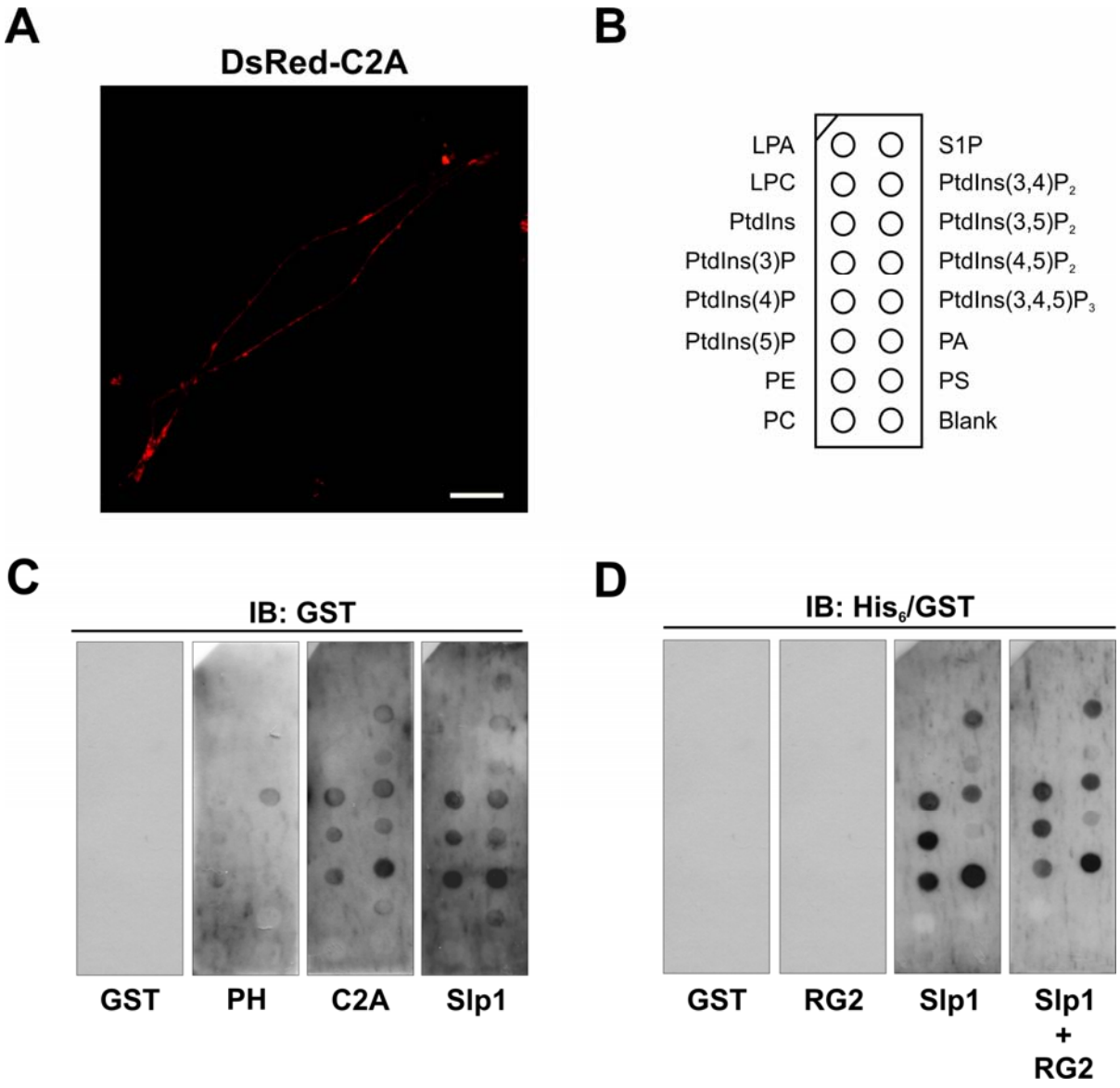

Figure 3.6: Slp1 binds via C2A to phospholipids.
A: C2A domain of Slp1 localizes to the plasma membrane. LNCaP cells were transiently transfected with C-terminally DsRed-tagged C2A domain of Slp1. 24 h post-transfection, cells were analyzed by confocal microscopy. Scale bar: 10 µm.
B: Schematic representation of phospholipids spotted on a nitrocellulose membrane (PIPStrip). 100 pmol of biologically active phospholipids were spotted onto a nitrocellulose membrane as indicated and used in protein phospholipid overlay assays.
C: C2A domain of Slp1 and full-length Slp1 bind to phospholipids. PIPStrips were incubated with 0.5 µg/ml of purified recombinant GST, GST-tagged PLCδ1 PH domain, GST-tagged C2A domain and GST-tagged full-length Slp1. Bound proteins were detected by immunoblot with anti-GST antibody.
D: Binding of Rap1GAP2 does not affect phospholipid binding of Slp1. PIPStrips were overlayed with 0.5 µg/ml of purified recombinant GST, His_6-tagged Rap1GAP2, GST-tagged Slp1 and GST-tagged Slp1 together with His_6-tagged Rap1GAP2. Bound proteins were detected by immunoblot with anti-His_6 and anti-GST antibodies.
LPA: Lysophosphatidic acid; LPC: Lysophosphocho-line; PtdIns: Phosphatidylinositol; PtdInsP: Phosphatidyl-inositolmonophosphate; $PtdInsP_2$: Phosphatidylinositolbisphosphate; $PtdInsP_3$: Phosphatidylinositoltris-phosphate; PE: Phosphatidylethanolamine; PC: Phosphatidylcholine; S1P: Sphingosine-1-phosphate; PA: Phosphatidic acid; PS: Phosphatidylserine.

Rap1GAP2 is able to bind to phospholipids by itself, one additional membrane was incubated with His_6-Rap1GAP2 protein only. GST was used as negative control. As shown in Fig.3.6D,

no binding of Rap1GAP2 or GST to phospholipids was observed. Importantly, addition of Rap1GAP2 did not change the phospholipid binding ability of Slp1. Taken together, binding of Rap1GAP2 to the C2A domain of Slp1 does not affect the lipid binding ability of full-length Slp1, suggesting that simultaneous binding of Slp1 to Rap1GAP2 and phospholipids can occur.

3.2.3 Rap1GAP2 interacts through the -*TKXT*- motif with Slp1

Rap1GAP2 is a modular protein composed of a central catalytic GAP domain, a dimerization domain, the N-terminal 14-3-3 binding site and a large serine-rich C-terminus of low structural organization and so far unknown function. To map the binding site(s) for Slp1 in Rap1GAP2, truncation mutants of Rap1GAP2 were generated and used in GST-Slp1 pull-down assays (Fig.3.7A). As shown in Fig.3.7B, Slp1 bound to wild-type Rap1GAP2 and Rap1GAP2ΔNterm mutant lacking the N-terminal part with equal potency. In contrast, no binding was detected between Slp1 and a C-terminally truncated Rap1GAP2 mutant (Rap1GAP2ΔCterm), suggesting that the binding site for Slp1 is harbored within the C-terminus of Rap1GAP2.

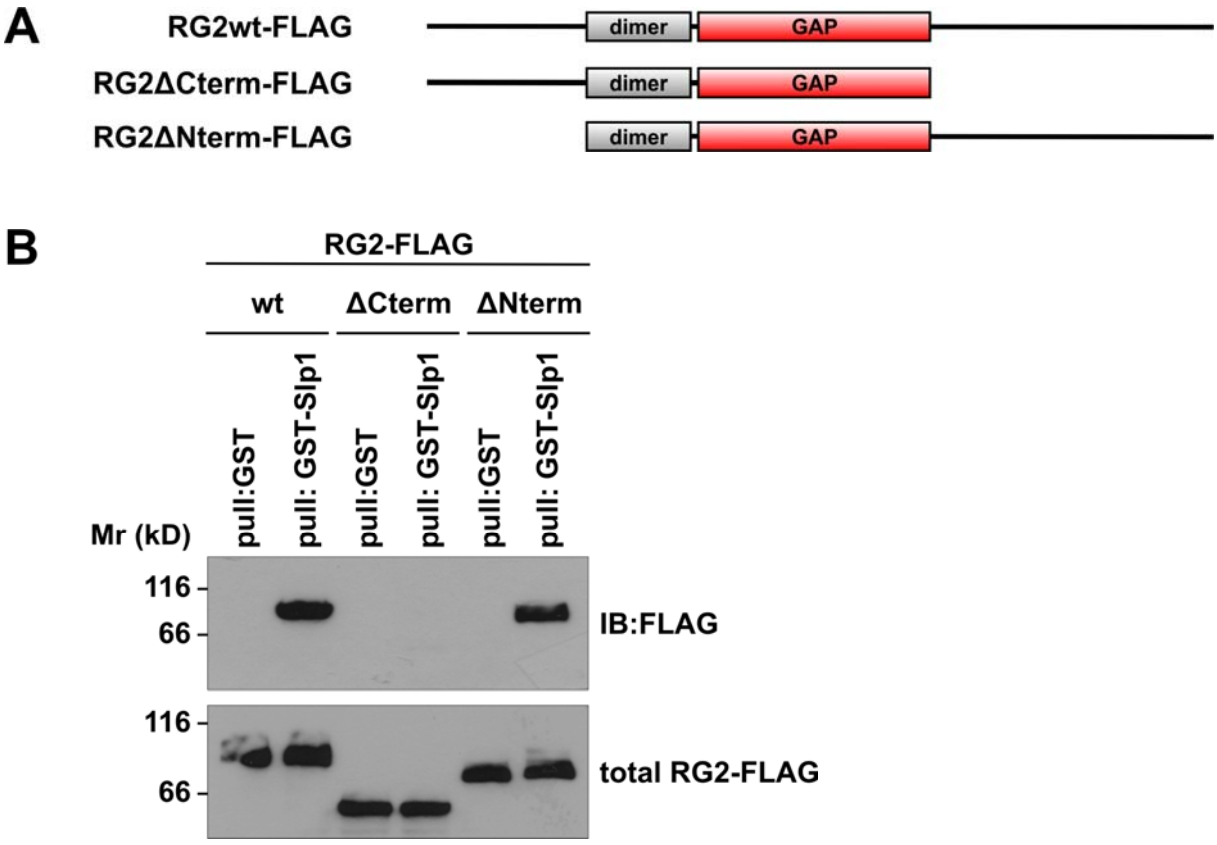

Figure 3.7: Slp1 interacts with the C-terminus of Rap1GAP2.
A: Schematic representation of FLAG-tagged Rap1GAP2 truncation mutants. C-terminally FLAG-tagged truncation mutants of Rap1GAP2 (RG2) were used in pull-down assays. Rap1GAP2ΔCterm lacks amino acids 467-715, whereas Rap1GAP2ΔNterm lacks amino acids 1-121.

B: Pull-down of transfected FLAG-tagged Rap1GAP2 truncation mutants with GST-Slp1. HeLa cells were transiently transfected with either FLAG-tagged Rap1GAP2 (RG2-FLAG) wild-type or different FLAG-tagged Rap1GAP2 truncation mutants as indicated in A. Cells were lysed, and pull-down assays using GST and GST-Slp1 were performed. Precipitates were analyzed for the presence of Rap1GAP2 by immunoblot using anti-FLAG antibody. The *upper panel* shows precipitation results, and the *lower panel* expression levels of Rap1GAP2 proteins (total RG-FLAG, 2% input).

To narrow down the Slp1 binding site, additional truncation mutants of Rap1GAP2 were generated and used in GST-Slp1 pull-down assays (Fig.3.8A). Since no binding between Slp1 and the N-terminus of Rap1GAP2 (amino acids 1-121) was observed (data not shown), these mutants were constructed as VSV-tagged at the N-terminus lacking amino acids 1-121 and varying in the length of their C-termini. As shown in Fig.3.8B, Slp1 bound to Rap1GAP2ΔNterm C1, C2, C3, C4, and C5 mutants, whereas no binding was detected between Slp1 and Rap1GAP2ΔNterm C6, C7 and C8 mutants. These results indicate that the binding site for Slp1 is located within the C-terminal region of amino acids 526-534 of Rap1GAP2.

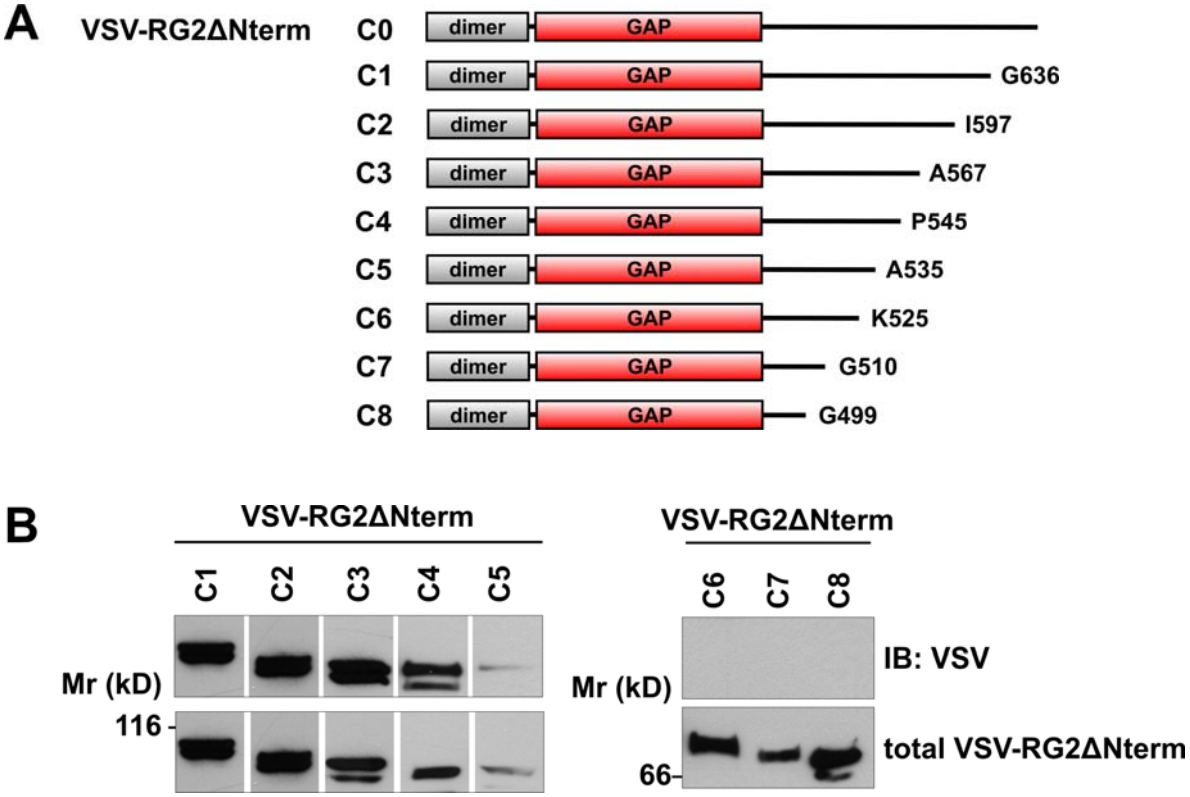

Figure 3.8: Slp1 interacts with a short sequence within the C-terminus of Rap1GAP2.
A: Schematic representation of VSV-tagged Rap1GAP2ΔNterm truncation mutants. N-terminally VSV-tagged Rap1GAP2 (RG2) mutants lacking amino acids 1-121 and varying in the length of their C-termini were used in pull-down assays.
B: Pull-down of transfected VSV-tagged Rap1GAP2ΔNterm truncation mutants with GST-Slp1. HeLa cells were transiently transfected with different VSV-tagged Rap1GAP2ΔNterm (VSV-RG2ΔNterm) mutants truncated at the C-terminus as indicated in A. Cells were lysed, and lysates were subjected to GST-Slp1 pull-down assays. Bound Rap1GAP2 was detected by immunoblot with anti-VSV antibody. The *upper panel* shows precipitation results, and the *lower panel* expression levels of Rap1GAP2 proteins (total VSV-RG2ΔNterm, 2% input).

In order to specify the residues that are responsible for binding of Rap1GAP2 to Slp1, deletion mutants of Rap1GAP2 were generated, based on the information gained from the truncational analysis above. Rap1GAP2Δ522-527 mutant lack amino acids 522-527, whereas in the control mutant Rap1GAP2Δ536-542 amino acids 536-542 were deleted (Fig.3.9A). Both mutants were overexpressed in HeLa cells, and cell lysates were subjected to GST-Slp1 pull-down assays. As shown in Fig.3.9B, Rap1GAP2Δ536-542 mutant bound Slp1 comparable to wild-type Rap1GAP2, whereas Rap1GAP2Δ522-527 mutant did not bind Slp1, suggesting that the sequence EVTKTT (amino acids 522-527 of Rap1GAP2) mediates binding of Rap1GAP2 to Slp1. To determine the role of each amino acid residue within this motif, consecutive alanine point mutants of the EVTKTT sequence were generated and tested in GST-Slp1 pull-down assays. As shown in Fig.3.9C, mutation of E522 to alanine did not affect binding of Slp1 to Rap1GAP2. Mutation of V523 or T526 to alanine only slightly reduced binding, whereas mutation of T524, K525 or T527 almost completely abolished binding of Slp1 to Rap1GAP2, indicating that amino acids T524, K525 and T527, the so-called -*TKXT*- motif, are important for binding of Slp1 to Rap1GAP2. In addition, the importance of the T527 residue was supported by the observation that the VSV-tagged Rap1GAP2ΔNterm C6 mutant was not able to bind to Slp1, although it contains the residues EVTK (amino acids 522-525 of Rap1GAP2) and lacks only T526 and T527 (Fig.3.8A). Nevertheless, deletion of T527 was sufficient to abrogate binding of Rap1GAP2 to Slp1 (Fig.3.8B and Fig.3.9C). To confirm and substantiate these data using a complementary approach, peptide binding assays were performed. For this purpose, short peptides containing the key sequence EVTKTT in wild-type form or with one amino acid mutated to alanine were synthesized on a cellulose membrane (ImmunoGlobe Antikörpertechnik) and incubated with purified recombinant GST-Slp1. As shown in Fig.3.9D, if T524, K525 and T527 were mutated, no binding of GST-Slp1 was detected. Interestingly, mutation of E522 to alanine led to a stronger binding of GST-Slp1. Taken together, these experiments indicate that the residues T524, K525 and T527 in the C-terminal part of Rap1GAP2 constitute the binding site for Slp1 within Rap1GAP2.

It is conceivable that phosphorylation of the two threonine residues, T524 and T527, within the -*TKXT*- motif of Rap1GAP2 could occur. To answer this question, peptides having either T524, T527 or both phosphorylated were tested in GST-Slp1 overlay assays. No binding of GST-Slp1 to the phosphorylated versions of the -*TKXT*- motif of Rap1GAP2 was observed (Fig.3.9D, *lanes 9, 10 and 11*), indicating that phosphorylation at the -*TKXT*- motif of Rap1GAP2 is not required and can even abolish Slp1 binding to Rap1GAP2.

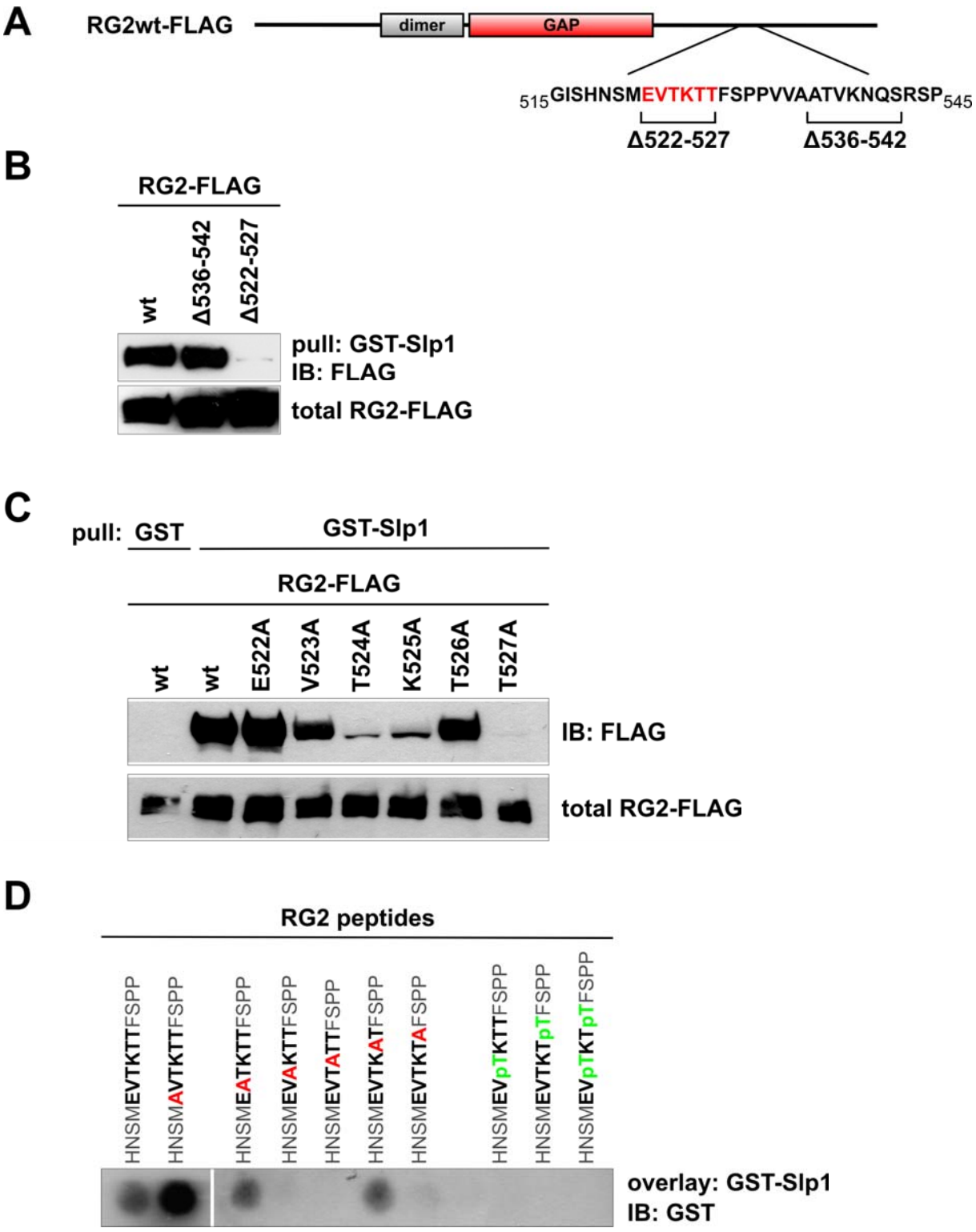

Figure 3.9: Binding of Rap1GAP2 to Slp1 is mediated through the -*TKXT*- motif of Rap1GAP2.
A: Schematic representation of Rap1GAP2 deletion mutants. C-terminally FLAG-tagged deletion mutants of Rap1GAP2 were used in pull-down assays. Rap1GAP2Δ522-527 lacks the sequence EVTKTT (amino acids 522-527 of Rap1GAP2), whereas in Rap1GAP2Δ536-542 amino acids 536-542 were deleted.
B: Pull-down of transfected Rap1GAP2 deletion mutants with GST-Slp1. Lysates of HeLa cells overexpressing either FLAG-tagged Rap1GAP2 wild-type (RG2-FLAG wt) or deletion mutants Rap1GAP2Δ536-542 as control and Rap1GAP2Δ522-527 were subjected to GST-Slp1 pull-down assays followed by immunoblot analysis using anti-FLAG antibody. The *upper panel* shows precipitation results, and the *lower panel* expression levels of Rap1GAP2 proteins (total RG2-FLAG, 2% input).

C: Pull-down of transfected Rap1GAP2 alanine point mutants with GST-Slp1. HeLa cells were transiently transfected with FLAG-tagged Rap1GAP2 wild-type (RG2-FLAG wt) or different Rap1GAP2 point mutants having each of the amino-acids within the EVTKTT sequence (amino acids 522-527) changed to alanine as indicated. Cells were lysed, and lysates were subjected to GST-Slp1 pull-down assays followed by immunoblot analysis with anti-FLAG antibody. The *upper panel* shows precipitation results, and the *lower panel* expression levels of Rap1GAP2 proteins (total RG2-FLAG, 2% input).
D: Peptide binding assay (PepSpot). Synthetic Rap1GAP2 (RG2) peptides covalently bound to a cellulose membrane containing either wild-type Rap1GAP2 EVTKTT sequence or with consecutive amino acids changed to alanine (A) or phosphorylated threonine residues (pT) as indicated were subjected to GST-Slp1 overlay assay followed by immunoblot analysis with anti-GST antibody.

Finally, to test if short peptides containing the key sequence EVTKTT of Rap1GAP2 or peptides carrying a deletion of this motif could affect binding of Slp1 to endogenous Rap1GAP2, GST-Slp1 pull-down assays were performed using human platelet lysate supplemented with either Rap1GAP2 wild-type or Rap1GAP2ΔEVTKTT peptide. As shown in Fig.3.10B, addition of the wild-type peptide to platelet lysate blocked the interaction of Slp1 and Rap1GAP2, whereas addition of the mutant peptide did not affect binding of Slp1 to Rap1GAP2.

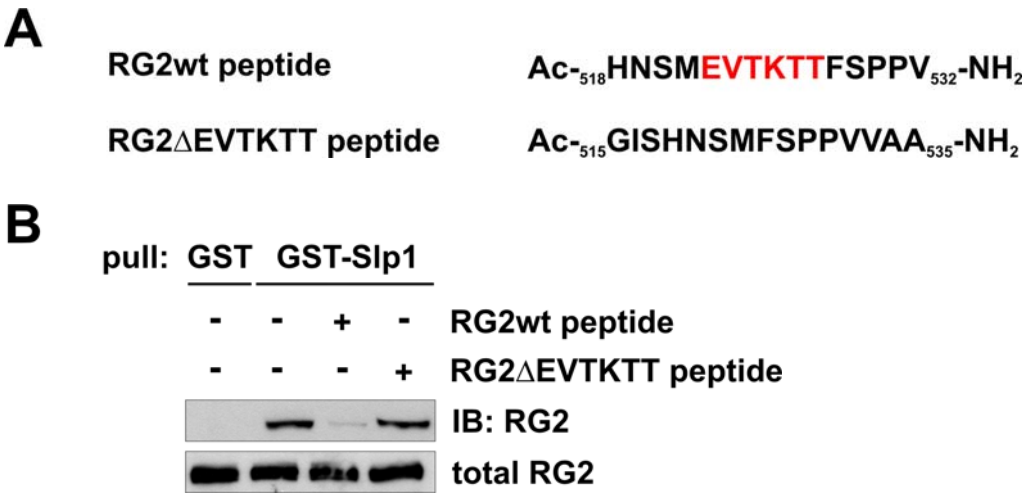

Figure 3.10: Rap1GAP2 wild-type peptide prevents binding of endogenous Rap1GAP2 protein to Slp1.
A: Schematic representation of Rap1GAP2 peptides. Synthetic Rap1GAP2 peptides were used in pull-down assays. Rap1GAP2 wild-type peptide contains the sequence HNSMEVTKTTFSPPV (amino acids 518-532 of Rap1GAP2). In contrast, Rap1GAP2ΔEVTKTT contains the sequence GISHNSMFSPPVVAA (amino acids 515-535 of Rap1GAP2 lacking amino acids 522-527).
B: Pull-down of endogenous Rap1GAP2 with GST-Slp1 from human platelets in absence or presence of Rap1GAP2 peptides. Native human platelet lysate or lysate supplemented with 100 µM of either Rap1GAP2 wild-type (RG2wt) peptide or Rap1GAP2ΔEVTKTT (RG2ΔEVTKTT) peptide were subjected to GST-Slp1 pull-down assays. The precipitates were analyzed for the presence of endogenous Rap1GAP2 protein by immunoblot using anti-Rap1GAP2 antibody. The *upper panel* shows precipitation results, and the *lower panel* expression levels of endogenous Rap1GAP2 (total RG2, 2% input). The used anti-Rap1GAP2 antibody was produced using an N-terminal peptide of Rap1GAP2 (amino acids 1-32) as antigen (Schultess et al. 2005). Therefore, it recognizes Rap1GAP2 protein only and does not detect Rap1GAP2 peptides.

In summary, the mapping experiments revealed residues T524, K525 and T527, the so-called -*TKXT*- motif, within the C-terminus of Rap1GAP2 as the binding site for Slp1 and

showed that phosphorylation at the -*TKXT*- motif is not required for binding of Slp1 to Rap1GAP2.

3.2.4 Rap1GAP2/Slp1 interaction is enhanced upon activation of PKA in platelets

In previous studies of our group we could show that Rap1GAP2 is phosphorylated by cGMP- and cAMP-dependent protein kinases (cGK and cAK, also called PKG and PKA) *in-vitro* and in intact platelets, and identified serine 7 as one phosphorylation site (Schultess et al. 2005, Hoffmeister et al. 2008). We demonstrated that PKG- and PKA-induced phosphorylation of serine 7 inhibits binding of 14-3-3 to Rap1GAP2 in platelets, and conversely, platelet activation by ADP and thrombin increases 14-3-3 binding to Rap1GAP2 (Hoffmeister et al. 2008). Therefore, we were interested in investigating if binding of Slp1 to Rap1GAP2 is also affected upon platelet activation or platelet inhibition. To this end, GST-Slp1 pull-down assays were performed using lysates of platelets preincubated with various platelet activators or inhibitors. To determine if platelet activation could impair Slp1 binding to Rap1GAP2, washed human platelets were treated with thrombin and ADP as indicated (Fig.3.11A). Platelets were lysed, and lysates were incubated with GST and GST-Slp1. The precipitates were analyzed for the presence of endogenous Rap1GAP2 using anti-Rap1GAP2 antibody. As shown in Fig.3.11A, treatment of platelets with thrombin and ADP did not affect Slp1 binding to endogenous Rap1GAP2. To investigate if activation of cAMP-dependent protein kinase in platelets would influence binding of Slp1 to Rap1GAP2, a set of experiments was performed. In order to induce activation of PKA, washed human platelets were treated with prostaglandin I_2, forskolin, and Sp-5,6-DCI-cBiMPS as indicated (Fig.3.11B-D). PGI_2 initiates platelet inhibition through interaction with specific G protein-coupled receptors on the platelet surface (*1.2.1*). Forskolin stimulates cAMP production through direct activation of adenylyl cyclase (Seamon et al. 1981, Insel et al. 1982), and Sp-5,6-DCI-cBiMPS is a membrane permeable cAMP analogue and direct activator of PKA (Sandberg et al. 1991). After treatment platelets were lysed, and lysates were subjected to GST-Slp1 pull-down assays. The precipitates were analyzed for the presence of endogenous Rap1GAP2 by immunoblot. As shown in Fig.3.11B to D, at each step of activation a concentration-dependent increase in binding of Slp1 to Rap1GAP2 was observed. Phosphorylation of VASP, a well established PKG and PKA substrate in platelets, was in direct correlation with the PKA activity and detected by immunoblot using phosphospecific anti-P-VASP antibody (Smolenski et al. 1998, Li et al. 2003). To further evaluate the specificity of PKA activation on Slp1/Rap1GAP2 binding, platelets were treated with Rp-8-Br-cAMPS, a specific PKA inhibitor, either alone or with forskolin on top (Fig.3.11E). GST-Slp1 pull-down assays were performed as described above. As shown in Fig.3.11E, no increase in binding of Slp1 to Rap1GAP2 was observed if platelets pretreated with Rp-8-Br-cAMPS were

treated with forskolin. Inhibition of PKA by Rp-8-Br-cAMPS was reflected in decreased phosphorylation of VASP. In order to confirm this PKA effect on Slp1/Rap1GAP2 binding in a different system, HeLa cells were used. Cells were transfected with FLAG-tagged Rap1GAP2 either alone or in combination with the PKA inhibitor PKI. On the following day, cells were washed and incubated in serum-free medium without or with forskolin. Cells were lysed, and lysates were subjected to GST-Slp1 pull-down assays. As shown in Fig.3.11F, inhibition of PKA by PKI resulted in decreased binding of Slp1 to transfected Rap1GAP2. Probably due to a high basal phosphorylation state of Rap1GAP2 or other PKA substrates involved in Rap1GAP2/Slp1 complex formation in HeLa cells, no increase in Slp1 binding to Rap1GAP2 upon forskolin treatment was observed.

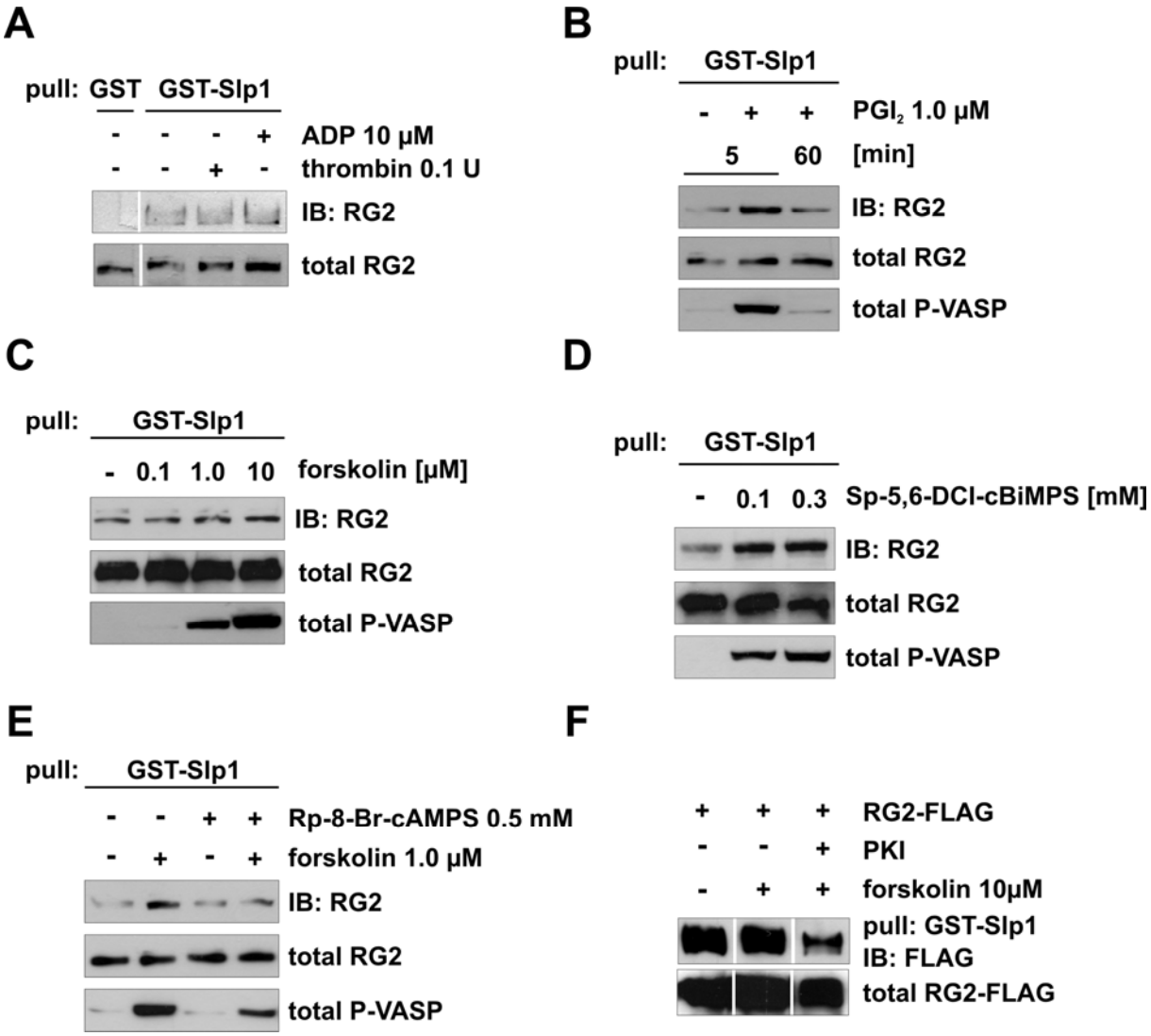

Figure 3.11: Activation of PKA in platelets increases binding of Slp1 to endogenous Rap1GAP2.
A: ADP and thrombin do not alter binding of Slp1 to Rap1GAP2. Washed human platelets were treated without or with 10 µM ADP or with 0.1 U/ml thrombin for 1 min at 37°C. Platelets were lysed, and lysates were subjected to GST-Slp1 pull-down assays. GST was used as negative control. The precipitates were examined for the presence of bound endogenous Rap1GAP2 protein by immunoblot using anti-Rap1GAP2 antibody. The *upper panel* shows precipitation results, and the *lower panel* expression levels of endogenous Rap1GAP2 (total RG2, 2% input).

B, C and **D:** Activation of PKA in platelets results in increased binding of Slp1 to endogenous Rap1GAP2. Washed human platelets were treated without or with PGI_2 (B), forskolin (C) or Sp-5,6-DCl-cBiMPS (D) as indicated. Platelets were lysed, and lysates were subjected to GST-Slp1 pull-down assays followed by immunoblot analysis using anti-Rap1GAP2 antibody. The *upper panel* shows precipitation results, and the *lower panel* expression levels of endogenous Rap1GAP2 (total RG2, 2% input). Phosphorylation of VASP was detected with anti-P-VASP antibody (total P-VASP, 2% input, *lower panel*).
E: Inhibition of PKA in platelets abrogates forskolin-stimulated increase in binding of Slp1 to endogenous Rap1GAP2. Washed human platelets were treated without or with 0.5 mM Rp-8-Br-cAMPS for 30 min at 37°C. Then, platelets were incubated without or with 1 µM forskolin for 20 min at 37°C. Platelets were lysed, and lysates were subjected to GST-Slp1 pull-down assays followed by immunoblot analysis with anti-Rap1GAP2 antibody. The *upper panel* shows precipitation results, and the *lower panel* expression levels of endogenous Rap1GAP2 (total RG2, 2% input). Phosphorylated VASP was detected by immunoblot using anti-P-VASP antibody (total P-VASP, 2% input*, lower panel*).
F: Inhibition of PKA in transfected HeLa cells results in decreased binding of Slp1 to Rap1GAP2. HeLa cells were transiently transfected with FLAG-tagged Rap1GAP2 without or with PKI. 24 h post-transfection cells were treated without or with 10 µM forskolin for 20 min at 37°C. Then, cells were lysed, and lysates were subjected to GST-Slp1 pull-down assays. The precipitates were analyzed for the presence of bound Rap1GAP2 with anti-FLAG antibody (*upper panel*). The *lower panel* shows expression levels of Rap1GAP2 (total RG2-FLAG, 2% input).

Taken together, activation of PKA in platelets enhanced binding of Slp1 to endogenous Rap1GAP2. The PKA effect is specific, because inhibition of PKA by a specific PKA inhibitor in platelets abolished the increase of Slp1 binding to Rap1GAP2 upon forskolin treatment. In HeLa cells, co-expression of Rap1GAP2 and PKI resulted in decreased Slp1 binding to transfected Rap1GAP2.

3.3 Complex formation of Rap1GAP2, Slp1 and Rab27

3.3.1 Rap1GAP2, Slp1 and Rab27a form a trimeric complex and co-localize in transfected HeLa cells

Slp1 has been shown to bind to Rab27, a small GTPase involved in vesicle regulated exocytosis of many cell types (Fukuda 2005). Rab27 is expressed in 2 isoforms, Rab27a and Rab27b, that share 71 % identity at amino acid level (Pereira-Leal and Seabra 2001). To first confirm binding of Slp1 to both, Rab27a and Rab27b, co-immunoprecipitation experiments were performed. HeLa cells were transfected with EGFP-tagged Rab27a or Rab27b, which were kindly provided by Prof. Dr. M. C. Seabra, London, UK, and myc-tagged Slp1 either alone or in combination. 24 h post-transfection, cells were lysed, and Rab27 was immunoprecipitated using anti-GFP antibody. The precipitates were analyzed for the presence of bound Slp1 by immunoblot. As shown in Fig.3.12A and B, Slp1 bound to both, Rab27a and Rab27b. Interestingly, binding of Slp1 to Rab27b was much weaker than to Rab27a. To determine if Slp1, Rab27 and Rap1GAP2 form a trimeric complex, HeLa cells were transfected with epitope-tagged versions of Slp1, Rab27a and Rap1GAP2. Two days later, cells were lysed, and lysates were subjected to co-immunoprecipitation experiments using anti-FLAG antibody. Rab27a could only be detected in precipitates from cell lysates containing all three proteins, indicating that Rab27a, Slp1 and Rap1GAP2 indeed form a trimeric complex in intact mammalian cells (Fig.3.12C). This result was further confirmed in a

reverse experiment using anti-VSV antibody (Fig.3.12D). Unfortunately, due to very weak binding of Rab27b to Slp1 and insufficient expression levels of VSV-tagged Rab27b, a trimeric complex composed of Rab27b, Slp1 and Rap1GAP2 could not be proven. However, given the fact that Rab27b binds to Slp1 and Slp1 binds to Rap1GAP2, complex formation of Rab27b, Slp1 and Rap1GAP2 is quite conceivable.

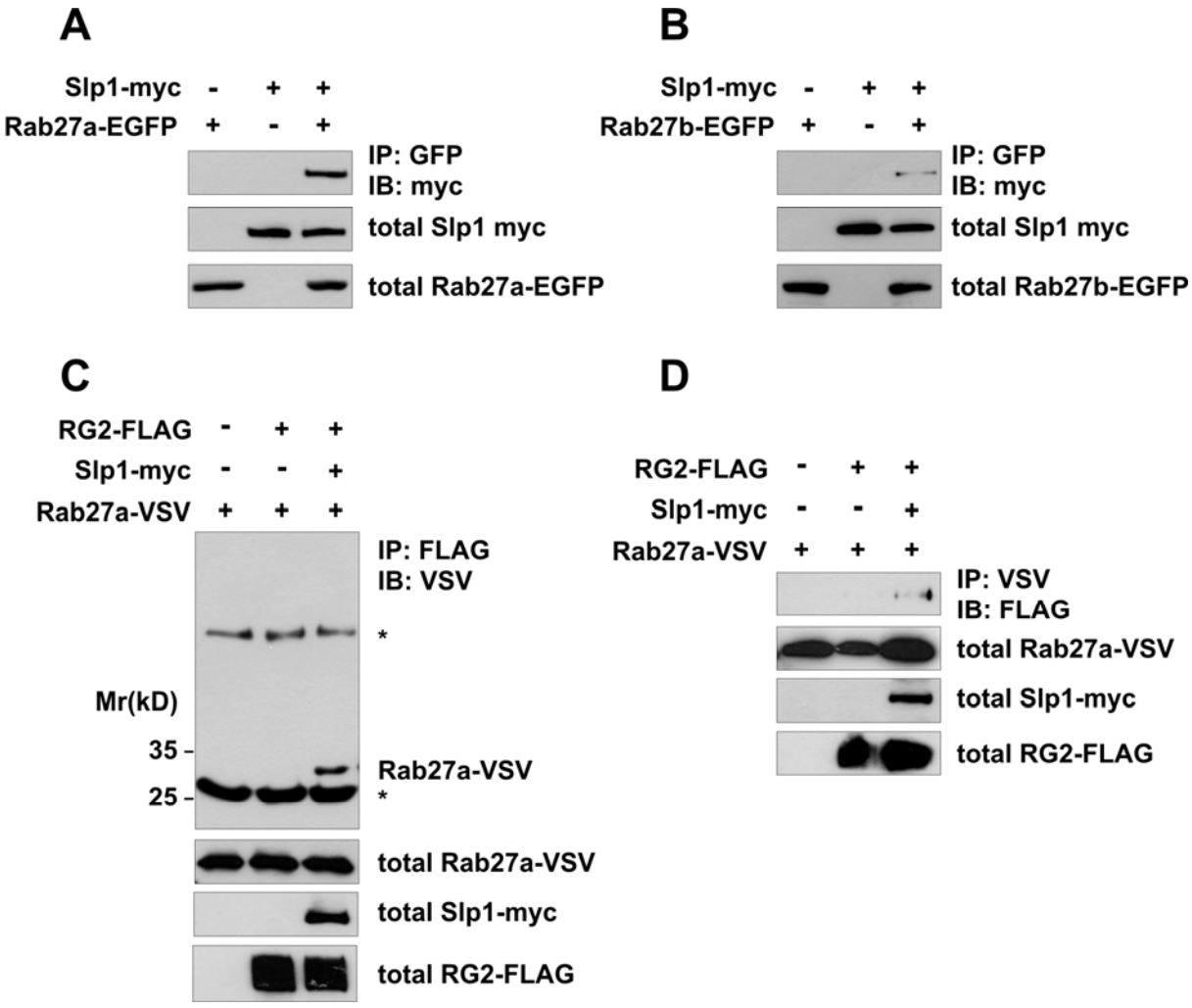

Figure 3.12: Rap1GAP2, Slp1 and Rab27 form a trimeric complex in transfected HeLa cells.
A and **B:** Slp1 binds to both, Rab27a and Rab27b. HeLa cells were transiently transfected with myc-tagged Slp1 and EGFP-tagged Rab27a (A) or Rab27b (B) either alone or in combination. Cells were lysed, and Rab27 was immunoprecipitated using anti-GFP antibody. The precipitates were examined for the presence of bound Slp1 with anti-myc antibody (*upper panel*). The *two lower panels* show expression levels of Slp1 (total Slp1-myc, 2% input) and Rab27 (total Rab27-EGFP, 2% input).
C and **D:** Co-immunoprecipitation of transfected Rap1GAP2 in complex with Slp1 and Rab27a. HeLa cells were transiently transfected with VSV-tagged Rab27a alone, together with FLAG-tagged Rap1GAP2, or with FLAG-tagged Rap1GAP2 and myc-tagged Slp1. Cells were lysed, and Rap1GAP2 was immunoprecipitated with anti-FLAG antibody (C) and Rab27a with anti-VSV antibody (D), respectively. The precipitates were analyzed for the presence of Rab27a using anti-VSV antibody (C) and Rap1GAP2 using anti-FLAG antibody (D). The *upper panel* shows the precipitation results. Immunoglobulin heavy and light chains are marked with asterisk (*) (C, *upper panel*). The *lower panels* demonstrate total amounts of transfected Rab27a-VSV (total Rab27a-VSV, 2% input), Slp1-myc (total Slp1-myc, 2% input) and Rap1GAP2-FLAG (total RG2-FLAG, 2% input).

To investigate the subcellular localization of Rab27, Slp1 and Rap1GAP2, HeLa cells were co-transfected with EGFP-tagged Rab27a, myc-tagged Slp1 and VSV-tagged Rap1GAP2. Cells were fixed, permeabilized and immunostained with tag-specific primary and dye-labelled secondary antibodies. Subsequent immunofluorescence analysis revealed a partial co-localization of all three proteins in the cytosol as well as at the plasma membrane (Fig.3.13).

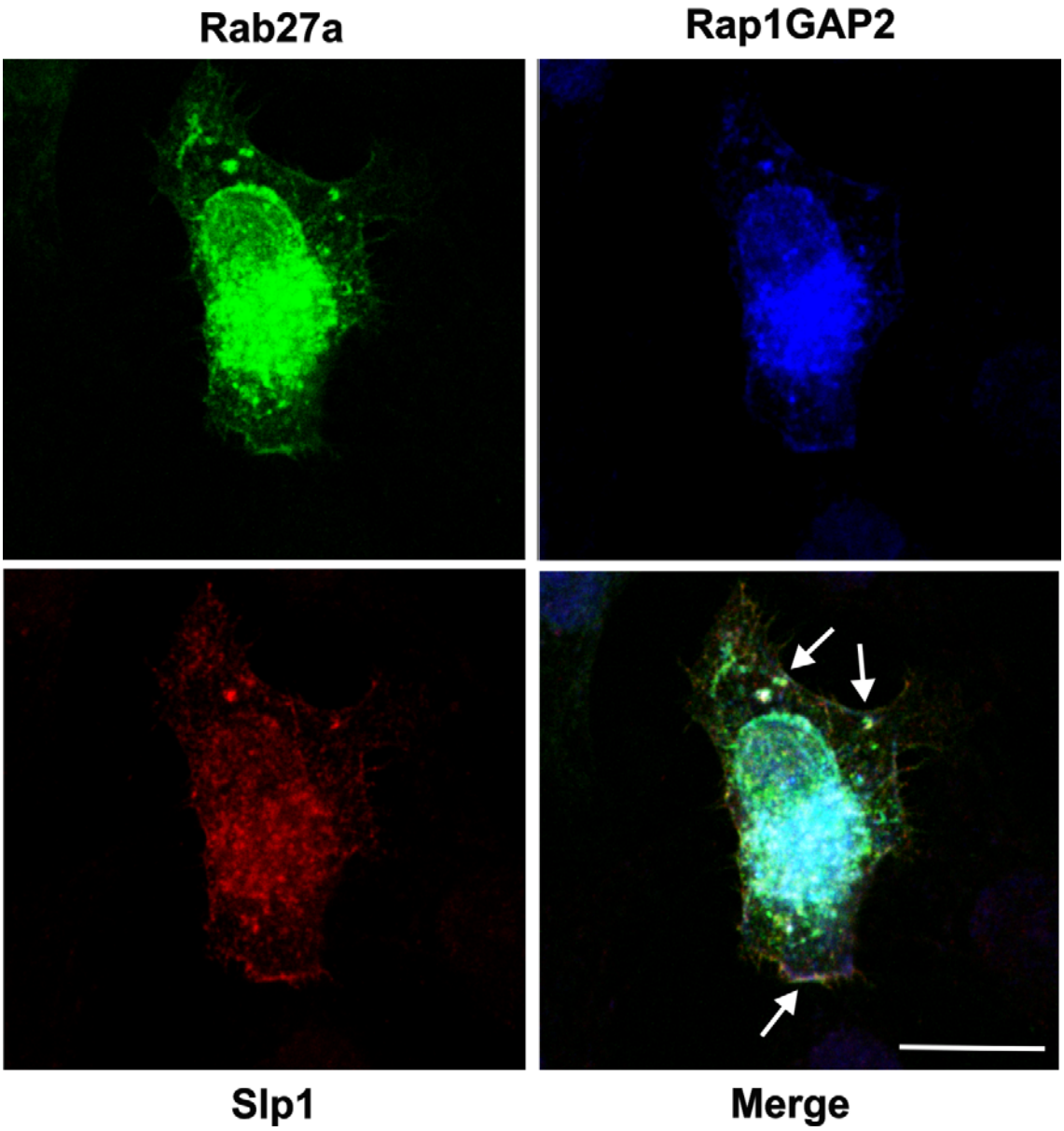

Figure 3.13: Co-localization of transfected Rap1GAP2, Slp1 and Rab27a.
Co-localization of EGFP-tagged Rab27a, VSV-tagged Rap1GAP2 and myc-tagged Slp1 overexpressed in HeLa cells was analyzed by immunofluorescence as described in Materials and Methods (*2.3.4)*. Arrows indicate co-localization of all three proteins. Scale bar: 10 µm.

3.3.2 Rap1GAP2, Slp1 and Rab27 form a trimeric complex in human platelets

Both isoforms of Rab27 are present in platelets (Barral et al. 2002). To demonstrate that Slp1 interacts with endogenous Rab27 expressed in human platelets, GST-Slp1 pull-down assays were performed. The monoclonal anti-Rab27a antibody, which was used to detect bound Rab27a, recognized both Rab27 isoforms (data not shown). Thus, the band for Rab27 most likely represents a mixture of Rab27a and Rab27b (Fig.3.14A). In reverse experiments using purified recombinant GST-Rab27a and GST-Rab27b, binding of endogenous Slp1 from human platelet lysate was observed to both isoforms of Rab27 (Fig.3.14B). Moreover, Slp1 bound to both, GTP- and GDP-loaded Rab27a and Rab27b equally well. To verify complex formation of Slp1, Rab27 and Rap1GAP2 at endogenous level in human platelets, co-immunoprecipitation experiments using platelet lysates were performed. As shown in Fig.3.14C, endogenous Rab27 was successfully co-immunoprecipitated with endogenous Slp1 and Rap1GAP2 from platelets.

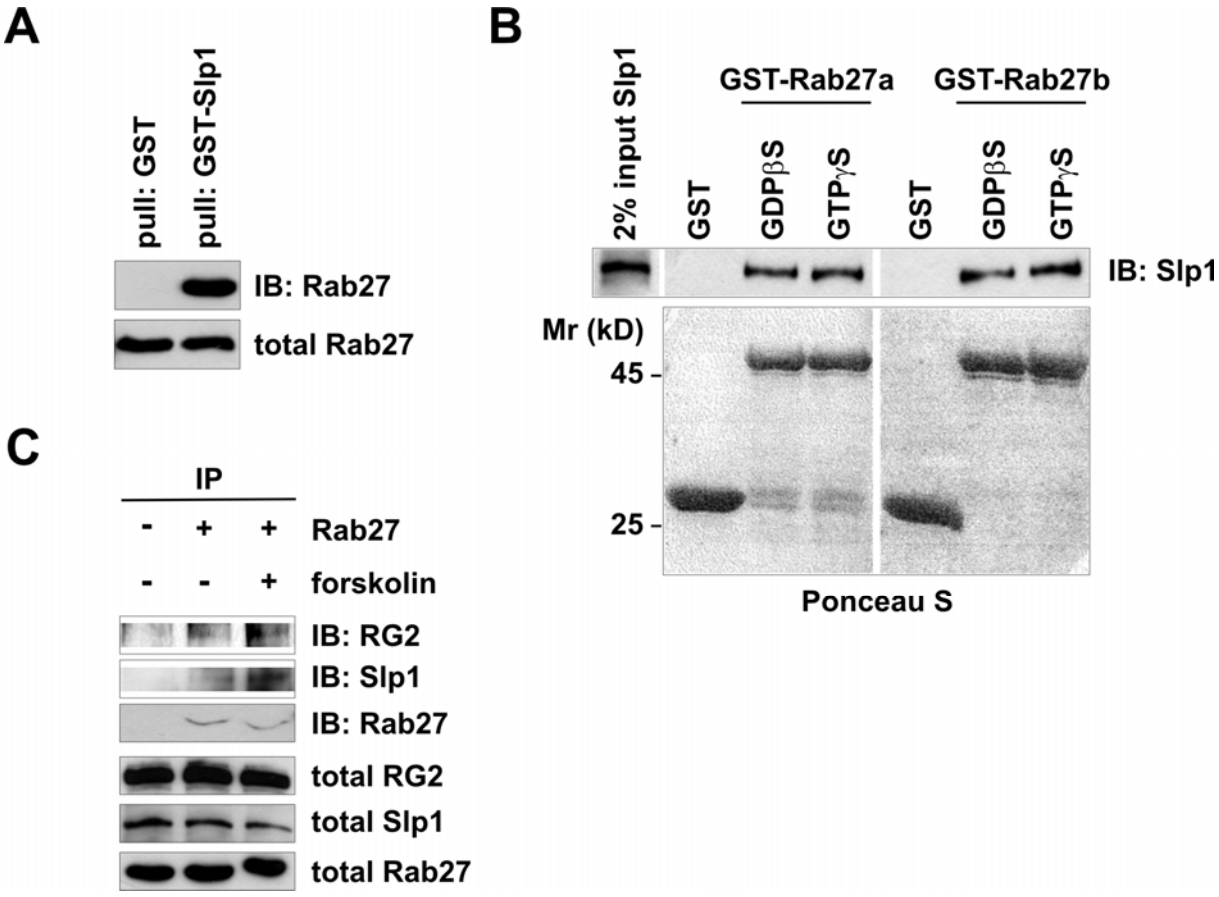

Figure 3.14: Rap1GAP2, Slp1 and Rab27 form a trimeric complex in platelets.
A: Pull-down of endogenous Rab27 with GST-Slp1. Human platelet lysate was subjected to GST-Slp1 pull-down assay followed by immunoblot analysis using anti-Rab27a antibody which recognizes both isoforms, Rab27a and Rab27b. The *upper panel* shows precipitation results, and the *lower panel* expression levels of endogenous Rab27 protein (total Rab27, 2% input).

B: Pull-down of endogenous Slp1 with GST-Rab27. Purified recombinant GST fusion proteins of Rab27a and Rab27b loaded either with GDPβS or GTPγS were used to precipitate endogenous Slp1 from human platelet lysate. Equal amounts of purified GST protein were used as negative control. The precipitates were analyzed for the presence of bound Slp1 by immunoblot with anti-Slp1 antibody (*upper panel*). The *lower panel* shows the amounts of GST and GST-Rab27 used for precipitation.
C: Co-immunoprecipitation of endogenous Rap1GAP2 in complex with Slp1 and Rab27. Washed human platelets were treated with 10 µM of forskolin for 20 min at 37°C as indicated. Platelets were lysed, and lysates containing endogenous Rab27, Rap1GAP2 and Slp1 were subjected to co-immunoprecipitation using anti-Rab27a antibody. The precipitates were examined for the presence of Rap1GAP2 and Slp1 by immunoblot using anti-Rap1GAP2 and anti-Slp1 antibodies (*first and second panels from top*). Precipitated Rab27 was controlled by immunoblot using anti-Rab27a antibody (*third panel from top*). As indicated in A, the Rab27 band most likely consists of both isoforms, Rab27a and Rab27b. The *three lower panels* show expression levels of endogenous Rap1GAP2 (total RG2, 2% input), Slp1 (total Slp1, 2% input) and Rab27 (total Rab27, 2% input).

Notably, treatment of platelets with forskolin resulted in stronger binding of Rab27 to Slp1, suggesting that activation of PKA and probably subsequent PKA phosphorylation of either Slp1 and/or Rab27 could impact complex formation by Slp1, Rab27 and Rap1GAP2 (Fig.3.14D, *lane 3*).

3.3.3 Slp1 is phosphorylated by PKA *in-vitro*

To evaluate if Slp1 could be a substrate of PKA, *in-vitro* kinase assays were performed. To this end, HeLa cells were transiently transfected with myc-tagged Slp1. Expressed protein was precipitated with anti-myc antibody and subjected to *in-vitro* phosphorylation using γ-[^{32}P] ATP and purified catalytic subunit of PKA, which was kindly provided by Dr. E. Butt-Dörje, Würzburg, Germany. As shown in Fig.3.15A, strong phosphorylation of Slp1 by PKA was observed. By means of the computational tool ScanSite (http://scansite.mit.edu), two serine residues of Slp1 corresponding to the consensus sequence -(R/K)$_2$-X-S/T- for phosphorylation by protein kinase A were predicted: serine 111 (-RKKS-) and serine 301 (-RRRS-). In order to identify the exact phosphorylation site(s), candidate serine residues were mutated to alanine. Mutation of serine 111 completely abolished *in-vitro* phosphorylation of Slp1 by PKA, whereas mutation of serine 301 only marginally reduced phosphorylation (Fig.3.15B). Using the computational tool SMART (*Simple Modular Architecture Research Tool*, http://smart.embl-heidelberg.de) for protein domain identification, the Rab27 binding SHD of Slp1 was assigned to amino acids 30 to 150, meaning that serine 111 residue is located within this domain. To investigate whether PKA phosphorylation of Slp1 at serine 111 could alter Slp1 binding to Rab27, co-immunoprecipitation experiments were performed. For this purpose, Hela cells were transiently transfected with myc-tagged wild-type Slp1 and serine-111-to-alanine mutant either alone or in combination with VSV-tagged Rab27a. 48 h post-transfection, cells were lysed, and Rab27a was immunoprecipitated with anti-VSV antibody. The precipitates were examined for the presence of Slp1 by immunoblot using anti-myc antibody. Serine-to-alanine mutation of residue 111 of Slp1 strongly reduced binding of Slp1 to Rab27a (Fig.3.15C).

Taken together, Slp1 is *in-vitro* phosphorylated by PKA, and serine 111 was identified as phosphorylation site. Mutation of serine 111 to alanine resulted in decreased binding of Slp1 to Rab27 in transfected mammalian cells.

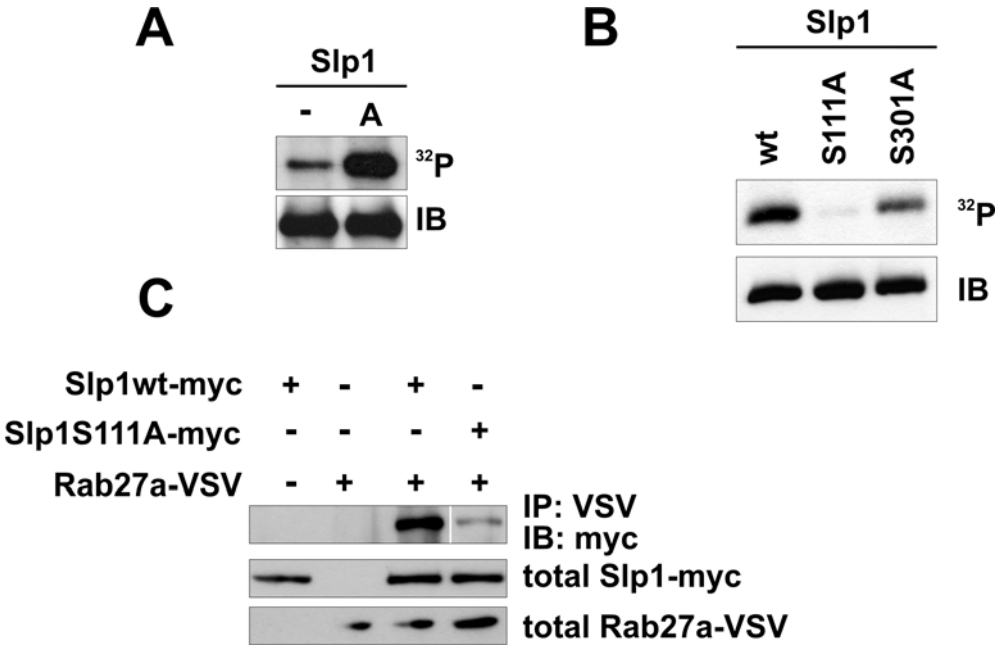

Figure 3.15: Slp1 is phosphorylated by PKA.
A: Slp1 is *in-vitro* phosphorylated by PKA. HeLa cells were transiently transfected with myc-tagged Slp1. Expressed Slp1 protein was immunoprecipitated with anti-myc antibody, and *in-vitro* kinase assays were performed using γ-[^{32}P]-ATP and purified catalytic subunit of PKA (*designated* A). As negative control no kinase was added (*designated* -). To detect ^{32}P incorporation, proteins were separated by SDS-PAGE, blotted on a nitrocellulose membrane, and exposed to film (^{32}P, *upper panel*). The expression levels of Slp1 were determined by immunoblot using anti-myc antibody followed by ECL detection (IB, *lower panel*).
B: Mutation of serine 111 to alanine abolishes *in-vitro* phosphorylation of Slp1 by PKA. Hela cells were transiently transfected with myc-tagged wild-type (wt) Slp1 and mutants of Slp1 having serine-to-alanine mutations of serine 111 (S111A) or serine 301 (S301A). Expressed proteins were immunoprecipitated with anti-myc antibody, and *in-vitro* kinase assays were performed as described in A. The *upper panel* shows ^{32}P incorporation, and the *lower panel* the expression levels of Slp1 proteins detected by immunblot using anti-myc antibody (IB).
C: Mutation of serine 111 to alanine reduces binding of Slp1 to Rab27a in transfected cells. HeLa cells were transiently transfected with myc-tagged wild-type Slp1 and Slp1S111A mutant having serine 111 changed to alanine either alone or together with VSV-tagged Rab27a. Cells were lysed, and Rab27a was immunoprecipitated with anti-VSV antibody. The precipitates were analyzed for the presence of bound Slp1 by immunoblot using anti-myc antibody (*upper panel*). The *two lower panels* show expression levels of Slp1 (total Slp1-myc, 2% input) and Rab27a (total Rab27a-VSV, 2% input).

3.3.4 Identification of Slp1 interacting proteins in platelets

The next aim of the present study was to identify additional Slp1 interacting proteins in platelets. To this end, Slp1 affinity chromatography was performed using human platelet lysate as source for Slp1 binding proteins. Subsequent mass spectrometric analysis revealed fourteen new putative Slp1 interactors in platelets (Tab.3.1). A total of six proteins were identified as members of the Rab protein family that are believed to control intracellular membrane trafficking (Zerial and McBride 2001). The presence of Rab27 and Rab8 indicated that the method was successful. However, Rap1GAP2 was not identified. Binding of endogenous Rab8 to Slp1 was confirmed in GST-Slp1 pull-down assays using human platelet lysate (Fig.3.16). In contrast, binding of Rap1b to Slp1 could not be verified (data not shown). A total of four proteins were related to actin cytoskeleton, and among them myosin-9 (non-muscle myosin heavy chain IIA, NMHC-IIA) was identified yielding the most peptide matches. Other putative Slp1 interacting proteins were the dual specificity protein phosphatase 3 (DUSP3), ATP synthase O subunit (ATPO) and programmed cell death protein 10 (PDCD10). Platelet expression of all identified proteins was confirmed by protein database search using “PlateletWeb-Knowledgebase” (http://plateletweb.bioapps.bio-zentrum.uni-wuerzburg.de, Dittrich et al. 2008) and by protein database “Human Proteinpedia” (http://www. humanproteinpedia.org).

Taken together, affinity chromatography and mass spectrometric analysis revealed further Slp1 interacting proteins in platelets. Binding of Slp1 to endogenous Rab8 from human platelets was verified by GST-Slp1 pull-down assays.

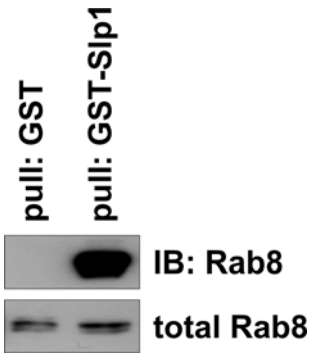

Figure 3.16: Slp1 interacts with endogenous Rab8 from platelets.
Washed human platelets were lysed, and lysates were subjected to GST-Slp1 pull-down assays. GST was used as negative control. The precipitates were analyzed for the presence of Rab8 by immunoblot using anti-Rab8 antibody. The *upper panel* shows precipitation results, and the *lower panel* the expression levels of endogenous Rab8 (total Rab8, 2% input).

Table 3.1: Slp1 interacting proteins in platelets.
Slp1 affinity chromatography and mass spectrometric analysis revealed 14 new putative Slp1 interacting proteins in human platelets. His_6-Slp1 was bacterially expressed, coupled to NHS-activated sepharose and incubated with human platelet lysate as described in Materials and Methods (*2.4.10*). After elution, bound proteins were separated by SDS-PAGE and stained with Coomassie Brilliant Blue. Protein bands were excised and analyzed by mass spectrometry.

Sample	Peptide Sequence	Mr (kD)	Accession Number	Protein
1	K.YDPTIEDSYRK.Q K.LVVLGSGGVGK.S R.VKDTDDVPMILVGNK.C R.QWNNCAFLESSAK.S	20	P61224	Rap1b
2	K.LQIWDTAGQER.F K.LLLIGDSGVGK.S	23	P62820 Q9H0U4	Rab1a/b
3	R.VASALPGMENVQEK.S K.LQLWDTAGQER.F	23	P20340 Q9NRW1	Rab6a/b
4	R.NIEEHASADVEK.M R.TITTAYYR.G K.LLLIGDSGVGK.S K.TYDYLFK.L	23	P61006 Q92930	Rab8a/b
5	R.IQIWDTAGQER.Y K.LLLIGDSGVGK.S	23	P59190	Rab15
6	R.VVYNAQGPNGSSGK.A K.TQIPDTVNGGNSGNLDGEKPPEKK.K K.LLALGDSGVGK.T K.YGIPYFETSAATGQNVEK.A	25	O00194	Rab27b
7	K.DSSQSPSQVDQFCK.E K.DNINIEEAAR.F	25	Q13637	Rab32
8	R.ELEDATETADAMNR.E K.KLVWVPSDK.S R.HEMPPHIYAITDTAYR.S K.NLPIYSEEIVEMYK.G K.NFINNPLAQADWAAK.K R.QLEEAEEEAQR.A K.DLEAHIDSANK.N R.EMEAELEDERK.Q R.EQLEEEEEAKHNLEK.Q K.NKHEAMITDLEER.L R.TEMEDLMSSKDDVGK.S K.QIATLHAQVADMK.K K.ASITALEAK.I R.EDQSILCTGESGAGK.T K.IAQLEEQLDNETK.E K.RQAQQERDELADEIANSSGK.G K.LKDVLLQVDDERR.N K.EQADFAIEALAK.A R.RGDLPFVVPR.R R.IAEFTTNLTEEEK.S	225	P35579	Myosin-9
9	K.EAFNMIDQNR.D K.LNGTDPEDVIR.N R.FTDEEVDELYR.E	20	P19105 P24844	Myosin regulatory light chain 2
10	R.VFDKEGNGTVMGAELR.H R.HVLVTLGEK.M R.ALGQNPTNAEVLK.V	16	P08590 P60660	Myosin light polypeptide 3/6
11	R.QGNMTAALQAALK.N K.ALAAGGVGSYVR.V R.NGVDLLMK.Y	16	O15511	Actin-related protein 2/3 complex subunit 5
12	R.IYVGNASVAQDIPK.L K.DSGITYLGIK.A R.AADFIDQALAQK.N	20	P51451	Dual specificity protein phosphatase 3
13	R.YATALYSAASL.Q K.VAASVLNPYVK.R K.SFLQGQVLK.L K.TDPSILGGMIVR.I	23	P48047	ATP synthase O subunit
14	R.VNLSAAQTLR.A K.ENPGLTQDIIMK.I	25	Q9BUL8	Programmed cell death protein 10

3.4 Functional analysis of the Rap1GAP2/Slp1 interaction

To determine the function of the interaction between Rap1GAP2 and Slp1, two strategies were defined and pursued: firstly, the functional relevance of the interaction in terms of Rap1GAP2 function in Rap1-mediated cell adhesion, and secondly, the functional significance of the interaction in terms of Slp1 function in Rab27-mediated secretion.

3.4.1 *In-vitro* GAP assay

As GTPase activating protein of Rap1, Rap1GAP2 contains a central catalytic GAP domain that is required to confer GTPase activity towards Rap1 (Schultess et al. 2005). Rap1 is a small GTPase that regulates integrin function and thus cell adhesion (Bos 2005). In order to investigate if Slp1 binding to Rap1GAP2 could affect the GTPase activity of Rap1GAP2, *in-vitro* GAP assays were performed. HeLa cells were transiently transfected with the appropriate plasmids of Rap1GAP2 and Slp1. Expressed proteins were affinity purified using anti-FLAG antibody. In parallel, Rap1b was purified from *Escherichia coli* BL21 and loaded with [^{32}P]-GTP as described in Materials and Methods (*2.5.1*). Precipitated Slp1 and Rap1GAP2 proteins either alone or in complex were added to GTP-loaded Rap1b and incubated at 25°C for 30, 60 and 120 sec. Released [^{32}P] was counted by liquid scintillation, and plotted as percentage of input [^{32}P]-GTP bound to Rap1b. As shown in Fig.3.17 and expected, Slp1 itself did not exhibit any GTPase activity. In contrast, in samples containing Rap1GAP2 a time-dependent increase in GAP activity was observed. However, no differences between free and Slp1 bound Rap1GAP2 was detected, indicating that Slp1 binding to Rap1GAP2 did not affect the catalytic GTPase activity of Rap1GAP2 *in-vitro*.

3.4.2 Cell adhesion assay

Rap1GAP proteins are known to inhibit Rap1-mediated adhesion of intact cells (Bos et al. 2001). As described in *3.4.1*, Slp1 binding had no effect on the catalytic GTPase-activating function of Rap1GAP2 *in-vitro*. However, binding of Slp1 to Rap1GAP2 could affect the subcellular distribution of Rap1GAP2 leading to local changes of Rap1-GTP levels within the cell. Therefore, functional consequences of Slp1 binding to Rap1GAP2 on cell adhesion were studied.

HeLa cells expressing endogenous Rap1 were transiently transfected with pRluc-N3 vector together with FLAG-tagged Rap1GAP2 and myc-tagged Slp1 either alone or in combination. Control cells were transfected with pRluc-N3 expressing luciferase only. One day after transfection, cells were seeded onto fibronectin-coated plates. Adherent cells were quantified

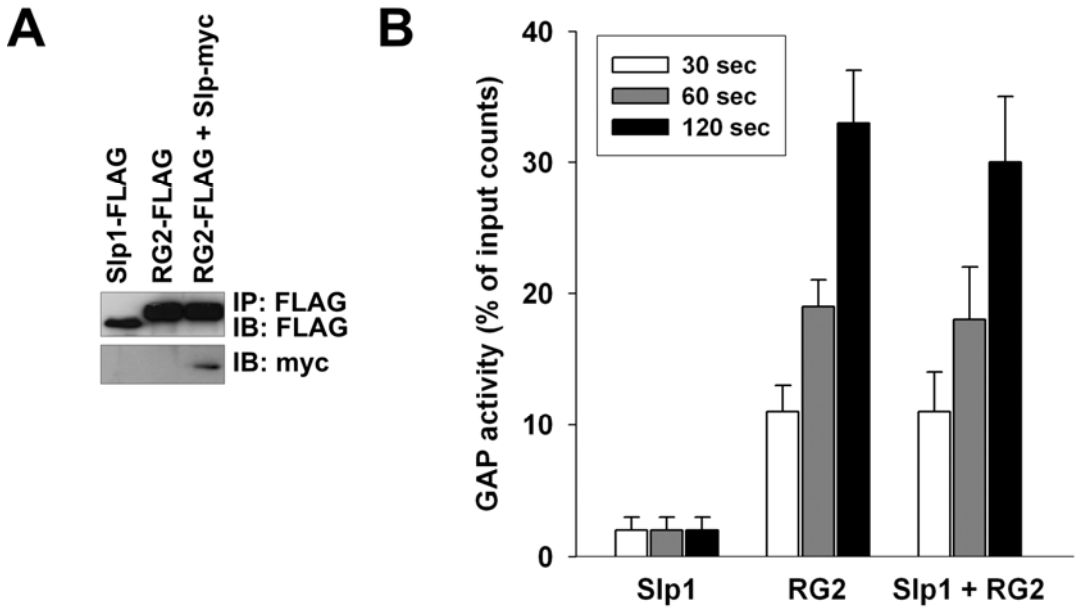

Figure 3.17: Slp1 binding does not affect the GAP activity of Rap1GAP2 *in-vitro*.
HeLa cells were transiently transfected with FLAG-tagged Slp1, FLAG-tagged Rap1GAP2 and FLAG-tagged Rap1GAP2 together with myc-tagged Slp1. Expressed proteins were affinity purified using anti-FLAG agarose beads. The amounts of precipitated Slp1 and Rap1GAP2 were analyzed by immunoblot using anti-FLAG antibody (**A**, *upper panel*). Presence of myc-tagged Slp1 bound to Rap1GAP2 was determined by immunoblot with anti-myc antibody (**A**, *lower panel*). In parallel, His_6-tagged Rap1b was purified from *E.coli* and loaded with [^{32}P]-GTP as described in Materials and Methods (*2.5.1*). Precipitated Slp1 and Rap1GAP2 proteins were added to the GTP-loaded Rap1b, and reactions were incubated at 25°C. Aliquots were removed at indicated time points, amounts of released [^{32}P] were determined by liquid scintillation counting, and plotted as percentage of input Rap1b-bound [^{32}P]-GTP counts. Shown data (**B**) represent the means $\pm$ SD of three independent experiments performed in triplicate.

as described in Materials and Methods (*2.5.2*), and plotted as percentage relative to the total amount of seeded cells. Expression levels of Rap1GAP2 and Slp1 were analyzed by immunoblotting using tag-specific antibodies (Fig.3.18A). As shown in Fig.3.18B, Rap1GAP2 reduced cell adhesion to more than 50 % of mock-transfected cells, whereas Slp1 did not alter cell adhesion. Adhesion of HeLa cells overexpressing both, Rap1GAP2 and Slp1, was similar to cells overexpressing Rap1GAP2 only. In conclusion, Slp1 binding to Rap1GAP2 did not affect the inhibitory function of Rap1GAP2 on Rap1-mediated cell adhesion.

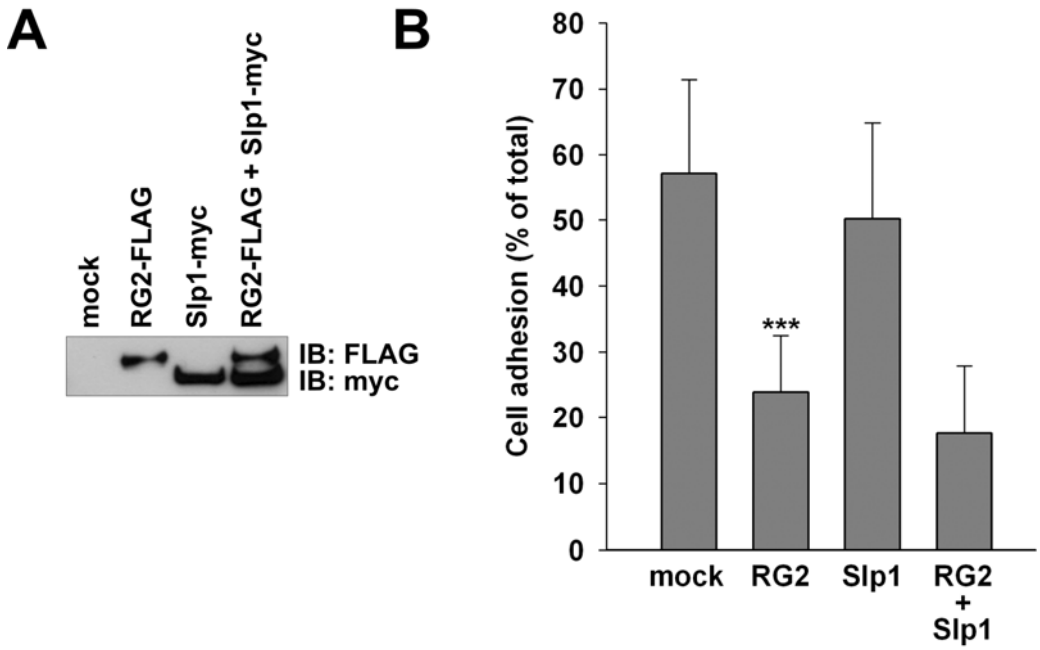

Figure 3.18: Slp1 binding does not affect Rap1GAP2-mediated inhibition of cell adhesion.
HeLa cells were transiently transfected with pRluc-N3 vector expressing luciferase together with FLAG-tagged Rap1GAP2 and myc-tagged Slp1 either alone or in combination. Control cells were transfected with pRluc-N3 vector only (mock). 24 h post-transfection cells were seeded onto fibronectin-coated plates. Adherent cells were quantified and plotted as percentage of the total amount of seeded cells. Shown data (**B**) represent the means ± SD of ten independent experiments performed in quintuplicate. The difference in adhesion between mock-transfected cells and cells transfected with Rap1GAP2 is expressed as $p < 0.001$ and considered as statistically significant. In all experiments equal levels of Rap1GAP2 and Slp1 expression were confirmed by immunoblot using anti-FLAG and anti-myc antibodies (**A**).

3.4.3 Prostate-specific antigen secretion assay

Slp1 was previously shown to be expressed in human prostate carcinoma LNCaP cells and to be involved in secretion of prostate-specific antigen and prostate-specific acid phosphatase in these cells (Johnson et al. 2005). Moreover, LNCaP cells express Rab27a, and Rab27a was demonstrated to regulate the secretion of both, PSA and PSAP (Johnson et al. 2005).

To elucidate the functional consequences of Slp1 binding to Rap1GAP2 in secretion, secretion of PSA was studied. LNCaP cells expressing endogenous Slp1 and Rab27a were transiently transfected with FLAG-tagged Rap1GAP2 (RG2) or the empty vector as negative control (mock). 12 h post-transfection, cells were incubated in absence (DMSO control) or presence of the androgen 6α-fluorotestosterone. LNCaP cells are androgen-responsive, and upon androgen treatment growth and secretion of these cells accelerated. Cells were stimulated for 36 h. Then, cell medium was collected and concentration of secreted PSA was determined using a specific PSA ELISA kit as described under Materials and Methods (*2.5.3*). The secretion of androgen-stimulated mock transfected cells was designated as 100 % secretion. Expression levels of Rap1GAP2 were examined by immunoblot using anti-

FLAG antibody. As expected, upon treatment of LNCaP cells with 6α-fluorotestosterone, expression of Rap1GAP2 was markedly increased compared to untreated cells (Fig.3.19A). In addition, cells overexpressing Rap1GAP2 showed significantly higher baseline (DMSO control) and 6α-fluorotestosterone-stimulated secretion of PSA, compared to mock transfected cells (Fig.3.19B), suggesting a stimulatory role for Rap1GAP2 in secretion.

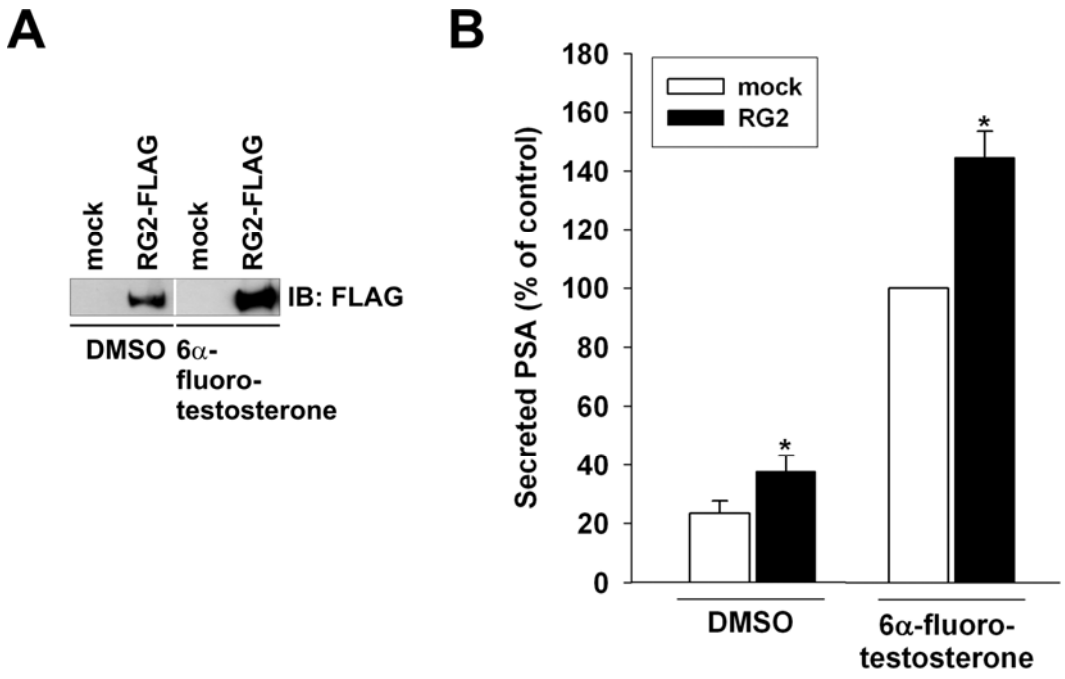

Figure 3.19: Rap1GAP2 stimulates the secretion of PSA in transfected LNCaP cells.
LNCaP cells were transiently transfected with empty vector pcDNA4/TO (mock) or FLAG-tagged Rap1GAP2 (RG2-FLAG). 12 h post-transfection cells were stimulated with 100 nM 6α-fluorotestosterone. Control cells were treated with DMSO. After 36 h cell medium was collected, and concentration of PSA was evaluated using a specific PSA ELISA kit. Shown data (**B**) are means ± SD of eight independent experiments performed in triplicate. The secretion of 6α-fluorotestosterone-stimulated mock cells was arbitrarily designated as 100 % secretion. The difference in PSA secretion between mock and Rap1GAP2 transfected cells is expressed as $p < 0.05$ and considered as statistically significant. In all experiments Rap1GAP2 expression was analyzed by immunoblot using anti-FLAG antibody (**A**).

3.4.4. Serotonin secretion assay of platelet dense granules

To confirm the Rap1GAP2 effect on secretion and to further investigate the impact of Rap1GAP2/Slp1 complex formation in this process, serotonin secretion from platelet dense granules was studied. In platelets, Rab27 has previously been shown to regulate dense granule secretion by interacting with Munc13-4 (Shirakawa et al. 2004). In the present work, the Rab27 binding protein Slp1 has been demonstrated to be expressed in platelets, too (Fig.3.4C). Moreover, Slp1 binds to Rap1GAP2, and a trimeric complex composed of Rap1GAP2, Slp1 and Rab27 is formed in platelets (Fig.3.14D). Therefore, to elucidate the roles of Slp1 and Rap1GAP2 in platelet dense granule secretion, a serotonin secretion assay

using streptolysin-O permeabilized human platelets was established (Flaumenhaft 2004, Shirakawa et al. 2005). Released serotonin which forms a fluorophore with *ortho*-phthalaldehyde was determined using Wallac Victor 1420 Multilabel Counter by a chemical fluorimetric method (*2.5.4,* Holmsen and Dangelmaier 1989).

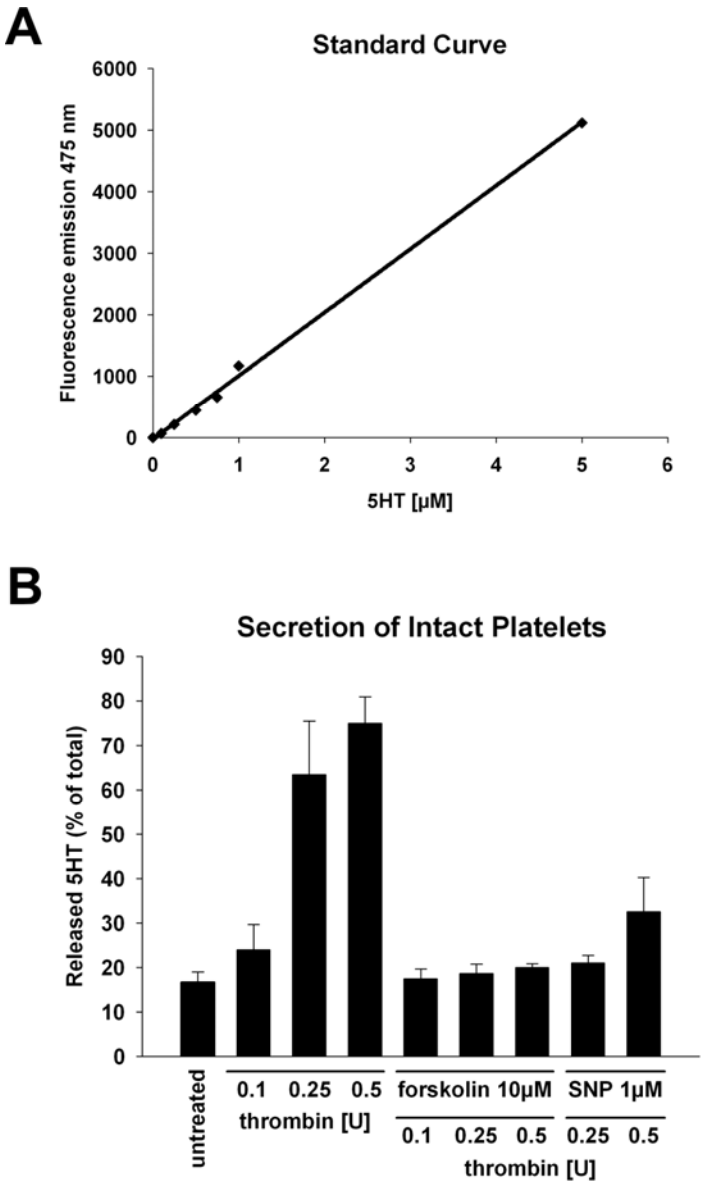

Figure 3.20: Validation of serotonin secretion assay (1).
A: Determination of serotonin creatinine sulfate as standard. Different concentrations ranging from 0 to 5 µM of serotonin creatinine sulfate were measured as described in Materials and Methods (*2.5.4*).
B: Agonist-induced serotonin secretion of intact platelets. Washed human platelets were treated as indicated. Serotonin (5HT) secretion was determined as described in Materials and Methods (*2.5.4*), and plotted as percentage of total serotonin stored in platelet dense granules. Shown data represent the means ± SD of at least three independent experiments.

To first test the accuracy of serotonin determination, serotonin creatinine sulfate was measured as standard. Different concentrations were used ranging from 0 to 5 µM. As shown in Fig.3.20A, a straight standard curve was produced. From the experiments hereafter, the total amount of serotonin in the platelet preparations varied from 2 to 6 µM depending on the donor with a mean platelet concentration of 1 x 10^8 platelets/ml.

It is known that platelet activators (e.g. thrombin) induce secretion of platelet granules, whereas platelet inhibitors (e.g. forskolin, SNP) inhibit platelet granule secretion (Aktas et al. 2003). Therefore and for further assay validation, serotonin secretion of intact platelets treated with platelet activators and inhibitors was evaluated. As shown in Fig.3.20B and expected, treatment of platelets with different concentrations of thrombin induced a concentration-dependent serotonin secretion of platelet dense granules. Up to 75 % $\pm$ 6 of total stored serotonin were released upon treatment of platelets with 0.5 U/ml of thrombin, while baseline serotonin release was 17 % $\pm$ 2. Conversely, treatment of platelets with forskolin or SNP resulted in an almost entire inhibition of thrombin-induced serotonin secretion. The amounts of released serotonin were comparable to that of untreated platelets (Fig.3.20B).

Given the fact that platelets are anucleate cells, they are not amenable to transfection. Therefore, we decided to permeabilize platelets in order to introduce proteins or peptides of interest. Platelets were permeabilized using the pore forming bacterial toxin streptolysin-O, which was a generous gift of Prof. Dr. S. Bhakdi, Mainz, Germany. Streptolysin-O binds as monomer to cellular membranes containing cholesterol, i.e. platelet plasma membrane, followed by oligomerization into ring-shaped structures, which then surround pores of about 30 nm in diameter (Palmer et al. 1998). Importantly, intracellular membranes are not disrupted, preventing thereby the release of granular contents. Assessment of permeabilization was carried out by evaluating the leakage of the cytosolic marker lactate dehydrogenase (LDH), which was monitored by immunoblot. As shown in Fig.3.21A, LDH was detectable in the supernatants of permeabilized platelets only. In contrast, no LDH was present in supernatants of non-permeabilized platelets (Fig.3.21A*, right panel*).

Granule secretion of permeabilized platelets can be stimulated with various agents. Strong activators such as thrombin capable of stimulating intact platelets, as shown in Fig.3.20B, induce granule secretion only within few minutes following permeabilization. However, due to leakage of cytosol, molecules critical for signal transduction diffused from the platelets interior, resulting in platelet irresponsiveness (data not shown). Therefore, to induce granule secretion of permeabilized platelets, calcium ions and the non-hydrolysable GTP analogue guanosine 5`-O-[γ-thio] triphosphate (GTPγS) were used. In order to optimize the time of Ca^{2+} and GTPγS stimulation, kinetics of Ca^{2+}- and GTPγS-induced granule secretion of streptolysin-O permeabilized platelets was analyzed. As shown in Fig.3.21B, Ca^{2+}-induced

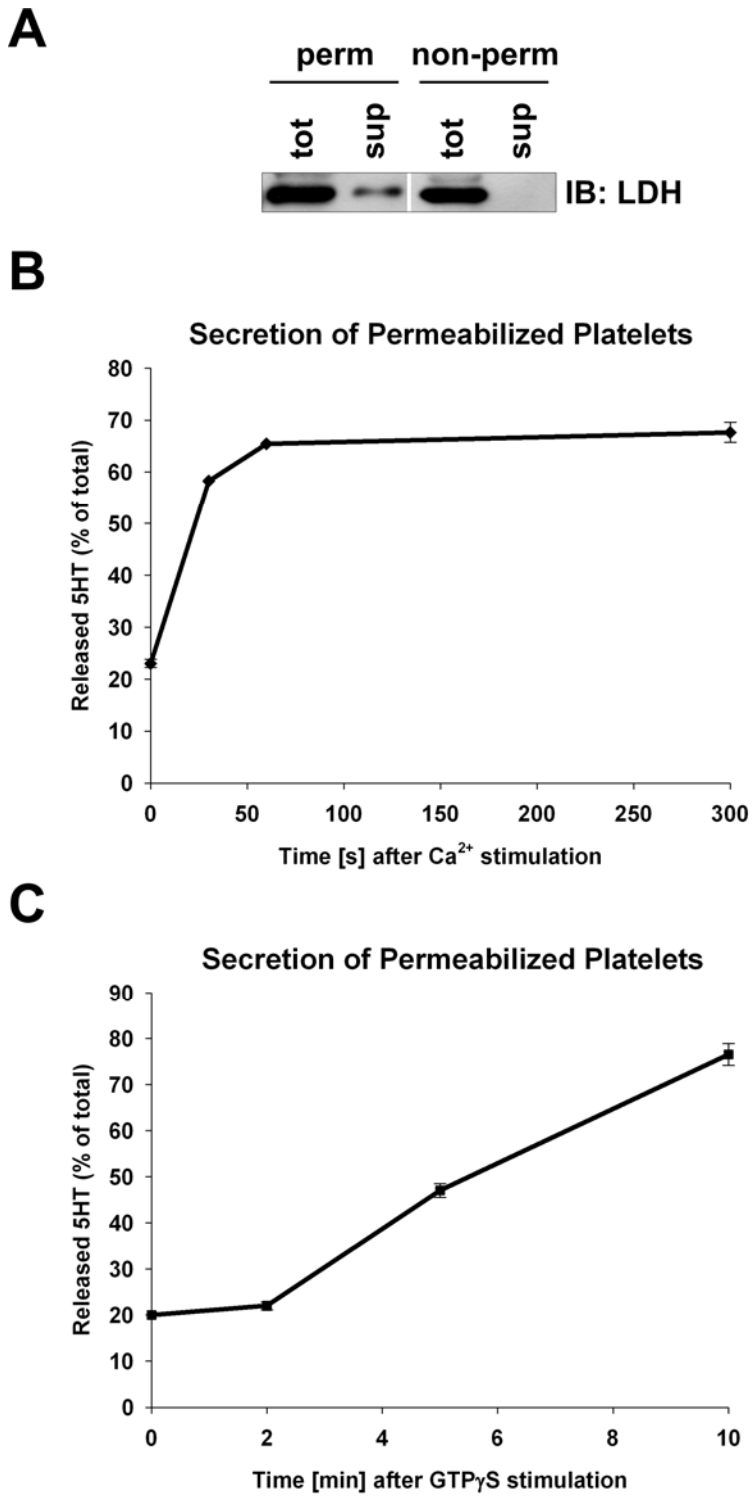

Figure 3.21: Validation of serotonin secretion assay (2).
A: Assessment of platelet permeabilization. Washed human platelets were permeabilized using 0.6 µg/ml streptolysin-O as indicated, and centrifuged. Aliquots of supernatants (sup) and total platelet suspensions (tot) of permeabilized and non-permeabilized platelets were mixed with 3x SDS electrophoresis loading buffer and boiled for 5 min. Proteins were separated by SDS-PAGE and blotted onto a nitrocellulose membrane. The presence of lactate dehydrogenase (LDH) was determined by immunoblot using anti-LDH antibody.
B and **C:** Time-dependent Ca^{2+}- and GTPγS-induced serotonin secretion of permeabilized platelets. Permeabilized platelets were stimulated with Ca^{2+} (B) or GTPγS (C) for the indicated periods of time. Released serotonin (5HT) was measured as described in Materials and Methods (*2.5.4*).

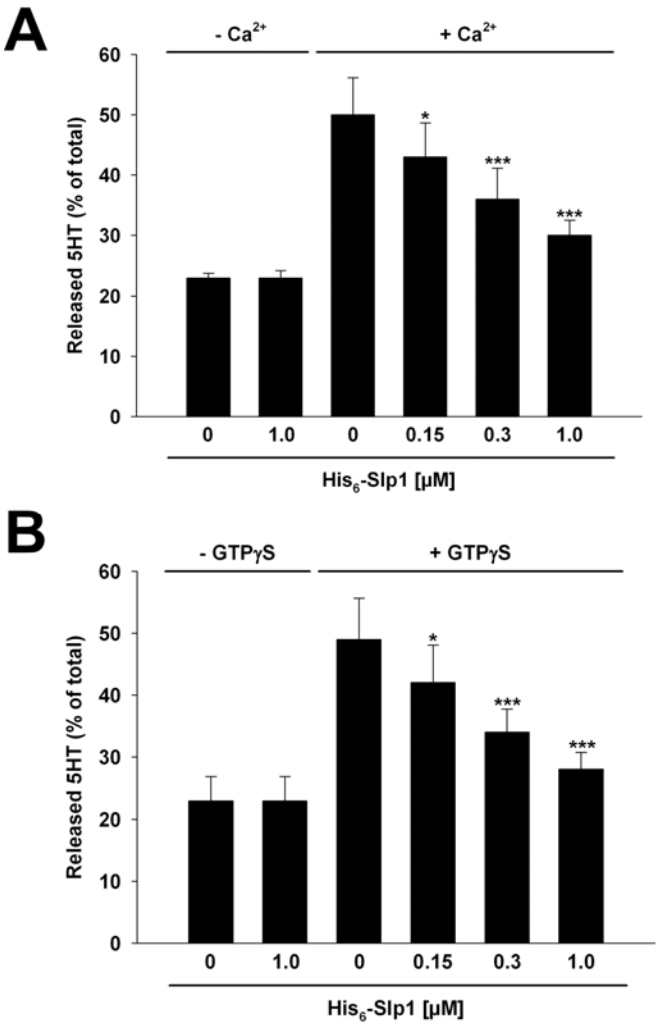

Figure 3.22: Slp1 inhibits platelet dense granule secretion in a dose-dependent manner.
A: Ca^{2+}-induced dense granule secretion after incubation of permeabilized platelets with Slp1. Permeabilized platelets were incubated with the indicated concentrations of purified recombinant His_6-tagged Slp1 and then stimulated with Ca^{2+} for 1 min. For baseline serotonin secretion platelets were left unstimulated in absence or presence of Slp1. Baseline and Ca^{2+}-induced secretion of dense granules were analyzed by measuring released serotonin (5HT) as described in Materials and Methods (*2.5.4*). The results shown are expressed as means ± SD of three independent experiments performed in triplicate. *P* values are expressed as follows * $p < 0.05$ and *** $p < 0.001$ and considered as statistically significant.
B: GTPγS-induced dense granule secretion after incubation of permeabilized platelets with Slp1. Permeabilized platelets were incubated with the indicated concentrations of purified recombinant His_6-tagged Slp1 and then stimulated with GTPγS for 5 min. Baseline and GTPγS-induced secretion of dense granules were analyzed by measuring released serotonin (5HT) as described in Materials and Methods (*2.5.4*). The results shown are expressed as means ± SD of three independent experiments performed in triplicate. *P* values are expressed as follows * $p < 0.05$ and *** $p < 0.001$ and considered as statistically significant.

dense granule secretion was very quick, and granules were efficiently secreted within 1 min after stimulation. In contrast, GTPγS-induced dense granule secretion was much slower (Fig.3.21C). While almost 70 % of stored serotonin was released after 1 min stimulation with Ca^{2+}, the same amount of serotonin was released after 10 min stimulation with GTPγS. Thus, we decided to stimulate permeabilized platelets with Ca^{2+} for 1 min and GTPγS for 5 min.

To test whether Slp1 and Rap1GAP2 are involved in platelet dense granule secretion, permeabilized platelets were incubated with purified recombinant Slp1 and Rap1GAP2 proteins. Upon incubation of permeabilized platelets with purified recombinant Slp1, Ca^{2+}- and GTPγS-induced dense granule secretion was significantly inhibited (Fig.3.22). The inhibitory effect of Slp1 was dose-dependent, while baseline serotonin secretion was not affected by Slp1 (Fig.3.22). In contrast, incubation of permeabilized platelets with purified recombinant wild-type Rap1GAP2 significantly enhanced Ca^{2+}- and GTPγS-induced dense granule release (Fig.3.23A). Baseline levels of serotonin secretion were not changed by Rap1GAP2 (Fig.3.23A). To investigate the relevance of the Rap1GAP2/Slp1 interaction in

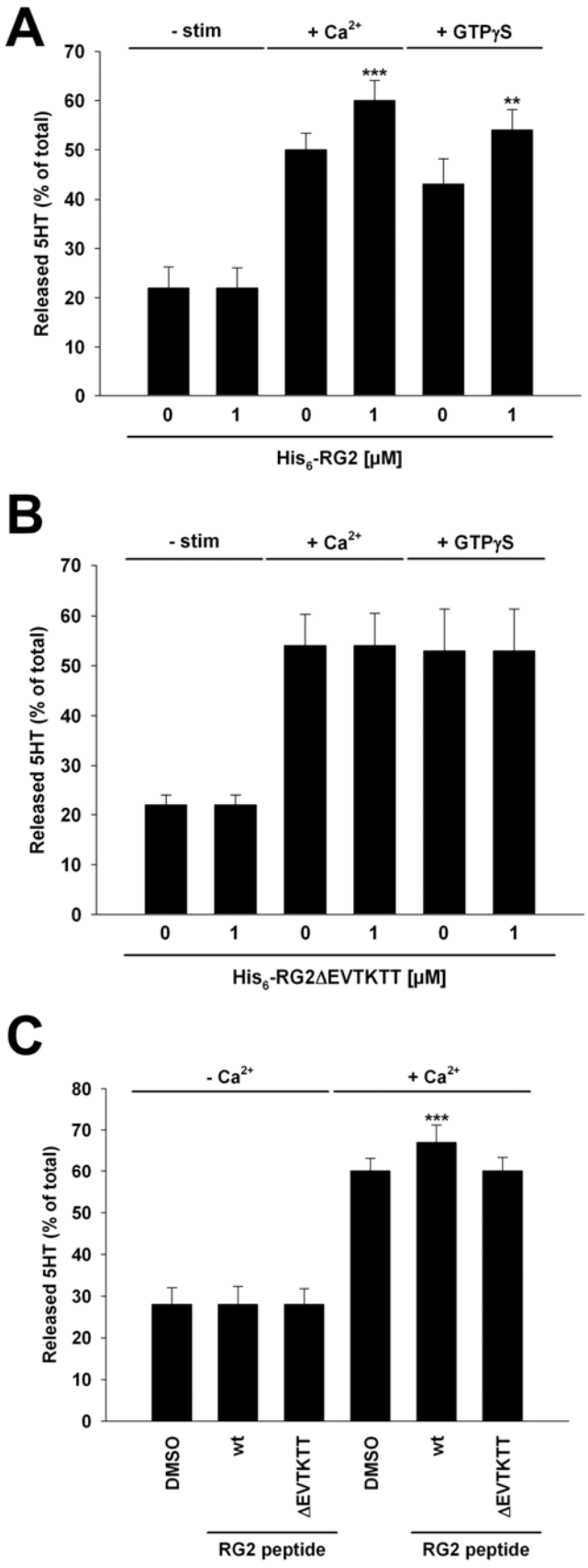

Figure 3.23: Rap1GAP2 augments platelet dense granule secretion by binding to Slp1.

A: Ca^{2+}- and GTPγS-induced dense granule secretion after incubation of permeabilized platelet with wild-type Rap1GAP2. Permeabilized platelets were incubated with or without 1 µM of purified recombinant His_6-tagged wild-type Rap1GAP2 and then stimulated with Ca^{2+} for 1 min or with GTPγS for 5 min. For baseline serotonin secretion, platelets were left unstimulated (-stim) in absence or presence of Rap1GAP2. Baseline and induced secretion of dense granules were analyzed by measuring released serotonin (5HT) as described in Materials and Methods (*2.5.4*). The results shown are expressed as means ± SD of three independent experiments performed in triplicate. *P* values are expressed as follows ** $p < 0.01$ and *** $p < 0.001$ and considered as statistically significant.

B: Ca^{2+}- and GTPγS-induced dense granule secretion after incubation of permeabilized platelet with Rap1GAP2ΔEVTKTT mutant that is deficient in Slp1 binding. Permeabilized platelets were incubated with or without 1 µM of purified recombinant His_6-tagged Rap1GAP2ΔEVTKTT mutant which does not bind Slp1. Then, platelets were stimulated with Ca^{2+} for 1 min or with GTPγS for 5 min. For baseline serotonin secretion, platelets were left unstimulated (-stim) in absence or presence of Rap1GAP2 ΔEVTKTT. Baseline and induced secretion of dense granules were analyzed by measuring released serotonin (5HT) as described in Materials and Methods (*2.5.4*). The results shown are expressed as means ± SD of seven independent experiments performed in triplicate.

C: Permeabilized platelets were incubated with 100 µM of Rap1GAP2 wild-type peptide (RG2wt peptide) or Rap1GAP2 peptide lacking the Slp1 binding motif EVTKTT (RG2ΔEVTKTT peptide). The solvent DMSO was used as negative control. Baseline and Ca^{2+}-induced secretion of dense granules were analyzed by measuring released serotonin (5HT) as described in Materials and Methods (*2.5.4*). The results shown are expressed as means ± SD of five independent experiments performed in triplicate. *P* values are expressed as follows *** $p < 0.001$ and considered as statistically significant.

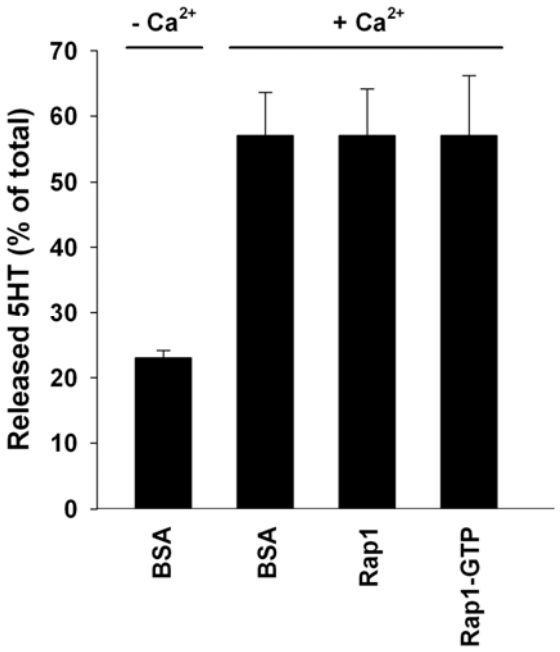

Figure 3.24: Rap1GAP2 effect on platelet dense granule secretion is not mediated by Rap1.
Ca^{2+}-induced dense granule secretion after incubation of permeabilized platelets with Rap1. Permeabilized platelets were incubated with 1 µM of either BSA as control or purified recombinant His_6-tagged native Rap1b or Rap1b loaded with GTP. Then, platelets were stimulated with Ca^{2+} for 1 min. Baseline and Ca^{2+}-induced secretion of dense granules were analyzed by measuring released serotonin (5HT) as described in Materials and Methods (*2.5.4*). The results shown are expressed as means ± SD of five independent experiments performed in triplicate.

secretion, Rap1GAP2ΔEVTKTT mutant deficient in Slp1 binding was purified and tested in the serotonin secretion assay. Incubation of permeabilized platelets with this mutant had no effect on Ca^{2+}- and GTPγS-induced dense granule secretion (Fig.3.23B). In order to corroborate the Rap1GAP2 effect on secretion, Rap1GAP2 peptides, described in *3.2.3,* were tested in secretion assays of permeabilized platelets. The wild-type Rap1GAP2 peptide containing the Slp1 binding -*TKXT*- motif, but not the mutant Rap1GAP2 peptide lacking this motif, augmented Ca^{2+}-induced platelet dense granule secretion (Fig.3.23C). To assure the Rap1GAP2 function in platelet secretion to be independent of the GAP activity of Rap1GAP2, permeabilized platelets were incubated with purified recombinant Rap1 either native or GTP-loaded. As expected, no effect on Ca^{2+}-induced serotonin secretion of platelet dense granules was observed (Fig.3.24). The same results were obtained if permeabilized platelets were incubated with Rap1 and stimulated with GTPγS (data not shown).

In summary, to study the functional relevance of the interaction between Rap1GAP2 and Slp1 in platelet secretion, a serotonin secretion assay using streptolysin-O permeabilized human platelets was set up and validated. Incubation of permeabilized platelets with purified recombinant Slp1 markedly decreased dense granule secretion, whereas addition of purified Rap1GAP2 increased secretion. The stimulation of dense granule secretion by Rap1GAP2 was independent of its GTPase activity but dependent on its ability to bind to Slp1, and deletion of the Slp1-binding -*TKXT*- motif abolished the Rap1GAP2 effect on secretion. Thus, from these data we conclude that Slp1 and Rap1GAP2 play a role in platelet dense granule secretion, and that the effect of Rap1GAP2 depends on the binding of Rap1GAP2 to Slp1.

4. DISCUSSION

4.1 Interaction of Rap1GAP2 and Slp1

4.1.1 The Slp1 binding *-TKXT-* motif of Rap1GAP2

Rap1GAP2 is a unique protein in platelets because it is the only GTPase activating protein of Rap1 expressed in these cells (Schultess et al. 2005). In order to understand the regulation of Rap1GAP2 and to identify possible new functions for this protein, a genetic two-hybrid screening for interacting proteins was performed in yeast using Rap1GAP2 as bait. In addition to the previously described 14-3-3 protein (Hoffmeister et al. 2008), the tandem C2 domain containing protein synaptotagmin-like protein 1 (Slp1) was found to interact with Rap1GAP2. The direct interaction of Rap1GAP2 and Slp1 was verified in yeast as well as in transfected mammalian cells (Fig.3.1 and Fig.3.2). It was shown that Slp1 is expressed in platelets, and the interaction of endogenous Slp1 and Rap1GAP2 was demonstrated by engagement of 14-3-3 (Fig.3.4). 14-3-3 proteins bind to phosphorylated serine 9 within the N-terminus of Rap1GAP2 (Hoffmeister et al. 2008). The serine- and threonine-rich C-terminus of Rap1GAP2, however, has so far been of unknown function. In the present work it was demonstrated that at least part of this C-terminal region of Rap1GAP2 is involved in protein-protein interactions. Mapping studies revealed that Rap1GAP2 binds through amino acids T524-K525-X-T527 within its C-terminus to the C2A domain of Slp1. The Slp1 binding *-TKXT-* motif was verified by three complementary approaches, i.e. pull-down assays using alanine point mutants of Rap1GAP2 protein (Fig.3.9C) and peptide binding assays using either immobilized (Fig.3.9D) or solubized (Fig.3.10) Rap1GAP2 peptides, respectively. Interestingly, this *-TKXT-* motif is not conserved in Rap1GAP1, the closest relative of Rap1GAP2 (Schultess et al. 2005). Consequently, no binding between Rap1GAP1 and Slp1 was observed (Fig.3.3). In Rap1GAP1, both threonine residues are changed to alanines, whereas the lysine residue K525 which corresponds to K503 in Rap1GAP1 is present (Schultess et al. 2005). However, K503 does not suffice to mediate binding of Rap1GAP1 to Slp1. Database search (http://www.ncbi.nlm.nih.gov/blast/Blast.cgi) revealed the *-TKXT-* motif in numerous proteins (e.g. lipoxygenase homology domain containing protein 1, accession number Q8IVV2.2; NEDD4, accession number P46934; phospholipase D2, accession number 014939.2; PTEN-induced putative kinase protein 1, accession number Q9BXM7). However, it remains to be investigated whether any of these proteins are capable of Slp1 binding. The outcome of such binding studies would help define the biochemical value of the *-TKXT-* motif in terms of having a general role in mediating binding to C2 domains. At present, the *-TKXT-* motif of Rap1GAP2 represents a unique new binding motif for the C2A domain of Slp1. The Slp1 binding *-TKXT-* motif could be involved in subcellular

targeting of Rap1GAP2 to the plasma membrane via Slp1 and we indeed observed a co-localization of Rap1GAP2 and Slp1 at the plasma membrane in transfected HeLa cells (Fig.3.13).

4.1.2 The role of the C2 domains of Slp1

C2 domains are generally considered as phospholipid binding domains (Lemmon 2008), and in particular, the C2A domain of Slp1 has been described to bind to phosphoinositides *in-vitro* and in transfected mammalian cells (Catz et al. 2002). Overexpressed DsRed-tagged C2A domain of Slp1 exclusively localized to the plasma membrane in LNCaP cells (Fig.3.6A), and the same was previously observed and reported for the EGFP-C2A chimera in transfected NIH3T3 cells (Catz et al. 2002). Thus, the C2A domain of Slp1 is sufficient and required for Slp1 binding to the plasma membrane. On the other hand, mapping studies in this work revealed that the C2A domain of Slp1 serves as a protein-protein interaction domain and mediates binding of Slp1 to Rap1GAP2. Certain C2 domains have been observed to be involved in protein-protein interactions before. Protein-protein interactions mediated by C2 domains include e.g. the interaction of the C1 and C2 domain of protein kinase C (Kheifets and Mochly-Rosen 2007) and the binding of the C2 domain to the catalytic GAP domain in SynGAP (Pena et al. 2008). In contrast to the C2A domain, the role of the C2B domain of Slp1 remains to be determined. In pull-down assays using the isolated C2B domain of Slp1, no binding to Rap1GAP2 was observed (Fig.3.5). Nonetheless, an engagement of the C2B domain of Slp1 in protein-protein and/or protein-membrane interactions cannot be ruled out. In particular, a cooperative function of both C2 domains of Slp1 appears to be conceivable. For example, the C2 domains of the Ca^{2+}-sensor protein synaptotagmin-I have recently been shown to function synergistically in promoting Ca^{2+}-dependent membrane fusion (Martens et al. 2007, Stein et al. 2007, Fuson et al. 2007, reviewed by Martens and McMahon 2008). Because of similarities observed between the C2A domain of Slp1 and the C2 domains of synaptotagmin-I one could speculate that binding of Slp1 to Rap1GAP2 might be modulated by calcium. However, the two C2 domains of Slp1 are not very likely to bind calcium ions because some aspartic residues known to be involved in calcium binding by synaptotagmins are not conserved in Slp1. To address this point experimentally, we performed pull-down assays in absence or presence of calcium. No difference in binding of Slp1 to Rap1GAP2 was observed (data not shown). This observation renders a possible role for calcium in Slp1/Rap1GAP2 interaction rather unlikely. Moreover, previous studies suggested that increased intracellular calcium concentration decreases binding of the C2A domain of Slp1 to membranes (Catz et al. 2002).

In order to further assess whether the C2A domain of Slp1 is capable of binding to phospholipids and thus plasma membrane and to Rap1GAP2 simultaneously, phospholipid binding (or protein lipid overlay) assays were performed. As expected, the C2A domain and the full-length Slp1 protein bound to phospholipids (Fig.3.6). Interestingly, the lipid specificity of both was different compared to that observed previously (Catz et al. 2002). Both, the C2A domain and Slp1 bound preferentially to phosphatidic acid followed by phosphatidyl-inositolmono- and -bisphosphates. Binding to PtdIns(3,4,5)P_3 was apparent, but rather weak. However, one has to argue that protein lipid overlay assays, albeit fast and convenient, often yield inconsistent results which are mostly due to experimental deviations associated with lipid deposition and preservation on the nitrocellulose membrane. For example, monophosphorylated phosphoinositides such as PtdIns(3)P, PtdIns(4)P, PtdIns(5)P most stably associate with the nitrocellulose membrane and thus tend to give the strongest results (Narayan and Lemmon 2006). Therefore, to define the exact lipid specificity of Slp1 and its C2A domain, additional experiments (e.g. studies in solution using specific lipid vesicles) are required. Nonetheless, protein lipid overlay assays as they have been carried out in this work are sufficient to state that Slp1 binds via its C2A domain to phospholipids and thus the plasma membrane, and that the phospholipid binding ability of Slp1 is not affected by binding of Rap1GAP2.

4.1.3 Phosphorylation at the -*TKXT*- motif of Rap1GAP2

The Slp1 binding -*TKXT*- motif of Rap1GAP2 contains two threonines that could be subject to phosphorylation, and recently the C2 domain of PKCδ was reported to be a phosphotyrosine binding domain (Benes et al. 2005). However, data of the present study suggest that phosphorylation is not required for binding of the C2A domain of Slp1 to the -*TKXT*- motif of Rap1GAP2 (Fig.3.9). On the other hand, platelet inhibition by activation of protein kinase A resulted in enhanced binding of Slp1 to endogenous Rap1GAP2 (Fig.3.11). These data suggest that either Rap1GAP2 or other protein(s) that is/are possibly involved in binding of Rap1GAP2 to Slp1 are phosphorylated by PKA, and that this phosphorylation impacts complex formation of Rap1GAP2 and Slp1 in platelets. From previous studies of our group we know that Rap1GAP2 is a substrate of both, PKA and PKG (Schultess et al. 2005). For example, phosphorylation of serine 7 by PKA and PKG inhibits binding of 14-3-3 to Rap1GAP2, and conversely, phoshorylation of serine 9 by a so far unidentified kinase increases 14-3-3 binding to Rap1GAP2 (Hoffmeister et al. 2008). Supposed that direct phosphorylation of Rap1GAP2 is responsible for the increase in binding of Slp1 to Rap1GAP2, phosphorylation does not occur at the -*TKXT*- motif. *In-vitro* kinase assays revealed that neither T524 nor T527 are phosphorylated by the purified catalytic subunit of PKA (data not shown). Therefore, it is reasonable to assume that the PKA phosphorylation

site is elsewhere within Rap1GAP2 and that this site once phosphorylated is able to positively modulate the interaction of Rap1GAP2 and Slp1. For instance, serine 549 corresponds to the consensus sequence -$(R/K)_2$-X-S/T- for phosphorylation by PKA (http://scansite.mit.edu/motifscan_seq.phtml). However, mutation of serine 549 to alanine did not affect phosphorylation by PKA in *in-vitro* kinase assays (Schultess et al. 2005), and it did not alter binding of Slp1 to Rap1GAP2 in transfected forskolin-treated HeLa cells (data not shown). Recently, a phosphopeptide of Rap1GAP2, comprising the sequence TTFS*PPVVAATVK (amino acids 526-538 of Rap1GAP2), in which serine 529 was phosphorylated, was identified in HeLa cells (Beausoleil et al. 2006). However, mutation of serine 529 to alanine did not affect binding of Slp1 to Rap1GAP2 in transfected cells (data not shown). Thus, the questions whether direct PKA phosphorylation of Rap1GAP2 is responsible for the enhanced binding of Slp1 to Rap1GAP2 and which serine or threonine residue(s) is/are phosphorylated remain to be answered. Also the issue of other protein(s) that could be phosphorylated by PKA and upon phosphorylation could modulate complex formation of Slp1 and Rap1GAP2 is subject for future studies.

Taken together, in the present work Slp1 was identified and verified as a new direct binding partner of Rap1GAP2 in platelets, and has been shown to bind through its C2A domain to the -*TKXT*- motif of Rap1GAP2. Evidence suggests that Slp1 binding to Rap1GAP2 is not affected by calcium or phosphorylation at the -*TKXT*- motif. However, activation of protein kinase A in platelets resulted in enhanced binding of Slp1 to Rap1GAP2. Supposed that PKA directly phosphorylates Rap1GAP2, the exact phosphorylation site remains to be defined. On the other hand, it is also possible that some other protein(s) is/are involved in complex formation between Slp1 and Rap1GAP2 and upon kinase activation modulate binding of Slp1 to Rap1GAP2 in platelets.

4.2 Complex formation of Slp1, Rab27, Rap1GAP2 and other proteins

4.2.1 The Slp1/Rab27 complex

Slp1 is a Rab27 binding protein and is known to interact with Rab27a and Rab27b via its N-terminal Slp homology domain (SHD). Moreover, binding of Slp1 to Rab27 has been reported to be nucleotide-dependent, i.e. Slp1 binds to the GTP-bound form of Rab27 (Kuroda et al. 2002, Strom et al. 2002). In the present work binding of Slp1 to Rab27 was verified in transfected cells and in platelets, and Rap1GAP2 was shown to join the Slp1/Rab27 complex (Fig.3.12 and Fig.3.14).

Binding of Slp1 to Rab27 was first confirmed by co-immunoprecipitation experiments in transfected cells. Therein, binding of Slp1 to Rab27a was stronger than to Rab27b (Fig.3.12).

In pull-down assays, however, binding of Slp1 to both Rab27 isoforms was similar (Fig.3.14). This discrepancy was probably due to different protein amounts of Rab27 used in these different approaches, i.e. co-immunoprecipitation and pull-down experiments, and especially, slight variations in binding of Slp1 to Rab27a or Rab27b, as they might exist, could have been blurred by much higher amounts of Rab27 used in pull-down assays. Therefore, in order to precisely and definitely assess the affinity of Slp1 binding to Rab27a and Rab27b, further studies (e.g. real time and quantitative analysis of the Slp1/Rab27 interaction using BIAcore technology) will be necessary. Notably, also binding of Munc13-4 to Rab27a has been shown to be stronger than its binding to Rab27b (Shirakawa et al. 2004). The question whether the nucleotide state of Rab27 has an effect on Slp1 binding was addressed in pull-down assays using GDP- versus GTP-loaded Rab27. No difference in binding was observed (Fig.3.10). These data confirm recent findings by Johnson et al. 2005 and Hattula et al. 2006, arguing against a role for the nucleotide state of Rab27 in Slp1/Rab27 complex formation. For example, also Slp4/granuphilin-a has been reported to bind Rab27 independently of the nucleotide state of the Rab protein (Fukuda 2005). Additionally, there is evidence suggesting that binding of Slp1 to Rab27 is regulated by phosphorylation. Recently, it was demonstrated that Slp1 is a substrate of protein kinase B (PKB, also termed Akt) and is phosphorylated by this kinase mainly at serine 241 which is located in proximity to the phospholipid binding C2A domain of Slp1 (Johnson et al. 2005). Accordingly, phosphorylation of Slp1 by PKB did not alter binding of Slp1 to Rab27. Instead, phosphorylation of Slp1 by PKB led to the dissociation of Slp1 from the plasma membrane and consequently, redistribution of Slp1 into the cytosol in LNCaP cells (Johnson et al. 2005). In the present work, *in-vitro* kinase assays revealed that Slp1 is a substrate of protein kinase A, and serine 111, which is localized within the Rab27 binding Slp homology domain, was identified as phosphorylation site (Fig.3.15). In platelets activation of PKA resulted in enhanced binding of Slp1 to Rab27 (Fig.3.14), indicating that phosphorylation of Slp1 by PKA could affect binding of Slp1 to Rab27, and indeed, mutation of serine 111 to alanine diminished binding of Slp1 to Rab27 in transfected cells (Fig.3.15). However, it is also possible that Rab27 itself is subject to phosphorylation and likewise, phosphorylation of Rab27 could impinge on binding of Rab27 to Slp1.

Altogether, the results of the present study suggest a constitutive binding of Slp1 to Rab27 in platelets and indicate that Slp1/Rab27 complex formation is affected by phosphorylation. Since Slp1 binding to Rab27 occurred independently of the nucleotide state of the Rab protein and since Rab27 associates with granules only in its GTP-bound state (Behnia and Munro 2005, Barral et al. 2002), it is likely that different pools of Slp1 are present in platelets (Fig.4.1). Slp1 that is bound to GDP-Rab27 may be soluble (reserve cytosolic pool), whereas Slp1 associated with GTP-Rab27 may mainly localize to platelet dense granules (active granule-associated pool). Moreover, the ability of the C2A domain of Slp1 to bind to

phospholipids and thus the plasma membrane suggests that Slp1 may also localize to the plasma membrane in platelets. Thus, it is reasonable to assume that Slp1 might be able to shift between these three distinct subcellular compartments, and accordingly, this might determine the functionality of the Slp1 protein. In particular, association of Slp1 with GTP-Rab27 on platelet dense granules might turn Slp1 into a Rab27 effector, and subsequent interaction of Slp1 with other proteins and/or lipids might help to position the granules to cellular targets (e.g. actin cytoskeleton or plasma membrane). Of course, further studies will be required in order to foremost precisely define the subcellular distribution of Slp1 in platelets and to answer the question of whether and how this distribution might be regulated.

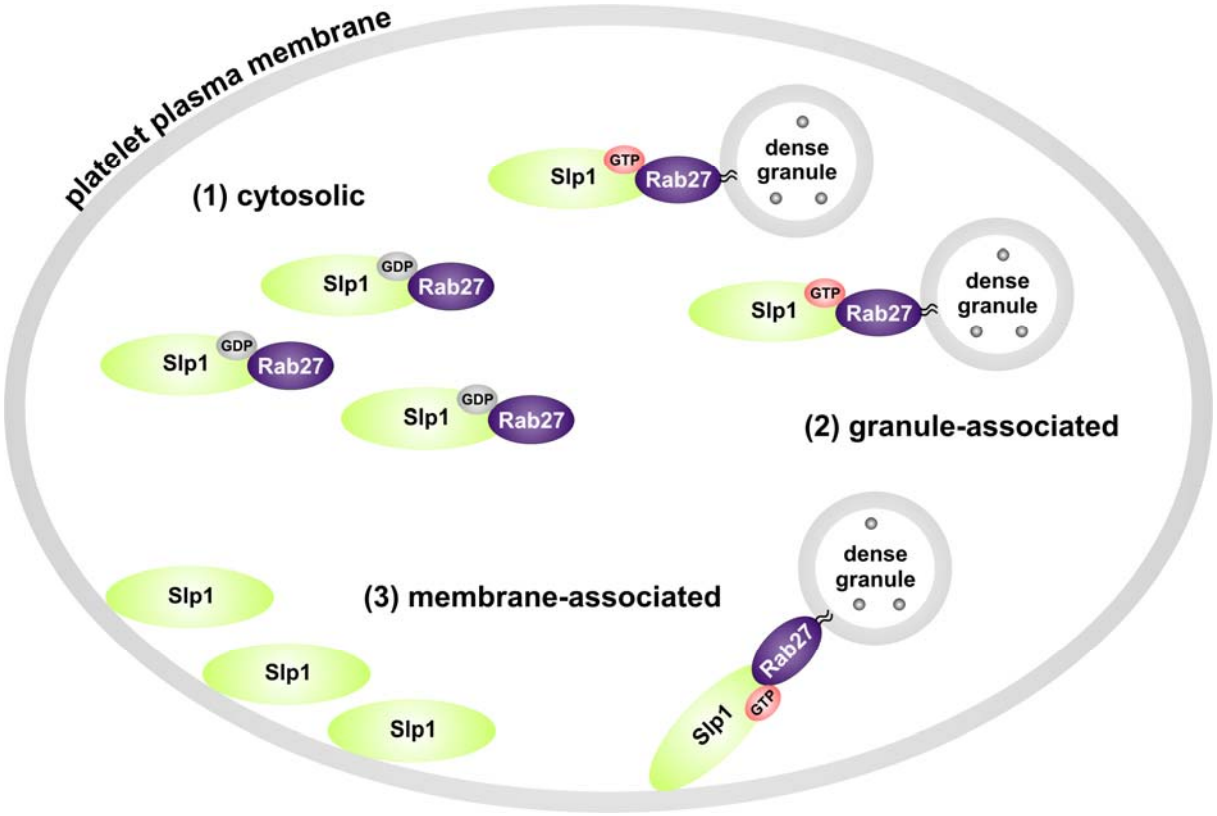

Figure 4.1: Possible subcellular distribution of Slp1 in platelets.
Slp1 is a Rab27 and membrane binding protein and might therefore distribute between three different subcellular compartments in platelets: (1) due to its binding to the inactive GDP-bound form of Rab27 Slp1 is cytosolic; (2) binding of Slp1 to the active GTP-bound form of Rab27, however, shifts Slp1 to platelet dense granules and turns it into a Rab27 effector; (3) finally, membrane binding of Slp1 positions the Slp1 protein at the plasma membrane and/or promotes tethering/docking of Rab27-coated dense granules to the plasma membrane during platelet secretion.

4.2.2 The platelet Slp1 interactome

Rab27 has been shown to regulate platelet dense granule secretion (Shirakawa et al. 2004, Tolmachova et al. 2007). It probably acts by promoting granule motility or by enhancing docking and fusion of granules with the plasma membrane (Seabra and Coudrier 2004, Behnia and Munro 2005, Fukuda 2006). For these functions Rab27 needs to interact with effector proteins, and Slp1 is the second Rab27 effector protein identified in platelets, in addition to Munc13-4 (this work, Shirakawa et al. 2004). In some cases the Rab27/effector protein complex in turn associates with other proteins (e.g. myosin, SNARE or SNARE regulatory proteins) to mediate membrane transport, docking and fusion. For example, Slac2-a/melanophilin simultaneously interacts with Rab27 and the cytoskeletal motor protein myosin Va, thereby enabling melanosome transport in melanocytes (Strom et al. 2002). The Rab27 binding protein Slp4/granuphilin-a directly binds to syntaxin-1a (Torii et al. 2002) and Munc18-1 (Coppola et al. 2002), both important for membrane docking and fusion. In addition, Slp4 is also known to bind to Rab8 and Rab3 at least *in-vitro* (Fukuda 2005). Recently, Slp1 has also been reported to bind to Rab8 in transfected HeLa cells (Hattula et al. 2006). However, the existence of the endogenous Slp1/Rab8 complex e.g. in platelets has not yet been demonstrated. The results of the present work clearly show that Slp1, Rab27 and Rap1GAP2 form a trimeric complex in transfected cells and in platelets, and demonstrate that this complex is affected by phosphorylation (Fig.3.14). In order to identify further proteins that could be involved in the complex formation around Slp1 in platelets, Slp1 affinity chromatography was performed. On the whole, fourteen new putative Slp1 interacting proteins were identified in platelets (Tab.3.1). The presence of Rab27 and Rab8 argues for the success of this biochemical method, and binding of Rab8 to Slp1 was confirmed in pull-down assays (Fig.3.16). The fact that Slp1 interacts with both Rab27 and Rab8 in platelets is of particular interest. Both Rab proteins might functionally overlap. For example, Rab27 and Rab8 colocalize on zymogen granules in pancreatic acinar cells and on melanosomes in melanocytes, and they are both involved in actin-based movement and secretion of these organelles (Chen et al. 2004, Chen et al. 2005, Faust et al. 2008, Fukuda et al. 2002, Chabrillat et al. 2005). In platelets, however, Rab8 has been reported to be present on alpha granules, whereas Rab27 mainly localizes to dense granules (Karniguian et al. 1993, Barral et al. 2002). Therefore, one could speculate that in contrast to Rab27 and in addition to Rab4, Rab8 could play a role in secretion of alpha granules in platelets. However, experimental proof is still missing. In addition, Rab8 has been implicated to regulate the formation of cell shape (Hattula et al. 2006) and cell polarity (Sato et al. 2007). In contrast to Rab8, binding of Rap1 to Slp1 could not be verified in pull-down assays, suggesting that Rap1 is a false-positive because of its very high expression level in platelets (data not shown). On the other hand, absence of Rap1GAP2 on the Slp1 affinity column might be

caused by low expression of Rap1GAP2 in platelets, and could potentially be tackled by forskolin treatment of platelets to enhance Rap1GAP2 binding to Slp1. The presence of Rab32 among the six Rab proteins that were purified with Slp1 is remarkable. Rab32 functions as an A-kinase anchoring protein, as it associates with protein kinase A in intact cells (Alto et al. 2002). In addition, Rab32 has been implicated in protein trafficking in melanosomes (Wasmeier et al. 2006), and has recently been shown to regulate melanosome transport in *Xenopus melanophores* by PKA recruitment (Park et al. 2007). As Slp1 is a substrate of protein kinase A (Fig.3.15), binding of Slp1 to Rab32 might provide an opportunity to spatially and temporally control phosphorylation of Slp1 by PKA in platelets. The presence of myosin-9 (non-muscle myosin heavy chain IIA, NMHC-IIA) together with myosin regulatory light chain 2 and myosin light polypeptide 3 and 6 might be important as well. Myosin-9 is encoded by *MYH9,* and is the only myosin heavy chain isoform expressed in platelets (Sellers 2000). Mutations in *MYH9* are responsible for the so-called *MYH9*-related disorders, i.e. May-Hegglin anomaly, Fechtner syndrome, Sebastian syndrome and Epstein syndrome, which are characterized by the triad of thrombocytopenia, large platelets and leukocyte inclusions (Seri et al. 2003). Myosin-9 is a heterohexameric protein, and becomes activated by phosphorylation of its regulatory light chain subunit. Myosin-9 plays a central role in the cytoskeletal rearrangements underlying platelet shape change during activation, and in platelet secretion (Blockmans et al. 1995, Nishikawa et al 1980, Watanabe et al. 2001).

Altogether, the identified new putative Slp1 interacting proteins are interesting and promising. However, it remains unclear if all these proteins bind to the same macromolecular complex around Slp1 or whether there may be different subcomplexes. In the present study Slp1 was found to interact with Rap1GAP2 in platelets and the trimeric complex of Rap1GAP2, Slp1 and Rab27 was proven. However, it appears unlikely that for example Rab8 can be found within this complex. Slp1 might rather bind to either Rab27 or Rab8 and act as effector protein in separate secretory processes. According to its subcellular localization in platelets (Karniguian et al. 1993), one could speculate that Rab8 regulates platelet alpha granule secretion by e.g. involving the formation of the trimeric complex of Slp1, Rab8 and Rap1GAP2. In addition, myosin-9 might be engaged into these complexes and might help to promote granule motility by connecting platelet alpha and dense granules with the actin cytoskeleton. Certainly, the identified Slp1 interacting proteins complement the Slp1 interactome in platelets (Fig.4.2). The platelet Slp1 interactome can be drawn based on the data of the present study, previously published data and predicted platelet protein-protein interactions by PlateletWeb-Knowledgebase (http://plateletweb.bioapps.biozentrum.uni-wuerzburg.de). PlateletWeb-Knowledgebase allows creating a “virtual” platelet by combining

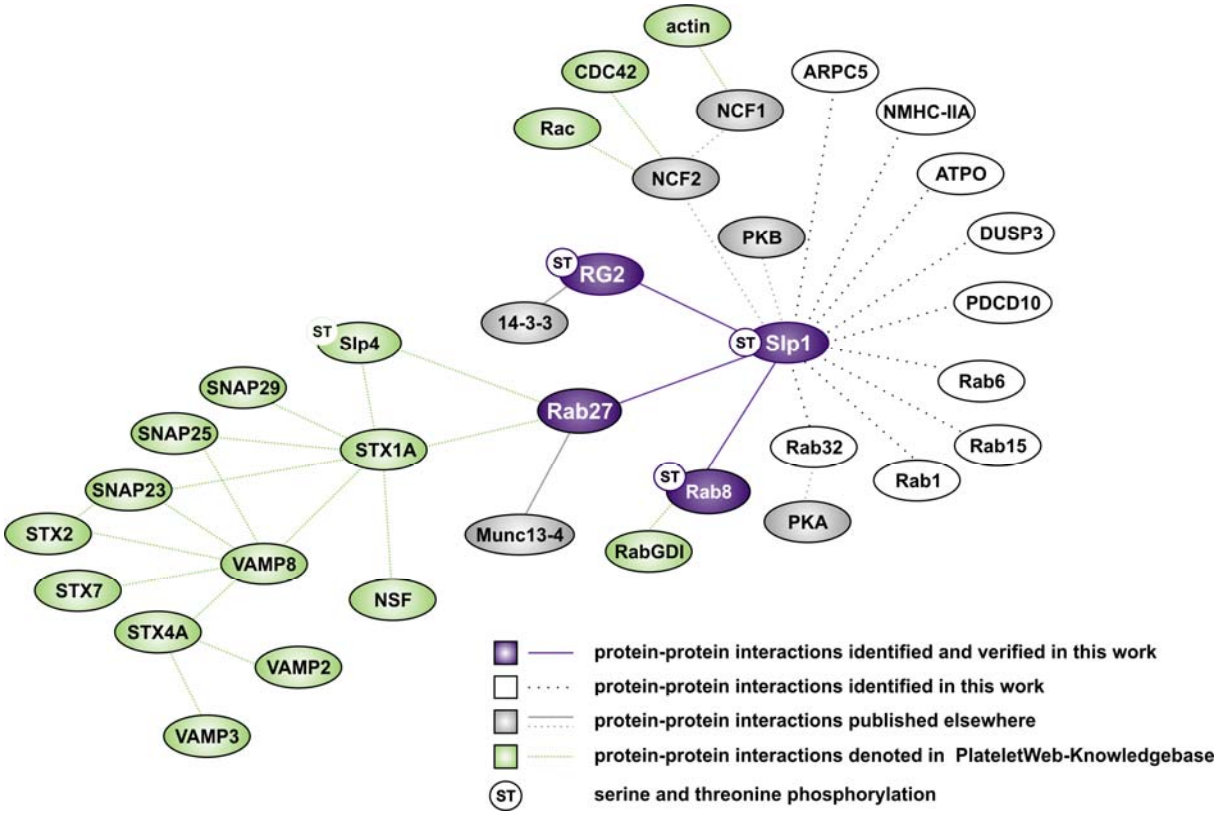

Figure 4.2: The Slp1 interactome in platelets.
Protein-protein interactions that were verified in platelets in the present work are *colored in violet* and *indicated by violet solid line.* Protein-protein interactions that were published and demonstrated in platelets by others are *colored in grey* and *indicated by grey solid line.* Protein-protein interactions that were published by others but need to be verified in platelets are *colored in grey* and *indicated by grey dashed line*. Protein-protein interactions that were identified by affinity chromatography and mass spectrometric analysis but need to be verified by alternative approaches are *uncolored* and *indicated by dashed line*. Protein-protein interactions that are predicted by PlateletWeb-Knowledgebase (http://plateletweb.bioapps.biozentrum.uni-wuerzburg.de) are *colored in green* and *indicated by green dashed line*. ST denotes serine and threonine phosphorylation. ARPC5: actin-related protein 2/3 complex subunit 5; ATPO: ATP synthase subunit O; CDC42: cell division cycle 42; DUSP3: dual specificity protein phosphatase 3; NMHC-IIA: non-muscle myosin heavy chain IIA, also myosin-9; NCF1; neutrophil cytosolic factor 1 (also termed $p47^{phox}$ subunit of NADPH oxidase); NCF2: neutrophil cytosolic factor 2 (also termed $p67^{phox}$ subunit of NADPH oxidase); NSF: N-ethylmaleimide-sensitive factor; PDCD10: programmed cell death protein 10; PKB: protein kinase B; RabGDI: Rab GDP dissociation inhibitor; RG2: Rap1GAP2; Slp: synaptotagmin-like protein; STX: syntaxin; VAMP; vesicle-associated membrane protein.

large scale proteome and transcriptome data with literature-curated data of the Human Protein Reference Database (http://www.hprd.org) (Dittrich et al. 2008). For example, previous publications demonstrated that Slp1 stably associates with PKB (Johnson et al. 2005), and directly interacts with $p67^{phox}$ subunit of NADPH oxidase (NCF2, McAdadra Berkowitz et al. 2001). Although these interactions were not demonstrated in platelets, they are predicted by PlateletWeb-Knowledgebase. Additionally, Slp4 is known to bind to Rab27 (Fukuda 2005). However, the Slp4/Rab27 complex has not yet been verified in platelets. On the other hand, Slp4 expression and its binding to Rab27 in platelets are predicted by PlateletWeb-Knowledgebase. Interestingly, within the platelet Slp1 interactome, Slp1 interacting proteins can be grouped into secretion-related proteins such as Rab and SNARE

proteins and into signaling- or cytoskeleton-related proteins such as Rap1GAP2, PKB, NMHC-IIA and NCFs linking Slp1 to Rac, CDC42 and actin (Fig.4.2). Moreover, the fact that several proteins of the platelet Slp1 interactome are subject to phosphorylation suggests a dynamic regulation of the protein-protein interactions by kinases and phosphates. So far, the results of the present study demonstrate that phosphorylation by protein kinase A modulates the formation of the trimeric complex of Slp1, Rab27 and Rap1GAP2. However, since Slp1 is a substrate of both, PKA and PKB (this work, Johnson et al. 2005), and Rap1GAP2 is known to be phosphorylated by both, PKA and PKG (Schultess et al. 2005), other kinases could be involved as well. In consequence, protein-protein interaction patterns might be significantly rearranged, leading to the so-called dynamic Slp1 interactome in platelets.
Finally, the question whether the new putative Slp1 interacting proteins constitute the complete list of Slp1 protein-protein interactions in platelets will need to be addressed in future studies. Further experiments will also help to validate the identified protein-protein interactions and clarify their relevance for platelet functions (e.g. platelet secretion of alpha and dense granules).

4.3 Involvement of Slp1 and Rap1GAP2 in platelet dense granule secretion

4.3.1 Serotonin secretion assay of permeabilized platelets

To determine the significance of the Slp1/Rap1GAP2 interaction for platelet function and in particular to dissect the roles of Slp1 and Rap1GAP2 in platelet secretion, a previously described technology was adopted and modified, in which platelets were permeabilized by the pore forming bacterial toxin streptolysin-O and secretion of serotonin was measured by a non-radioactive flourimetric method (Flaumenhaft 2004, Shirakawa et al. 2005, Holmsen and Dangelmaier 1989). Since platelets are anucleate cells, they cannot be transfected. Therefore, in order to be able to introduce peptides or proteins into platelets, they need to be permeabilized. In the present work, permeabilization at 30°C with 0.6 µg/ml streptolysin-O proved to allow access to the platelet cytosol without damaging the granule membranes, and was monitored by the appearance of lactate dehydrogenase in the supernatants of permeabilized platelets (Fig.3.21). Then, permeabilized platelets were incubated on ice with peptides and proteins of interest to equilibrate them into the platelet interior. Since streptolysin-O is inactive at 4°C, this cold step decreased the activity of the toxin, thereby lessening the extent of permeabilization of granule membranes (Ahnert-Hilger et al. 1989). When this step was performed at room temperature or extended over the time indicated in Materials and Methods (*2.4.5.*), an increase in the baseline secretion of serotonin from platelet dense granules was observed (data not shown). After rewarming to 30°C for 5 minutes, permeabilzed platelets were treated with 20 µM Ca^{2+} or 100 µM GTPγS to induce

secretion. Several groups have previously demonstrated that Ca^{2+} and GTPγS at the indicated concentrations can stimulate secretion of permeabilized platelets (Padfield et al. 1996, Sloan and Haslam 1997). Interestingly, granule secretion was induced rapidly after addition of Ca^{2+} and reached a plateau after 3 minutes (Fig.3.21). In contrast, GTPγS stimulated granule secretion only after a certain time lag, but once initiated, secretion occurred at comparable rates (Fig.3.21). The delay in GTPγS-induced secretion was perhaps due to the dilution of an important cytosolic factor. Such a dilution apparently has only a limited effect on the Ca^{2+}-induced secretion, although it also requires cytosol (Shirakawa et al. 2005). Alternatively, the delay might be caused by the need for a GDP-GTPγS exchange to activate a G protein which is not needed on Ca^{2+} stimulation. Thus, the difference in kinetics suggests that the two types of stimuli induce secretion through different but potentially parallel pathways. Ca^{2+} probably induces granule secretion by stimulating the final fusion step of the granule with the plasma membrane, whereas GTPγS stimulation might be mediated by small GTPases such as Rab27 or Ral (Padfield et al. 1996, Shirakawa et al. 2004, Kawato et al. 2008). In all cases, dense granule secretion was dependent on ATP, and the creatine phosphate/creatine phosphokinase system was used as an ADP scavenger.

The major difference between the properties of permeabilized and intact platelets was the extent of granule release. The extent of release from permeabilzed platelets was approximately 50 % of that seen for thrombin-induced secretion from intact platelets (Fig.3.20, Flaumenhaft 2004). This difference in release efficiency was again probably due to the dilution of important cytosolic components as they diffused from the platelets, and was further supported by the observation that permeabilized platelets became irresponsive to thrombin within few minutes following permeabilzation (data not shown). Additionally, it should be noted that platelet dense granule secretion was induced at 30°C rather than at 37°C, which also might account for some decrease in release efficiency.

4.3.2 The role of Slp1 in platelet dense granule secretion

Using the above assay a role for Slp1 in platelet dense granule secretion was assigned. Addition of purified recombinant Slp1 to permeabilized platelets strongly inhibited Ca^{2+}- and GTPγS-induced secretion of serotonin in a dose-dependent manner (Fig.3.22). This finding suggests that Slp1 is a negative regulator of platelet dense granule secretion. The inhibitory effect of Slp1 on platelet dense granule secretion was further supported by the observation that the isolated C2A domain of Slp1 augmented serotonin secretion of permeabilized platelets (data not shown). In line with the argument that the C2A domain might compete against a function of endogenous Slp1 protein, this result substantiates the inhibitory role of Slp1 in platelet secretion. However, the literature about effects of Slp1 on secretion in other cells is controversial. Slp1 has previously been demonstrated to positively regulate secretion

of prostate-specific antigen by prostate cells (Johnson et al. 2005) and secretion of azurophilic granules by granulocytes (Munafo et al. 2007). Studies in mice lacking Slp1, however, suggest an inhibitory role for Slp1 in amylase secretion by pancreatic acinar cells (Saegusa et al. 2008). Additionally, data obtained from studies of other Slp family members indicate that Slp proteins have cell type specific functions and may play both, stimulatory and inhibitory roles in secretion through diverse interactions with other proteins or the membrane (Rizo and Rosenmund 2008). For example, Slp2 has been shown to positively affect basal mucus secretion in gastric cells (Saegusa et al. 2006). Moreover, Slp2 has further been implicated in targeting Rab27-coated melanosomes to the plasma membrane in melanocytes (Kuroda and Fukuda 2004), and this effect was attributed to its N-terminal Rab27 binding domain and its C2A domain that mediates binding to phospholipids and thus the plasma membrane. Similarly, Slp2 has been proposed to dock glucagon containing granules to the plasma membrane in pancreatic α-cells (Yu et al. 2007). On the other hand, Slp4 has been reported to negatively regulate dense granule secretion by neuroendocrine PC12 cells (Fukuda et al. 2002) and insulin secretion by pancreatic β-cells (Gomi et al. 2005). The inhibitory effect of Slp4 on secretion is supposed to be mediated by its binding to Munc18-1 and syntaxin-1a (Torii et al. 2002, Coppola et al. 2002, Fukuda 2006). In contrast to Slp1, addition of Munc13-4 enhanced Ca^{2+}-induced secretion of platelet dense granules (Shirakawa et al. 2004). Since Munc13 proteins appear to play prominent roles in vesicle priming (Rizo and Rosenmund 2008), Munc13-4 could presumably be involved in priming of platelet dense granules with the plasma membrane (Fukuda 2005).

Altogether, the results of the present study clearly suggest that Slp1 negatively regulates platelet dense granule secretion. However, the exact molecular mechanism of Slp1 action in platelets remains yet to be determined. A further more detailed study will be required, including experiments on the role of other Slp1 domains and other Slp1 binding partners such as Rab27, Rab8, Rab32 and myosin-9 in platelet secretion.

4.3.3 The role of Rap1GAP2 in platelet dense granule secretion

Next, the role of Rap1GAP2 in secretion was analyzed. Studies in LNCaP cells pointed to a putative stimulatory role of Rap1GAP2 in secretion of prostate-specific antigen (Fig.3.19). Addition of purified recombinant Rap1GAP2 protein to permeabilized platelets led to a small but highly significant stimulation of platelet dense granule secretion. Rap1GAP2 augmented both, Ca^{2+}- and GTPγS-induced secretion of platelet dense granules (Fig.3.23A). Importantly, this effect was strictly dependent on the binding of Rap1GAP2 to Slp1. Deleting the Slp1 binding -*TKXT*- motif in Rap1GAP2 abolished the stimulatory effect of Rap1GAP2 on platelet secretion (Fig.3.23B). The Rap1GAP2 effect on platelet secretion was further confirmed by a complementary approach using Rap1GAP2 peptides. Rap1GAP2 wild-type peptide

containing the Slp1 binding -*TKXT*- motif augmented serotonin secretion comparable to the full-length Rap1GAP2 protein. In contrast, a mutant peptide lacking the -*TKXT*- motif had no effect on secretion (Fig.3.23C). Moreover, it was demonstrated that the stimulatory effect of Rap1GAP2 on secretion was not dependent on the GTPase activating function of Rap1GAP2 and thus Rap1. Given the fact that Rap1 was found to be associated with secretory granules in e.g. neutrophils and pancreatic acinar cells (Maridonneau-Parini and de Gunzburg 1992, Chen X et al. 2005), it has been speculated that Rap1 might be involved in secretion (Bos et al. 2001). However, we and others did not observe any effect of Rap1 on secretion of platelet dense granules (Fig.3.24, Shirakawa et al. 2004). In addition, Slp1 binding to Rap1GAP2 also had no effect on the catalytic GTPase activity of Rap1GAP2 in *in-vitro* GAP assays using purified proteins (Fig.3.17).

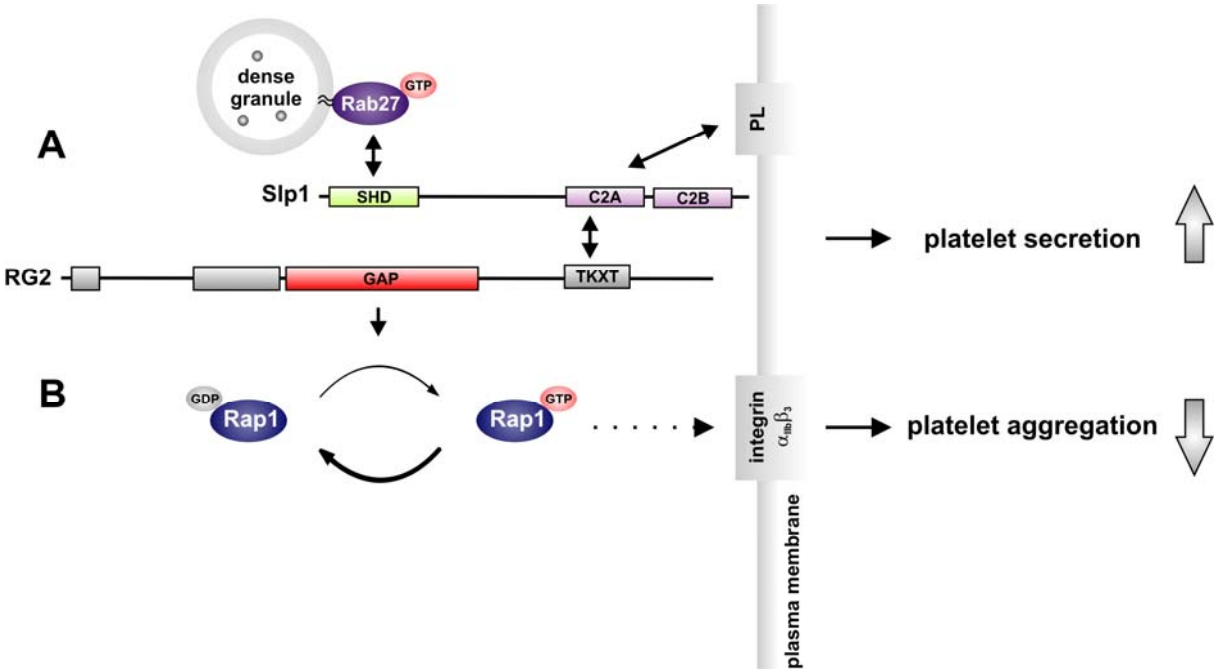

Figure 4.3: Rap1GAP2 is involved in both platelet secretion and aggregation.
The -*TKXT*-mediated interaction of Rap1GAP2 (RG2) with the Rab27 and membrane binding protein Slp1 is important for platelet dense granule secretion (**A**). Slp1 is recruited to Rab27 on platelet dense granules. By simultaneously interacting with Rab27 and phospholipids (*denoted by PL*) Slp1 presumably links dense granules with the plasma membrane. Rap1GAP2 interacts with Slp1 via the Slp1 binding -*TKXT*- motif and augments platelet dense granule secretion. On the other hand, Rap1GAP2 is a GTPase activating protein specific for Rap1 and is required for the GTPase function of Rap1 (**B**). Rap1GAP2 enables the formation of Rap1-GDP, thereby terminating the activatory effect of Rap1-GTP on platelet integrin $\alpha_{IIb}\beta_3$ (*denoted by dashed line*), leading to reduced platelet aggregation.

Thus, the results of the present study for the first time demonstrate that Rap1GAP2 is involved in secretion, and the stimulatory effect of Rap1GAP2 is mediated by a completely new mechanism, involving the interaction of Rap1GAP2 with the tandem C2 domain containing and Rab27 binding protein Slp1. To explain the Rap1GAP2 effect on secretion,

one could speculate that binding of the -*TKXT*- motif of Rap1GAP2 to the C2A domain of Slp1 positively affects the cooperation between the Slp1 tandem C2A and C2B domains (Fuson et al. 2007), which might be required for full activation of membrane fusion by both domains (Martens et al. 2007, Stein et al. 2007).

From these data we conclude that Rap1GAP2 and Slp1 are important new components of the protein machinery mediating platelet dense granule secretion. Since Rap1GAP2 is a regulator of Rap1 and thus of platelet aggregation, the findings of the present study suggest that Rap1GAP2 is involved in both, aggregation and secretion (Fig.4.3), and might serve to coordinate these crucial platelet functions.

5. FUTURE PERSPECTIVES

In the present work it was demonstrated that the tandem C2 domain containing and Rab27 binding protein Slp1 is expressed in platelets and interacts with the GTPase activating protein of Rap1, Rap1GAP2. Binding of Rap1GAP2 to Slp1 is mediated by the new *-TKXT-* protein motif in Rap1GAP2 that binds to the C2A domain of Slp1. Furthermore, both Slp1 and Rap1GAP2 were shown to be involved in platelet dense granule secretion. Of course, further experimentation will be required to clarify the exact molecular mechanism of Slp1 and Rap1GAP2 action in platelet secretion. For example, it will be necessary to analyze the subcellular distribution of Slp1 and Rap1GAP2 e.g. in resting and activated platelets. To this end, platelet fractionation assays and electron microscopy approaches could be used. Besides dense granules, platelets contain alpha granules and lysosomes. Thus, it is interesting to know whether Slp1 and Rap1GAP2 are involved in platelet dense granule secretion alone or whether they also play a role in platelet alpha and lysosomal granule release. This could be addressed in secretion assays of permeabilized platelets by monitoring the release of von Willebrand factor and β-hexosaminidase, respectively. Moreover, on the way to further unravel the molecular details of Slp1 and Rap1GAP2 action in platelet secretion, one could perform lipid binding assays using liposomes as described by Martens et al. 2007. For example, it has been reported that Slp2, a member of the synaptotagmin-like protein family, binds to Folch liposomes in a Ca^{2+}-independent manner and induces membrane curvature *in-vitro* (Martens et al. 2007), and this phenomenon was attributed to the presence of the two tandem C2 domains in Slp2. Thus, one could ask the question whether Slp1 or its tandem C2A and C2B domains are also capable of membrane deformation and how it might be affected by Rap1GAP2 protein or peptide containing the Slp1 binding *-TKXT-* motif. In addition to Slp1, database search using PlateletWeb-Knowledgebase (http://plateletweb.bioapps.biozentrum.uni-wuerzburg.de) revealed Slp4 to be present in platelets. It will be interesting to verify whether Slp4 is expressed in platelets and whether it also might be involved in platelet secretion. Initial studies were performed to analyze binding of Rap1GAP2 to Slp2, Slp3, Slp4, and Slp5, however, further experiments e.g. using purified Slp proteins will be required to conclusively exclude binding of Rap1GAP2 to Slp family members apart from Slp1. Moreover, a number of putative new Slp1 interacting proteins were identified in platelets. Binding of Slp1 to Rab8 was confirmed in pull-down assays, however, it remains to be investigated whether Slp1 and Rab8 interact at the complete endogenous level in platelets and whether a trimeric complex of Slp1, Rab8 and Rap1GAP2 can be formed. In addition, the question whether Rab8 is involved in platelet secretion has to be addressed in secretion assays of permeabilized platelets. Given the fact that multiple Rab27 binding proteins (e.g. Slp1 and Munc13-4) are present in platelets one

could also ask the question how these proteins discriminately bind to Rab27 or other Rab proteins (e.g. Rab8), and how they differentially, sequentially or synergistically function in the same cell. Moreover, the question how all these protein-protein interactions are regulated during platelet activation or platelet inhibition will be a future challenge. Finally, the obtained knowledge on the molecular mechanisms governing platelet granule secretion needs to be consolidated in order to develop new strategies for antiplatelet drugs. First evidence suggests that targeting the platelet secretory machinery might be an effective way to manage thrombosis *in-vivo*, i.e. limiting clot formation without inducing excessive bleeding (reviewed by Ren et al. 2008). In particular, the identification of the Slp1 binding -*TKXT*- motif raises the question of its pharmacological value in terms of being a potential target to modify platelet granule release. One could imagine developing specific and cell permeable -*TKXT*- peptidomimetics that bind Slp1 but do not augment but rather block platelet granule release. Structural analysis of the Rap1GAP2/Slp1 complex by means of crystallography approaches will help to proceed in that direction.

6. REFERENCES

Ahnert-Hilger G., Mach W., Föhr K.J., Gratzl M., (1989). Poration by alpha-toxin and streptolysin O: an approach to analyze intracellular processes. *Methods Cell Biol* 31:63-90.

Agatep R., Gietz, R.D., (1998): Transformation of Saccharomyces cerevisiae by the lithium acetate / single-stranded carrier DNA / polyethylene glycol protocol. *Technical Tips Online* 1

Ali B.R., Seabra M.C., (2005). Targeting Rab GTPases to cellular membranes. *Biochem Soc Trans* 33: 652-6

Alto N.M., Soderling J., Scott J.D., (2002). Rab32 is an A-kinase anchoring protein and participates in mitochondrial dynamics. *J Cell Biol* 158: 659-668.

Andrews R.K., Shen Y., Gardiner E.E., Dong J., Lopez J.A., Berndt M.C., (1999). The glycoprotein Ib-IX-V complex in platelet adhesion and signaling. *Thromb Haemost* 82: 357-64.

Andrews N.W. (2000). Regulated secretion of conventional lysosomes. *Trends Cell Biol* 10: 316-21.

Aszódi A., Pfeifer A., Ahmad M., Glauner M., Zhou X.H., Ny L., Andersson K.E., Kehrel B., Offermanns S., Fässler R., (1999). The vasodilator-stimulated phosphoprotein (VASP) is involved in cGMP- and cAMP-mediated inhibition of agonist-induced platelet aggregation, but is dispensable for smooth muscle function. *EMBO J* 18: 37-48.

Atkinson B., Dwyer K., Enjyoji K., Robson S.C., (2006). Ecto-nucleotidases of the CD39/NTPDase family modulate platelet activation and thrombus formation: potential as therapeutic targets. *Blood Cells Mol Dis* 36: 217-22.

Barral D.C., Ramalho J.S., Anders R., Hume A.N., Knapton H.J., Tolmachova T., Collinson L.M., Goulding D., Authi K.S., Seabra M.C., (2002). Functional redundancy of Rab27 proteins and the pathogenesis of Griscelli syndrome. *J Clin Invest* 110: 247-57.

Beausoleil S.A., Villen J., Gerber S.A., Rush J., Gygi S.P., (2006). A probability-based approach for high-throughput protein phosphorylation analysis and site localization. *Nat Biotechnol* 24:1285-92.

Behnia R., Munro S., (2005). Organelle identity and the signposts for membrane traffic. *Nature* 438: 597-604.

Benes C.H., Wu N., Elia A.E., Dharia T., Cantley L.C., Soltoff S.P., (2005). The C2 domain of PKC delta is a phosphotyrosine binding domain. *Cell* 121: 271-80.

Berg J.S., Powel B.C., Cheney R.E., (2001) A millennial myosin census. *Mol Biol Cell* 12: 780-94.

Bertoni A., Tadokoro S., Eto K., Pampori N., Parise L.V., White G.C., Shattil S.J., (2002). Relationships between Rap1b, affinity modulation of integrin alphaIIbbeta3, and the actin cytoskeleton. *J Biol Chem* 277: 25715-21.

Blockmans D., Deckmyn H., Vermylen J., (1995). Platelet activation. *Blood Rev* 9: 143-56.

Bos J.L., de Rooij J., Reedquist K.A., (2001). Rap1 signaling: adhering to new models. *Nat Rev Mol Cell Biol* 2: 369-77.

Bos J.L., de Bruyn K., Enserink J., Kuiperij B., Rangarajan S., Rehmann H., Riedl J., de Rooij J., van Mansfeld F., Zwartkruis F., (2003). The role of Rap1 in integrin-mediated cell adhesion. *Biochem Soc Trans* 31: 83-6.

Bos J.L., (2005). Linking Rap to cell adhesion. *Curr Opin Cell Biol* 17: 123-8.

Bos J.L., Rehmann H., Wittinghofer A., (2007). GEFs and GAPs: critical elements in the control of small G proteins. *Cell* 129: 865-77.

Brass L.F., (2003). Thrombin and platelet activation. *Chest* 124: 18-25.

Burgoyne R.D., Morgan A., (2003). Secretory granule exocytosis. *Physiol Rev* 83: 581-632.

Butt E., Abel K., Krieger M., Palm D., Hoppe V., Hoppe J., Walter U., (1994). cAMP- and cGMP-dependent protein kinase phosphorylation sites of the focal adhesion vasodilator-stimulated phosphoprotein (VASP) in vitro and in intact human platelets. *J Biol Chem* 269: 14509-17.

Camerer E., Huang W., Coughlin S.R., (2000). Tissue factor- and factor X-dependent activation of protease-activated receptor 2 by factor VIIa. *Proc Natl Acad Sci USA* 97: 5255-60.

Catz S.D., Johnson J.L., Babior B.M., (2002). The C2A domain of JFC1 binds to 3'-phosphorylated phosphoinositides and directs plasma membrane association in living cells. *Proc Natl Acad Sci USA* 99: 11652-7.

Chabrillat M.L., Wilhelm C., Wasmeier C., Sviderskaya E.V., Louvard D., Coudrier E., (2005). Rab8 regulates the actin-based movement of melanosomes. *Mol Biol Cell* 16: 1640-50.

Chen D., Bernstein A.M., Lemons P.P., Whiteheart S.W., (2000a). Molecular mechanisms of platelet exocytosis: role of SNAP-23 and syntaxin 2 in dense core granule release. *Blood* 95: 921-9.

Chen D., Lemons P.P., Schraw T., Whiteheart S.W., (2000b). Molecular mechanisms of platelet exocytosis: role of SNAP-23 and syntaxin 2 and 4 in lysosome release. *Blood* 96: 1782-8.

Chen X., Walker A.K., Strahler J.R., Simon E.S., Tomanicek-Volk S.L., Nelson B.B., Hurley M.C., Ernst S.A., Williams J.A., Andrews P.C., (2005). Organellar Proteomics – Analysis of pancreatic zymogen granules membranes. *Mol Cell Proteom* 5: 306-312.

Chintala S., Tan J., Gautam R., Rusiniak M.E., Guo X., Li W., Gahl W.A., Huizing M., Spritz R.A., Hutton S., Novak E.K., Swank R.T., (2007). The Slc35d3 gene, encoding an orphan nucleotide sugar transporter, regulates platelet-dense granules. *Blood* 109: 1533-40.

Chrzanowska-Wodnicka M., Smyth S.S., Schoenwaelder S.M., Fischer T.H., White G.C. II, (2005). Rap1b is required for normal platelet function and hemostasis in mice. *J Clin Invest* 115: 680-7.

Chung S.H., Polgar J., Reed G.L., (2000). Protein kinase C phosphorylation of syntaxin 4 in thrombin-activated human platelets. *J Biol Chem* 275: 25286-91.

Clary D.O., Griff I.C., Rothman J.E., (1990). SNAPs, a family of NSF attachment proteins involved in intracellular membrane fusion in animals and yeast. *Cell* 61: 709-21.

Colman R.W., (2004). Platelet cyclic adenosine monophosphate phosphodiesterases: targets for regulating platelet related thrombosis. *Semin Thromb Hemost* 30: 451-60.

Coppinger J.A., Maguire P.B., (2007). Insights into the platelet releasate. *Curr Pharm Des* 13: 2640-6.

Coppola T., Frantz C., Perret-Menoud V., Gattesco S., Hirling H., Regazzi R., (2002). Pancreatic beta- cell protein granuphillin binds Rab3 and Munc-18 and controls exocytosis. *Mol Biol Cell* 13: 1906-15.

Coughlin S.R., (2000). Thrombin signaling and protease-activated receptors. *Nature* 407: 258-64.

Coughlin S.R., (2005). Protease-activated receptors in hemostasis, thrombosis and vascular biology. *J Thromb Haemost* 3: 1800-14.

Crittenden J.R., Bergmeier W., Zhang Y., Piffath C.L., Liang Y., Wagner D.D., Housman D.E., Graybiel A.M., (2004). CalDAG-GEFI integrates signaling for platelet aggregation and thrombus formation. *Nat Med* 10: 982-6.

Danielewski O., Schultess J., Smolenski A.P., (2005). The NO/cGMP pathway inhibits Rap1 activation in human platelets via cGMP-dependent protein kinase I. *Thromb Haemost* 93: 319-25.

Danielewski O., (2005). Der NO/cGMP Signalweg reguliert das kleine G Protein Rap1B in humanen Thrombozyten. Dissertation zur Erlangung des Doktorgrades der Naturwissenschaften, Frankfurt a.M.

Daubie V., (2007). Pochet R., Houard S., Philippart P., Tissue factor: a mini-review. *J Tissue Eng Regen Med* 1: 161-9.

Daumke O., Weyand M., Chakrabarti P.P., Vetter I.R., Wittinghofer A., (2004). The GTPase-activating protein Rap1GAP uses a catalytic asparagine. *Nature* 429: 197-201.

Davi G., Patrono C., (2007). Platelet activation and atherothrombosis. *N Engl J Med* 357: 2482-94.

Denis M.M., Tolley N.D., Bunting M., Schwertz H., Jiang H., Lindemann S., Yost C.C., Rubner F.J., Albertine K.H., Swoboda K.J., Fratto C.M., Tolley E., Kraiss L.W., McIntyre T.M., Zimmermann G.A., Weyrich A.S., (2005). Escaping the nuclear confines: signal-dependent pre-mRNA splicing in anucleate platelets. *Cell* 122: 379-91.

Detter J.C., Zhang Q., Mules E.H., Novak E.K., Mishra V.S., Li W., McMurtrie E.B., Tchernev V.T., Wallace M.R., Seabra M.C., (2000). Swank R.T., Kingsmore S.F., Rab geranylgeranyl transferase alpha mutation in the gunmetal mouse reduces Rab prenylation and platelet synthesis. *Proc Natl Acad Sci USA* 97: 4144-9.

Dittrich M., Birschmann I., Mietner S., Sickmann A., Walter U., Dandekar T., (2008). Platelet protein interactions. Map, signaling components and phosphorylation groundstate. *Arterioscler Thromb Vasc Biol* 28: 1326-31.

Elzagallaai A., Rose S.D., Trifaro J.M., (2000). Platelet secretion induced by phorbol esters stimulation is mediated through phosphorylation of MARCKS: a MARCKS-derived peptide blocks MARCKS phosphorylation and serotonin release without affecting pleckstrin phosphorylation. *Blood* 95: 894-902.

Elzagallaai A., Rose S.D., Brandan N.C., Trifaro J.M., (2001). Myristoylated alanine-rich C kinase substrate phosphorylation is involved in thrombin-induced serotonin release from platelets. *Br J Haematol* 112: 593-602.

Faust F., Gomez-Lazaro M., Borta H., Agricola B., Schrader M., (2008). Rab8 is involved in zymogen granule formation in pancreatic acinar AR42J cells. *Traffic* 9: 964-79.

Flaumenhaft R., Croce K., Chen E., Furie B., Furie B.C., (1999). Proteins of the exocytotic core complex mediate platelet alpha-granule secretion: roles of vesicle-associated membrane protein, SNAP-23, and syntaxin 4. *J Biol Chem* 274: 2492-501.

Flaumenhaft R., (2003). Molecular basis of platelet granule secretion. *Arterioscler Thromb Vasc Biol* 23: 1152-60.

Flaumenhaft R., (2004). Platelet permeabilization. *Meth Mol Biol* 273: 365-78.

Franke B., Akkerman J.W., Bos J.L., (1997). Rapid Ca^{2+}-mediated activation of Rap1 in human platelets. *EMBO J* 16: 252-9.

Fukuda M., (2005). Versatile role of Rab27 in membrane trafficking: focus on the Rab27 effector families. *J Biochem* 137: 9-16.

Fukuda M., (2006). Rab27 and its effectors in secretory granule exocytosis: a novel docking machinery composed of a Rab27 effector complex. *Biochem Soc Trans* 34: 691-5.

Fukuda M., Kanno E., Saegusa C., Ogata Y., Kuroda T.S., (2002). Slp4-a/granuphillin-a regulates dense-core vesicle exocytosis in PC12 cells. *J Biol Chem* 277: 39673-78.

Fukuda M., Mikoshiba K., (2001). Synaptotagmin-like protein 1-3: a novel family of C-terminal-type tandem C2 proteins. *Biochem Biophys Res Commun* 281: 1226-33.

Fukuhara S., Chikumi H., Gutkind J.S., (2001). RGS-containing RhoGEFs: the missing link between transforming G proteins and Rho? *Oncogene* 20: 1661-8.

Fullard J.F., (2004). The role of the platelet glycoprotein IIb/IIIa in thrombosis and haemostasis. *Curr Pharm Des* 10: 1567-76.

Furie B., Furie B.C., Flaumenhaft R., (2001). A journey with platelet P-selectin: the molecular basis of granule secretion, signalling and cell adhesion. *Thromb Haemost* 86: 214-21.

Fuson K.L., Montes M., Robert J.J., Sutton R.B., (2007). Structure of human synaptotagmin 1 C2AB in the absence of Ca^{2+} reveals a novel domain association. *Biochemistry* 46: 13041-48.

Gachet C., (2008). P2 receptors, platelet function and pharmacological implications. *Thromb Haemost* 99: 466-72.

Gawaz M., (1999). Das Bluttplättchen, Thieme, Stuttgart.

Ginsberg M.H., Partridge A., Shattil S.J., (2005). Integrin regulation. *Curr Opin Cell Biol* 17: 509-16.

Gomi H., Mizutani S., Kasai K., Itohara S., Izumi T., (2005). Granuphilin molecularly docks insulin granules tot he fusion machinery. *J Cell Biol* 171: 99-109.

Häuser W., Knobeloch K.P., Eigenthaler M., Gambaryan S., Krenn V., Geiger J., Glazova M., Rohde E., Horak I., Walter U., (1999). Zimmer M., Megakaryocyte hyperplasia and enhanced agonist-induced platelet activation in vasodilator-stimulated phosphoprotein knockout mice. *Proc Natl Acad Sci USA* 96: 8120-5.

Hattula K., Furuhjelm J., Tikkanen J., Tanhuanpää K., Laakkonen P., Peränen J., (2006). Characterization of the Rab8-specific membrane traffic route linked to protrusion formation. *J Cell Sci* 119: 4866-77.

Hart M.J., Jiang X., Kozasa T., Roscoe W., Singer W.D., Gilman A.G., Sternweis P.C., Bollag G., (1998). Direct stimulation of the guanine nucleotide exchange activity of p115 RhoGEF by Galpha13. *Science* 280: 2112-4.

Hartwig J., Italiano J., Jr, (2003). The birth of the platelet. *J Thromb Haemost* 1: 1580-6.

Heemskerk J.W., Bevers E.M., Lindhout T., (2002). Platelet activation and blood coagulation. *Thromb Haemost* 88: 186-93.

Hodivala-Dilke K.M, McHugh K.P., Tsakiris D.A., Rayburn H., Crowley D., Ullman-Cullere M., Ross F.P., Coller B.S., Teitelbaum S., Hynes R.O., (1999). Beta3-integrin-deficient mice are a model for Glanzmann thrombasthenia showing placental defects and reduced survival. *J Clin Invest* 103: 229-38.

Hofmann F., Feil R., Kleppisch T., Schlossmann J., (2006). Function of cGMP-dependent protein kinases as revealed by gene deletion. *Physiol Rev* 86: 1-23.

Hoffmeister M., Riha P., Neumüller O., Danielewski O., Schultess J., Smolenski A.P., (2008). Cyclic nucleotide dependent protein kinases inhibit binding of 14-3-3 to the GTPase activating protein Rap1GAP2 in platelets. *J Biol Chem* 283: 2297-306.

Holmsen H., Dangelmaier C.A., (1989). Measurement of secretion of serotonin. *Meth Enzymol* 169: 205-10.

Holt O., Kanno E., Bossi G., Booth S., Daniele T., Santoro A., Arico M., Saegusa C., Fukuda M., Griffiths G.M., (2008). Slp1 and Slp2-a localize to the plasma membrane of CTL and contribute to secretion from the immunological synapse*. Traffic* 9: 446-57.

Houng A., Polgar J., Reed G.L., (2003). Munc18 syntaxin complexes and exocytosis in human platelets. *J Biol Chem* 278: 19627-33.

Insel P.A., Stengel D., Ferry N., Hanoune J., (1982). Regulation of adenylate cyclase of human platelet membranes by forskolin. *J Biol Chem* 257: 7485-90.

Italiano J.E., Jr., Shivdasani R.A., (2003). Megakaryocytes and beyond: the birth of platelets. *J Thromb Haemost* 1: 1174-82.

Italiano J.E., Jr, (2008). Platelets in hematologic and cardiovascular disorders: a clinical handbook. Cambridge University Press.

Jackson S.P., (2007). The growing complexity of platelet aggregation. *Blood* 109: 5087-95.

Jahn R., Scheller R.H., (2006). SNAREs – engines for membrane fusion. *Nat Rev Mol Cell Biol* 7: 631-43.

Jantzen H.M., Gousset L., Bhaskar V., Vincent D., Tai A., Reynolds E.E., Conley P.B., (1999). Evidence for two distinct G protein-coupled ADP receptors mediating platelet activation. *Thromb Haemost* 81: 111-7.

Jardin I., Lopez J.J., Pariente J.A., Salido G.M., Rosado J.A., (2008). Intracellular calcium release from human platelets: different messengers for multiple stores. *Trends Cardiovasc Med* 18: 57-61.

Jin J., Kunapuli S.P., (1998). Coactivation of two different G protein-coupled receptors is essential for ADP-induced platelet aggregation. *Proc Natl Acad Sci USA* 95: 8070-4.

Johnson J.L., Ellis B.A., Noack D., Seabra M.C., Catz S.D., (2005). The Rab27a-binding protein, JFC1, regulates androgen-dependent secretion of prostate-specific antigen and prostatic-specific acid phosphatase. *Biochem J* 391: 699-710.

Johnson J.L., Pacquelet S., Lane W.S., Eam B., Catz S.D., (2005). Akt regulates the subcellular localization of the Rab27a-binding protein JFC1 by phosphorylation. *Traffic* 6: 667-81.

Jurk K., Kehrel B.E., (2005). Platelets: physiology and biochemistry. *Semin Thromb Hemost* 31(4): 381-92.

Jurk K., Kehrel B.E., (2008). Dir Rolle von Thrombozyten bei Hämostase, Thrombose, Immunabwehr und Entzündung. *Dtsch Med Wochenschr* 133: 1130-5.

Kahn M.L., Nakanishi-Matsui M., Shapiro M.J., Ishihara H., Coughlin S.R., (1999). Protease-activated receptors 1 and 4 mediate activation of human platelets by thrombin. *J Clin Invest* 103: 879-87.

Karniguian A., Zahraoui A., Tavitian A., (1993). Identification of small GTP-binding rab proteins in human platelets: thrombin-induced phosphorylation of rab3b, rab6 and rab8 proteins. *Proc Natl Acad Sci USA* 90: 7647-51.

Kawato M., Shirakawa R., Kondo H., Higashi T., Ikeda T., Okawa K., Fukai S., Nureki O., Kita T., Horiuchi H., (2007). Regulation of platelet dense granule secretion by the Ral GTPase-exocyst pathway. *J Biol Chem* 283: 166-74.

Kehrel B.E., (2003). Blutplättchen: Biochemie und Physiologie. *Hämostaseologie* 23: 149-58.

Kheifets V., Mochly-Rosen D., (2007). Insight into intra- and inter-molecular interactions of PKC: design of specific modulators of kinase function. *Pharamcol Res* 55: 467-76.

King S.M., Reed G.L., (2002). Development of platelet secretory granules. *Semin Cell Dev Biol* 13: 293-302.

Klinz F.J., Seifert R., Schwaner I., Gausepohl H., Frank R., Schultz G., (1992). Generation of specific antibodies against the rap1A, rap1B and rap2 small GTP-binding proteins: analysis of rap and ras proteins in membranes from mammalian cells. *Eur J Biochem* 207: 207-13.

Kuroda T.S., Fukuda M., (2004). Rab27a-binding protein Slp2-a is required for peripheral melanosome distribution and elongated cell shape in melanocytes. *Nature Cell Biol* 6: 1195-1200.

Kuroda T.S., Fukuda M., Ariga H., Mikoshiba K., (2002). The Slp homology domain of synaptotagmin-like proteins 1-4 and Slac2 functions as a novel Rab27 binding domain. *J Biol Chem* 277: 9212-18.

Lemmon M.A., (2008). Membrane recognition by phospholipid-binding domains. *Nat Rev Mol Cell Biol* 9: 99-111.

Lemons P.P., Chen D., Bernstein A.M., Bennett M.K., Whiteheart S.W., (1997). Regulated secretion in platelets: identification of elements of the platelet exocytosis machinery. *Blood* 90: 1490-500.

Lemons P.P., Chen D., Whiteheart S.W., (2000). Molecular mechanisms of platelet exocytosis: requirements for alpha-granule release. *Biochem Biophys Res Commun* 267: 875-80.

Lesurtel M., Graf R., Aleil B., Walther D.J., Tian Y., Jochum W., Gachet C., Bader M., Clavien P.A., (2006). Platelet-derived serotonin mediates liver regeneration. *Science* 312: 104-7.

Li Z., Ajdic J., Eigenthaler M., Du X., (2003). A predominant role for cAMP-dependent protein kinase in the cGMP-induced phosphorylation of vasodilator-stimulated phosphoprotein and platelet inhibition in humans. *Blood* 101: 4423-9.

Luzio J.P., Pryor P.R., Bright N.A., (2007). Lysosomes: fusion and function. *Net Rev Mol Cell Biol* 8: 622-32.

Maridonneau-Parini I., de Gunzburg J., (1992). Association of rap1 and rap2 proteins with the specific granules of human neutrophils. Translocation to the plasma membrane during cell activation. *J Biol Chem* 267: 6396-402.

Martens S., McMahon H.T., (2008). Mechanisms of membrane fusion: disparate players and common principles. *Nat Rev Mol Cell Biol* 9: 543-56.

Martens S., Kozlov M.M., McMahon H.T., (2007). How synaptotagmin promotes membrane fusion. *Science* 316: 1205-08.

Massberg S., Grüner S., Konrad I., Garcia Arguinzonis M.I., Eigenthaler M., Hemler K., Kersting J., Schulz C., Muller I., Besta F., Nieswandt B., Heinzmann U., Walter U., Gawaz M., (2004). Enhanced in vivo platelet adhesion in vasodilator-stimulated phosphoprotein (VASP)-deficient mice. *Blood* 103: 136-42.

Miura Y., Kaibuchi K., Itoh T., Corbin J.D., Francis S.H., Takai Y., (1992). Phosphorylation of smg p21B/rap1B p21 by cyclic GMP-dependent protein kinase. *FEBS Lett* 297: 171-4.

McAdara Berkowitz J.K., Catz S.D., Johnson J.L., Ruedi J.M., Thon V., Babior B.M., (2001). JFC1, a novel tandem C2 domain-containing protein associated with the leukocyte NADPH oxidase. *J Biol Chem* 276: 18855-62.

Molino M., Barnathan E.S., Numerof R., Clark J., Dreyer M., Cumashi A., Hoxie J.A., Schechter N., Woolkalis M., Brass L.F., (1997). Interactions of mast cell tryptase with thrombin receptors and PAR-2. *J Biol Chem* 272: 4043-9.

Munafo D.B., Johnson J.L., Ellis B.A., Rutschmann S., Beutler B., Catz S.D., (2007). Rab27a is a key component of the secretory machinery of azurophilic granules in granulocytes. *Biochem J* 402: 229-39.

Munzel T., Feil R., Mülsch A., Lohmann S.M., Hofmann F., Walter U., (2003). Physiology and pathophysiology of vascular signaling controlled by cyclic guanosine 3`,5`-cyclic monophosphate-dependent protein kinase. *Circulation* 108: 2172-83.

Murugappan S., Shankar H., Kunapuli S.P., (2004). Platelet receptors for adenine nucleotides and thromboxane A2. *Semin Thromb Hemost* 30: 411-8.

Murugappan S., Tuluc F., Dorsam R.T., Shankar H., Kunapuli S.P., (2004). Differential role of protein kinase C delta isoform in agonist-induced dense granule secretion in human platelets. *J Biol Chem* 279: 2360-7.

Narayan K., Lemmon M.A., (2006). Determining selectivity of phosphoinositide-binding domains. *Methods* 39: 122-33.

Nishikawa M**.,** Tanaka T**.,** Hidaka H**.,** (1980). Ca^{2+}-calmodulin-dependent phosphorylation and platelet secretion. *Nature* 287: 863-5.

Niitsu Y., Jakubowski J.A., Sugidachi A., Asai F., (2005). Pharmacology of CS-747 (prasugrel, LY640315), a novel, potent antiplatelet agent with in vivo P2Y12 receptor antagonist activity. *Semin Thromb Hemost* 31: 184-94.

Norel X., (2007). Prostanoid receptors in the human vascular wall. *Scientific World J* 7: 1359-74.

Nurden P., Nurden A.T., (2008). Congenital disorders associated with platelet dysfunctions. *Thromb Haemost* 99: 253-63.

Nystedt S., Emilsson K., Wahlestedt C., Sundelin J., (1994). Molecular cloning of a potential proteinase activated receptor. *Proc Natl Acad Sci USA* 91: 9208-12.

Offermanns S., (2006). Activation of platelet function through G protein-coupled receptors. *Circ Res* 99: 1293-1304.

Okumara T., Hasitz M., Jamieson G.A., (1978). Platelet glycocalicin: interaction with thrombin and role as thrombin receptor of the platelet surface. *J Biol Chem* 253: 3435-43.

Padfield P.J., Panesar N., Henderson P., Baldassare J.J., (1996). Differential effects of G-protein activators on 5-hydroxytryptamine and platelet-derived growth factor release from streptolysin-O-permeabilized human platelets. *Biochem J* 314: 123-8.

Palmer M., Harris R., Freytag C., Kehoe M., Tranum-Jensen J., Bhakdi S., (1998). Assembly mechanism of the oligomeric streptolysin O pore: the early membrane lesion is lined by a free edge of the lipid membrane and is extended gradually during oligomerization. *EMBO J* 17: 1598-1605.

Park M., Serpinskaya A.S., Papalopulu N., Gelfand V.I., (2007). Rab32 regulates melanosome transport in Xenopous melanophores by protein kinase A recruitment. *Curr Biol* 17: 2030-34.

Patrono C., García Rodríguez L.A., Landolfi R., Baigent C., (2005). Low-dose aspirin for the prevention of atherothrombosis. *N Engl J Med* 353: 2373-83.

Patrono C, Rocco B., (2008). Aspirin: promise and resistance in the new millennium. *Arterioscler Thromb Vasc Biol* 28: 25-32.

Pena V., Hothorn M., Eberth A., Kaschau N**.,** Parret A**.,** Gremer L**.,** Bonneau F**.,** Ahmadian M.R**.,** Scheffzek K**.,** (2008). The C2 domain of SynGAP is essential for stimulation of the RapGTPase reaction. *EMBO Rep* 9: 350-5.

Pereira-Leal J.B., Seabra M.C., (2001). Evolution of the Rab family of small GTP-binding proteins. *J Mol Biol* 313: 889-901.

Polgar J., Chung S.H., Reed G.L., (2002). Vesicle-associated membrane protein 3 (VAMP-3) and VAMP-8 are present in human platelets and are required for granule secretion. *Blood* 100: 1081-3.

Polgar J., Reed G.L., (1999). A critical role for N-ethylmaleimide-sensitive fusion protein (NSF) in platelet granule secretion. *Blood* 94: 1313-8.

Polgar J., Lane W.S., Chung S.H., Houng A.K., Reed G.L., (2003). Phosphorylation of SNAP-23 in activated human platelets. *J Biol Chem* 278: 44369-76.

Reed G.L., Houng A.K., Fitzgerald M.L., (1999). Human platelets contain SNARE proteins and a Sec1p homologue that interacts with syntaxin 4 and is phosphorylated after thrombin activation: implications for platelet secretion. *Blood* 93: 2617-26.

Reed G.L., Fitzgerald M.L., Polgar J., (2000). Molecular mechanisms of platelet exocytosis: insights into the “secrete” life of thrombocytes. *Blood* 96: 3334-42.

Reed G.L., (2004). Platelet secretory mechanisms. *Semin Thromb Hemost* 30: 441-50.

Reinhard M., Jarchau T., Walter U., (2001). Actin-based motility: stop and go with Ena/VASP proteins. *Trends Biochem Sci* 26: 243-9.

Ren Q., Barber H.K., Crawford G.L., Karim Z.A., Zhao C., Choi W., Wang C., Hong W., Whiteheart S.W., (2007). Endobrevin/VAMP-8 is the primary v-SNARE for the platelet release reaction. *Mol Biol Cell* 18: 24-33.

Ren Q., Ye S., Whiteheart S.W., (2008). The platelet release reaction: just when you thought platelet secretion was simple. *Curr Opin Hematol* 15: 537-41.

Rendu F., Brohard-Bohn B., (2001). The release reaction: granules constituents, secretion and functions. *Platelets* 12: 261-73.

Rink T.J., Sanchez A., Hallam T.J., (1983). Diacylglycerol and phorbol ester stimulate secretion without raising cytoplasmic free calcium in human platelets. *Nature* 305: 317-9.

Rizo J., Rosenmund C., (2008). Synaptic vesicle fusion. *Nat Struct Mol Biol* 15: 665-74.

Rozenvayn N, Flaumehaft R., (2003). Protein kinase C mediates translocation of type II phosphatidylinositol 5-phosphate 4-kinase required for platelet alpha-granule secretion. *J Biol Chem* 278: 8126-34.

Ruggeri Z.M., (2002). Platelets in atherothrombosis. *Nat Med* 8: 1227-34.

Ruggeri Z.M., Mendolicchio G.L., (2007). Adhesion mechanisms in platelet function. *Circ Res* 100: 1673-85.

Saegusa C., Kanno E., Itohara S., Fukuda M., (2008). Expression of Rab27B-binding protein Slp1 in pancreatic acinar cells and ist involvement in amylase secretion. *Arch Biochem Biophys* 475: 87-92.

Saegusa C., Tanaka T., Tani S., Itohara S., Mikoshiba K., Fukuda M., (2006). Decreased basal mucus secretion by Slp2-a deficient gastric surface mucous cells. *Genes Cell* 11: 623-31.

Sandberg M., Butt E., Nolte C., Fischer L., Halbrügge M., Beltman J., Jahnsen T., Genieser H.G., Jastorff B., Walter U., (1991). Characterization of SP-5,6-dichloro-1-b-D-ribofuranosyl-benzimidazole-3`,5`-monophosphorothioate (SP-5,6-DCI-cBiMPS) as a potent and specific activator of cyclic-AMP-dependent protein kinase in cell extracts and intact cells. *Biochem J* 279: 521-7.

Sato T., Mushiake S., Kato Y., Sato K., Sato M., Takeda N., Ozono K., Miki K., Kubo Y., Tsuj A., Harada R., Harada A., (2007). The Rab8 GTPase regulates apical protein localization in internal cells. *Nature* 448: 366-9.

Savi P., Herbert J.M., (2005). Clopidogrel and ticlopidine: P2Y12 adenosine diphosphate-receptor antagonists for the prevention of atherothrombosis. *Semin Thromb Hemost* 318: 174-83.

Schultess J., Danielewski O., Smolenski A.P., (2005). Rap1GAP2 is a new GTPase-activating protein of Rap1 in human platelets. *Blood* 105: 3185-92.

Schwarz U.R., Walter U., Eigenthaler M., (2001). Taming platelets with cyclic nucleotides. *Biochem Pharmacol* 62: 1153-61.

Scrima A., Thomas S., Deaconescu D., Wittinghofer A., (2008). The Rap-RapGAP complex: GTP hydrolysis without catalytic glutamine and arginine residues. *EMBO J* 27: 1145-53.

Seabra M.C., Mules E.H., Hume A.N., (2002). Rab GTPases, intracellular traffic and disease. *Trends Mol Med* 8: 23-30.

Seamon K.B., Padgett W., Daly J.W., (1981). Forskolin: unique diterpene activator of adenylate cyclase in membranes and in intact cells. *Proc Natl Acad Sci USA* 78: 3363-7.

Sellers J.R., (2000). Myosins: a diverse superfamily. *Biochim Biophys Acta* 1496: 3-22.

Seri M., Pecci A., Di Bari F., et al., (2003). MYH9-related disease: May-Hegglin anomaly, Sebastian syndrome, Fechtner syndrome, and Epstein syndrome are not distinct entities but represent a variable expression of a single illness. *Medicine* 82: 203-15.

Shattil S.J., Newman P.J., (2004). Integrins: dynamic scaffolds for adhesion and signaling in platelets. *Blood* 104: 1606-15.

Shirakawa R., Yoshioka A., Horiuchi H., Nishioka H., Tabuchi A., Kita T., (2000). Small GTPase Rab4 regulates Ca^{2+}-induced alpha-granule secretion in platelets. *J Biol Chem* 275: 33844-9.

Shirakawa R., Higashi T., Tabuchi A., Yoshioka A., Nishioka H., Fukuda M., Kita T., Horiuchi H., (2004). Munc13-4 is a GTP-Rab27-binding protein regulating dense core granule secretion in platelets. *J Biol Chem* 279: 10730-7.

Shirakawa R., Higashi T., Kondo H., Yoshioka A., Kita T., Horiuchi H., (2005). Purification and functional analysis of a Rab27 effector Munc13-4 using a semiintact platelet dense granule secretion assay. *Meth Enzymol* 403: 778-88.

Sierko E., Wojtikiewicz M.Z., (2007). Inhibition of platelet function: does it offer a chance of better cancer progression control? *Semin Thromb Hemost* 33: 712-22.

Siess W., Winegar D.A., Lapetina E.G., (1990). Rap1-B is phosphorylated by protein kinase A in intact human platelets. *Biochem Biophys Res Commun* 170: 944-50.

Siess W., Grünberg B., (1993). Phosphorylation of rap1B by protein kinase A is not involved in platelet inhibition by cyclic AMP. *Cell Signal* 5: 209-14.

Sloan D.C., Haslam R.J., (1997). Protein kinase C-dependent and Ca2+-dependent mechanisms of secretion from streptolysin O-permeabilized platelets: effects of leakage of cytosolic proteins. *Biochem J* 328: 13-21.

Smolenski A., Bachmann C., Reinhard K., Hönig-Liedl P., Jarchau T., Hoschuetzky H., Walter U., (1998). Analysis and regulation of vasodilator-stimulated phosphoprotein serine 239 phosphorylation in vitro and in intact cells using a phsophospecific antibody. *J Biol Chem* 273: 20029-35.

Stein A., Radhakrishnan A., Riedel D., Fasshauer D., Jahn R., (2007). Synaptotagmin activates membrane fusion through a Ca^{2+}-dependent trans interaction with phospholipids. *Nat Struct Mol Biol* 14: 904-11.

Stichcombe J.C., Griffiths G.M., (1999). Regulated secretion from hematopoietic cells. *J Cell Biol* 147: 1-5.

Stork P.J.S., Dillon T.J., (2005). Multiple roles of Rap1 in hematopoietic cells: complementary versus antagonistic functions. *Blood* 106: 2952-61.

Strom M., Hume A.N., Tarafder A.K., Barkagianni E., Seabra M.C., (2002). A family of Rab27-binding proteins. Melanophilin links Rab27a and myosin Va function in melanosome transport. *J Biol Chem* 277: 25423-30.

Tolmachova T., Abrink M., Futter C.E., Authi K.S., Seabra M.C., (2007). Rab27b regulates number and secretion of platelet dense granules*. Proc Natl Acad Sci USA* 104: 5872-7.

Torii S., Zhao S., Yi Z., Takeuchi T., Izumi T., (2002). Granuphilin modulates the exocytosis of secrtory granules through interaction with syntaxin 1a. *Mol Cell Biol* 22: 5518-26.

Varga-Szabo D., Pleines I., Nieswandt B., (2008). Cell adhesion mechanisms in platelets. *Arterioscler Thromb Vasc Biol* 28: 403-12.

Von Hundelshausen P., Weber C., (2007). Platelets as immune cells: bridging inflammation and cardiovascular disease. *Circ Res* 100: 27-40.

Walker T.R., Watson S.P., (1993). Synergy between Ca2+ and protein kinase C is the major factor in determining the level of secretion from human platelets. *Biochem J* 289: 277-82.

Wang J., Arbuzova A., Hangyas-Mihalyne G., McLaughlin S., (2001). The effector domain of myristoylated alanine-rich C kinase substrate binds strongly to phosphatidylinositol 4,5-bisphosphate. *J Biol Chem* 276: 5012-9.

Wasmeier C., Romao M., Plowright L., Bennett D.C., Raposo G., Seabra M.C., (2006). Rab38 and Rab32 control post-Golgi trafficking of melanogenic enzymes. *J Cell Biol* 175: 271-81.

Watanabe Y., Ito M., Kataoka Y., Wada H., Koyama M., Feng J., Shiku H., Nishikawa M., (2001). Protein kinase C-catalyzed phosphorylation of an inhibitory phosphoprotein of myosin phosphatase is involved in human platelet secretion. *Blood* 97: 3798-805.

Wilson S.M., Yip R., Swing D.A., O'Sullivan T.N., Zhang Y., Novak E.K., Swank R.T., Russell L.B., Copeland N.G., Jenkins N.A., (2000). A mutation in Rab27a causes the vesicle transport defects observed in ashen mice. *Proc Natl Acad Sci USA* 97: 7933-8.

Yoshioka A., Horiuchi H., Shirakawa R., Nishioka H., Tabuchi A., Higashi T., Yamamoto A., Kita T., (2001). Molecular dissection of alpha- and dense-core granule secretion of platelets. *Ann N Y Acad Sci* 947: 403-6.

Yu M., Kasai K., Nagashima K., Torii S., Yokoto-Hashimoto H., Okamoto K., Takeuchi T., Gomi T., Izumi T., (2007). Exophilin4/Slp2-a targets glucagon granules to the plasma membrane through unique Ca^{2+}-inhibitory phospholipid-binding activity of the C2A domain. *Mol Biol Cell* 18: 688-96.

Zerial M., McBride H., (2001). Rab proteins as membrane organizers. *Nat Rev Mol Cell Biol* 2: 107-18.

7. APPENDIX

7.1 List of constructs

Table 7.1.1: Slp1 constructs

Name	Vector	Primer	Template	Source
GST-Slp1	pGEX-4T-3	235,236	Slp1_RZPD	this work
His_6-Slp1	pET28	563, 236	Slp1_RZPD	this work
GST-C2A	pGEX-4T-3	337,338	Slp1_RZPD	this work
GST-C2B	pGEX-4T-3	339,236	Slp1_RZPD	this work
GST-C2AB	pGEX-4T-3	337,236	Slp1_RZPD	this work
Slp1-myc	pcDNA3.1/myc-His	235, 336	Slp1_RZPD	this work
C2A-myc	pcDNA3.1/myc-His	337, 365	Slp1_RZPD	this work
Slp1ΔC2B-myc	pcDNA3.1/myc-His	235, 365	Slp1_RZPD	this work
Slp1S117A-myc	pcDNA3.1/myc-His	469, 470	Slp1_RZPD	this work
Slp1S311A-myc	pcDNA3.1/myc-His	471, 472	Slp1_RZPD	this work
Slp1-3xFLAG	pCMV-3Tag-3	235, 405	Slp1_RZPD	this work

Table 7.1.2: Rap1GAP2 constructs

Name	Vector	Primer	Template	Source
RG2-FLAG	pcDNA4/TO			A. Smolenski
RG2ΔCterm-FLAG	pcDNA4/TO			A. Smolenski
RG2Nterm-FLAG	pcDNA4/TO			M. Hoffmeister
RG2ΔNterm-FLAG	pcDNA4/TO			M. Hoffmeister
VSV-RG2ΔNterm-C1	pSG8-VSV-EGFP			J. Schultess
VSV-RG2ΔNterm-C2	pSG8-VSV-EGFP			J. Schultess

VSV-RG2ΔNterm-C3	pSG8-VSV-EGFP			J. Schultess
VSV-RG2ΔNterm-C4	pSG8-VSV-EGFP	367, 368	VSV-RG2ΔNterm	this work
VSV-RG2ΔNterm-C5	pSG8-VSV-EGFP	346, 347	VSV-RG2ΔNterm	this work
VSV-RG2ΔNterm-C6	pSG8-VSV-EGFP	369, 370	VSV-RG2ΔNterm	this work
VSV-RG2ΔNterm-C7	pSG8-VSV-EGFP	343, 344	VSV-RG2ΔNterm	this work
VSV-RG2ΔNterm-C8	pSG8-VSV-EGFP			J. Schultess
RG2Δ522-527 -FLAG	pcDNA4/TO	401,402	RG2-FLAG	this work
RG2Δ536-542 -FLAG	pcDNA4/TO	399,400	RG2-FLAG	this work
RG2E522A-FLAG	pcDNA4/TO	481,482	RG2-FLAG	this work
RG2V523A-FLAG	pcDNA4/TO	479,480	RG2-FLAG	this work
RG2T524A-FLAG	pcDNA4/TO	496,497	RG2-FLAG	this work
RG2K525A-FLAG	pcDNA4/TO	477,478	RG2-FLAG	this work
RG2T526A-FLAG	pcDNA4/TO	456, 457	RG2-FLAG	this work
RG2T527A-FLAG	pcDNA4/TO	452,453	RG2-FLAG	this work
RG2-VSV	pcDNA4/TO			M. Hoffmeister
RG2-His_6	pcDNA4/TO			M. Hoffmeister
RG2Δ522-527-His_6	pcDNA4/TO	401,402	RG2-His_6	this work

Table 7.1.3: Other Constructs

Name	Vector	Primer	Template	Source
T7-Slp2a	pEF-T7			M. Fukuda
T7-Slp3a	pEF-T7			M. Fukuda
T7-Slp4a	pEF-T7			M. Fukuda
T7-Slp5	pEF-T7			M. Fukuda

RG1-HA	pMT2-HA			J. Bos
His_6-Rap1B	pET28			M. Hoffmeister
GST-14-3-3	pGEX-4T-3			P. Riha
EGFP-rRab27a	pEGFP-C3			M. Seabra
EGFP-hRab27b	pEGFP-C3			M. Seabra
rRab27a-VSV	pcDNA4/TO	448,468	EGFP-rRab27a	this work
hRab27b-VSV	pcDNA4/TO	446, 447	EGFP-hRab27b	this work
GST-rRab27a	pGEX-4T-3	559, 560	EGFP-rRab27a	this work
GST-hRab27b	pGEX-4T-3	561, 562	EGFP-hRab27b	this work
PKI	pcDNA3			R. Maurer
Rap1GAP2-Gal4BD	pGBKT7			O. Danielewski
Slp1-Gal4AD	pACT2			A.Smolenski

7.2 List of primers

Table 7.2.1: Primers for cloning

Primer No.	Name	Sequence 5´→ 3`
235	Slp1-EcoRI-for	ATTGAATTCCATGCCCCAGAGGGGCCACCCATCG
236	Slp1-XhoI-rev	AATCTCGAGCTACGTCCTGGGGGCCAGG
336	Slp1-XhoI-rev	AATCTCGAGAACGTCCTGGGGGCCAGG
337	C2A-EcoRI-for	ATTGAATTCCATGGAGCTGCGCGTGCACGTGATC
338	C2A-XhoI-rev	AATCTCGAGCTAAGCCAGGTGGGCTCAGAGC
339	C2B-EcoRI-for	ATTGAATTCCATGGAGCTGCACTTCTGGGTG
365	C2A-XhoI-rev	AATCTCGAGAACCCGCTCGGGGGCAGTCCTG
405	Slp1-XhoI-rev	AATCTCGAGCGTCCTGGGGGCCAGGTTG

446	Rab27b-EcoRI-for	ATTGAATTCATGACCGATGGAGACTATG
447	Rab27b-VSV-XhoI-rev	AATCTCGAGCTACTTACCCAGGCGGTTCATTTCGATATCAGTGTAGCAGATACATTTCTTC
448	Rab27a-HindIII-for	ATTAAGCTTATGTCGGATGGAGATTATGAC
468	Rab27a-VSV-XhoI-rev	AATCTCGAGCTACTTACCCAGGCGGTTCATTTCGATATCAGTGTAACAGCCGCATAACCCCTTC
559	Rab27a-SmaI-for	ATTCCCGGGTCATGTCGGATGGAGATTATGAC
560	Rab27a-XhoI-rev	AATCTCGAGTCAACAGCCGCATAACCCCTTC
561	Rab27b-EcoRI-for	ATTGAATTCCATGACCGATGGAGACTATG
562	Rab27b-XhoI-rev	AATCTCGAGCTAGCAGATACATTTCTTCTC
563	Slp1-NheI-for	ATTGGCTAGCATGCCCCAGAGGGGCCACCCATCG

Table 7.2.2: Primers for mutagenesis

Primer No.	Name	Sequence 5´→ 3`
344	RG2ΔNC7-for	CAGTGGGGGCATCCCTGGCTGACTCAGCGGGGGCATCTCCCAC
345	RG2ΔNC7-rev	GTGGGAGATGCCCCCGCTGAGTCAGCCAGGGATGCCCCCACTG
346	RG2ΔNC5-for	CTCGCCTCCAGTGGTGGCGTGAACGGTGAAGAACCAGTCACGG
347	RG2ΔNC5-rev	CCGTGACTGGTTCTTCACCGTTCACGCCACCACTGGAGGCGAG
367	RG2ΔNC4-for	GAACCAGTCACGGAGTCCCTGAAAGCGACGCTCGGGGCTCTTC
368	RG2ΔNC4-rev	GAAGAGCCCCGAGCGTCGCTTTCAGGGACTCCGTGACTGGTTC
369	RG2ΔNC6-for	CAGCATGGAGGTCACCAAGTGAACCTTCTCGCCTCCAGTGGTG
370	RG2ΔNC6-rev	CACCACTGGAGGCGAGAAGGTTCACTTGGTGACCTCCATGCTG
399	RG2Δ536-542-for	CTCGCCTCCAGTGGTGGCGGCACGGAGTCCCATCAAGCGAC
400	RG2Δ536-542-rev	GTCGCTTGATGGGACTCCGTGCCGCCACCACTGGAGGCGAG
401	RG2Δ522-527-for	CATCTCCCACAACAGCATGTTCTCGCCTCCAGTGGTG
402	RG2Δ522-527-rev	CACCACTGGAGGCGAGAACATGCTGTTGTGGGAGATG

452	RG2T527A-for	GAGGTCACCAAGACCGCCTTCTCGCCTCCAGTG
453	RG2T527A-rev	CACTGGAGGCGAGAAGGCGGTCTTGGTGACCTC
469	Slp1S111A-for	CTATGCGCAGGAAGAAGGCCACCAGGGGAGACCAGGCTC
470	Slp1S111A-rev	GAGCCTGGTCTCCCCTGGTGGCCTTCTTCCTGCGCATAG
471	Slp1S301A-for	GCCGCCCGGCGCCGCCGCGCGGACCCCTACGTCAAAAG
472	Slp1S301A-rev	CTTTTGACGTAGGGGTCCGCGCGGCGGCGCCGGGCGGC
477	RG2K525A-for	CAGCATGGAGGTCACCGCGACCACCTTCTCGCCTCCAGTG
478	RG2K525A-rev	CACTGGAGGCGAGAAGGTGGTCGCGGTGACCTCCATGCTG
479	RG2V523A-for	CTCCCACAACAGCATGGAGGCCACCAAGACCACCTTCTCGCCTC
480	RG2V523A-rev	GAGGCGAGAAGGTGGTCTTGGTGGCCTCCATGCTGTTGTGGGAG
481	RG2E522A-for	CATCTCCCACAACAGCATGGCGGTCACCAAGACCACCTTCTC
482	RG2E522A-rev	GAGAAGGTGGTCTTGGTGACCGCCATGCTGTTGTGGGAGARG
496	RG2T524A-for	CACAACAGCATGGAGGTCGCCAAGACCACCTTCTCGCCTCCAG
497	RG2T524-rev	CTGGAGGCGAGAAGGTGGTCTTGGCGACCTCCATGCTGTTGTG

ZUSAMMENFASSUNG

1. Einleitung

Blutplättchen, auch Thrombozyten genannt, sind kernlose Zellen, die unter physiologischen Umständen eine wichtige Rolle in der primären Hämostase spielen. Nach einer Gefäßverletzung adhärieren Thrombozyten an Strukturen der freigelegten subendothelialen Matrix. Bei dieser primären Adhäsion werden Thrombozyten aktiviert und bilden durch Wechselwirkung untereinander ein zunächst fragiles Thrombozytenaggregat. Dieser initial gebildete Thrombus wird in der sekundären Hämostase durch Fibrin verfestigt und ermöglicht dann die stabile Abdichtung der Gefäßwandläsion gegenüber dem Blutstrom (Kehrel 2003). Die Aktivierung von Thrombozyten durch Adhäsion oder durch lösliche Plättchenaktivatoren bewirkt eine Formveränderung der Thrombozyten. Gleichzeitig werden intrazelluläre Speichergranula von Thrombozyten ausgeschüttet. Thrombozyten enthalten drei verschiedene Arten von Granula: alpha-Granula, dichte Granula und Lysosomen. Die Granula in Thrombozyten dienen als Speicherorte für Proteine und Substanzen, welche sowohl autokrin die Thrombozytenaktivierung verstärken als auch parakrin noch ruhende Thrombozyten aus der Blutzirkulation rekrutieren. Die dichten Granula in Thrombozyten enthalten niedermolekulare Substanzen wie zum Beispiel ADP, ATP, Ca^{2+} und Serotonin. In den alpha-Granula dagegen befinden sich vor allem Proteine, die für die Adhäsion, Aggregation und die Blutgerinnung wichtig sind. Zusätzlich enthalten alpha-Granula Zytokine und Wachtumsfaktoren. Die lysosomalen Granula in Thrombozyten enthalten hydrolytische Enzyme wie beispielsweise β-Hexosaminidase und Heparitinase (Gawaz 1999).

Im Gegensatz zur Sekretion der alpha-Granula, die durch Rab4 reguliert wird (Shirakawa et al. 2000), steuert das kleine G-Protein Rab27 die Sekretion der dichten Granula in Thrombozyten (Shirakawa et al. 2004). Rab27 befindet sich auf der Oberfläche der dichten Granula (Barral et al. 2002) und es wird angenommen, dass Rab27 vor allem die Motilität und das Andocken der Granula an die Plasmamembran fördert (Seabra und Coudrier 2004, Fukuda 2006). Für diese Funktion interagiert Rab27 mit unterschiedlichen Effektorproteinen und Munc13-4 wurde als das erste Rab27-bindende Protein in Thrombozyten beschrieben (Shirakawa et al. 2004). Weitere Proteine, die für die Sekretion der dichten Granula von Bedeutung sind, sind SNARE (soluble N-ethylmaleimide-sensitive-factor attachment receptor)-Proteine. SNARE-Proteine spielen eine wichtige Rolle bei der Fusion von Membranen. So wird die Fusion der dichten Granula mit der Plasmamembran durch das sich auf der Granulaoberfläche befindende (v)-SNARE-Protein VAMP-8 und den an der Plasmamembran angesiedelten (t)-SNARE-Proteinen syntaxin-2 und SNAP-23 vermittelt (Ren et al. 2007, Chen et al. 2000a).

Die Sekretion der Speichergranula geht eng mit der Aggregation von Thrombozyten einher. Durch *outside in* und *inside out signaling* werden Integrinrezeptoren auf der Oberfläche von Thrombozyten aktiviert. Eines der bedeutendsten Plättchenintegrine ist $\alpha_{IIb}\beta_3$, auch GPIIb-IIIa genannt. Im aktivierten Zustand bindet Integrin $\alpha_{IIb}\beta_3$ an Fibrinogen. Durch die Ausbildung von Fibrinogenbrücken erfolgt dann die Quervernetzung mehrerer Thrombozyten. Das kleine G-Protein Rap1 reguliert den Aktivitätszustand von Integrin $\alpha_{IIb}\beta_3$ und besitzt damit eine zentrale Rolle bei der Thrombozytenaggregation. Rap1 selbst durchläuft einen Aktivitätszyklus: GDP-gebundenes Rap1 ist inaktiv und GTP-gebundenes Rap1 ist aktiv. Die Aktivierung von Rap1 erfolgt mit Hilfe verschiedener GEF (guanine nucleotide exchange factor)-Proteine, welche den Austausch von GDP zu GTP fördern. In Thrombozyten sind CalDAG-GEFI und III sowie PDZ-GEF1 exprimiert (Schultess et al. 2005). Die Inaktivierung von Rap1 erfolgt durch Hydrolyse von GTP zu GDP und Phosphat. Da Rap1 eine nur sehr schwache eigene intrinsische GTPase Aktivität besitzt, beschleunigen Rap1-spezifische GAP (GTPase activating protein)-Proteine die Hydrolyse von GTP. Bisher sind zwei Familien von Rap1GAP-Proteinen bekannt (Stork und Dillon 2005). Zur ersten Familie gehören die Proteine SPA-1 und E6TP1α. Die zweite Familie umfasst die Proteine Rap1GAP1 und das von unserer Arbeitsgruppe kürzlich entdeckte Rap1GAP2. In Thrombozyten ist Rap1GAP2 das einzige GAP-Protein für Rap1 (Schultess et al. 2005). Rap1GAP2 enthält eine konservierte zentrale GAP-Domäne, eine N-terminale Bindungsstelle für 14-3-3-Proteine sowie einen großen C-terminalen Bereich mit bisher noch unbekannter Funktion. Die Aktivierung von Thrombozyten führt zur Phosphorylierung von Rap1GAP2 an Serin 9, woraufhin 14-3-3-Proteine an Rap1GAP2 binden und wahrscheinlich die GAP-Funktion hemmen (Hoffmeister et al. 2008).

2. Zielsetzung dieser Arbeit

Um weitere Einblicke in die Funktion und Regulation von Rap1GAP2 in Thrombozyten zu gewinnen, wurde ein Hefe-zwei-Hybrid-Screening durchgeführt (O. Danielewski und A. Smolenski, IBCII, Frankfurt). Neben 14-3-3-Proteinen (Hoffmeister et al. 2008), wurde das Rab27-bindende Protein synaptotagmin-like protein 1 (Slp1, auch JFC1 genannt) als neuer putativer Interaktionspartner von Rap1GAP2 gefunden. Ausgehend von den Ergebnissen dieses Hefe-zwei-Hybrid-Screenings waren die konkreten Ziele der vorliegenden Arbeit (1) die Bindung von Slp1 an Rap1GAP2 zu verifizieren, (2) die für die Bindung verantwortlichen Bindebereiche zu identifizieren, (3) die mögliche Komplexbildung von Rap1GAP2, Slp1, Rab27 und anderen Proteinen zu untersuchen sowie (4) die funktionale Bedeutung der Interaktion zwischen Rap1GAP2 und Slp1 zu bestimmen.

3. Ergebnisse und Diskussion

Slp1 ist ein neuer Interaktionspartner von Rap1GAP2 in Thrombozyten

Die direkte Interaktion zwischen Rap1GAP2 und Slp1 wurde zunächst durch Retransformation in Hefe bestätigt. Durch Transfektion von HeLa und COS-1 Zellen mit anschließenden Pulldown- und Koimmunpräzipitationsexperimenten wurde die Interaktion zwischen Rap1GAP2 und Slp1 in Säugerzellen verifiziert. Mit Hilfe des eigens hergestellten polyklonalen Slp1-Antikörpers konnte ferner gezeigt werden, dass Slp1 in Thrombozyten exprimiert wird. Weder der Slp1- noch unser Rap1GAP2-Antikörper eigneten sich zur Immunpräzipitation ihrer endogenen Antigene aus Thrombozyten. Um dennoch den Beweis für die Interaktion zwischen Rap1GAP2 und Slp1 auf endogener Ebene in Thrombozyten zu erbringen, wurde ein alternativer Lösungsansatz entwickelt und angewandt (Hoffmeister et al. 2008). Unter Ausnutzung der Fähigkeit von Rap1GAP2 an 14-3-3-Proteine zu binden, wurde aus *Escherichia coli* gereinigtes GST-14-3-3-Protein verwendet, um endogenes Rap1GAP2 und das daran gebundene Slp1 aus humanen Thrombozyten zu präzipitieren. In Kontrollversuchen wurde zuvor eine direkte Interaktion zwischen 14-3-3-Proteinen und Slp1 ausgeschlossen. Auf diese Art und Weise gelang es die Interaktion zwischen Rap1GAP2 und Slp1 auf endogener Ebene in Thrombozyten nachzuweisen.
Um die für die Bindung von Rap1GAP2 und Slp1 verantwortlichen Binderegionen zu identifizieren, wurden Mutations- und Peptidbindungsstudien durchgeführt. Es konnte gezeigt werden, dass die Bindung von Rap1GAP2 an Slp1 durch das -*TKXT*- Proteinmotiv im C-terminalen Bereich von Rap1GAP2 vermittelt wird. Das -*TKXT*- Motiv bindet Ca^{2+}-unabhängig an die C2A Domäne von Slp1. C2 Domänen sind im Allgemeinen als Phospholipidbindedomänen bekannt und speziell die C2A Domäne von Slp1 vermittelt die Bindung von Slp1 an die Plasmamembran (Lemmon 2008, Catz et al. 2002). Andererseits sind einige C2 Domänen auch an Protein-Protein-Interaktionen beteiligt (Kheifets und Mochly-Rosen 2007, Pena et al. 2008). In Lipidbindungsversuchen wurde nachgewiesen, dass Slp1 gleichzeitig sowohl an Phospholipide als auch an Rap1GAP2 binden kann. Die Aktivierung der Proteinkinase A in Thrombozyten verstärkte die Bindung von GST-Slp1 an endogenes Rap1GAP2. Zusammen mit der Tatsache, dass im -*TKXT*- Motiv von Rap1GAP2 zwei Threonine (T524 und T527) enthalten sind, ließ dieser Befund über eine Phosphorylierung am -*TKXT*- Motiv spekulieren. Nachfolgende Experimente sprachen jedoch gegen eine Phosphorylierung am -*TKXT*- Motiv von Rap1GAP2. Vielmehr konnte eine Phosphorylierung eines oder beider Threonine am -*TKXT*- Motiv von Rap1GAP2 die Bindung an Slp1 aufheben. Es bleibt demzufolge offen, ob eine Phosphoyrlierung durch Proteinkinase A am Rap1GAP2 an anderer Stelle als dem Slp1 bindenden -*TKXT*- Motiv erfolgt und folglich die Bindung von Slp1 an Rap1GAP2 positiv beeinflusst. Alternativ

könnten aber auch weitere an der Bindung von Rap1GAP2 und Slp1 beteiligte Proteine durch Proteinkinase A phosphoryliert werden und in Folge, die Komplexbildung zwischen Rap1GAP2 und Slp1 in Thrombozyten verstärken. Die detaillierte Rolle der Phosphorylierung bei der Regulation der Rap1GAP2/Slp1 Interaktion bleibt jedoch in zukünftigen Studien zu klären.

Komplexbildung von Slp1, Rab27 und Rap1GAP2

Slp1 bindet über die N-terminale Slp Homologiedomäne (SHD) an das kleine G-Protein Rab27, welches, wie bereits erwähnt, die Sekretion der dichten Granula in Thrombozyten reguliert (Fukuda 2005, Shirakawa et al. 2004). Rab27 besitzt zwei Isoformen Rab27a und Rab27b, die 71 % in ihrer Aminosäuresequenz übereinstimmen (Pereira-Leal und Seabra 2001). Beide Isoformen kommen in Thrombozyten vor (Barral et al. 2002). In der vorliegenden Arbeit wurde die direkte Interaktion zwischen Slp1 und Rab27 in Pulldown- und Koimmunpräzipitationsexperimenten bestätigt. Dabei konnte festgestellt werden, dass Slp1 unabhängig vom gebundenen Nukleotid an Rab27 bindet. Desweiteren konnte gezeigt werden, dass ein trimärer Komplex aus Slp1, Rab27 und Rap1GAP2 sowohl bei Überexpression in Säugerzellen als auch endogen in Thrombozyten gebildet wird. Um weitere Slp1-assoziierte Proteine, die an der Komplexbildung um Slp1, Rab27 und Rap1GAP2 in Thrombozyten beteiligt sein könnten, zu identifizieren, wurde ein affinitätschromatographisches Screening durchgeführt. Durch die anschließende massen-spektrometrische Analyse (Conway Institut, Dublin, Irland) konnten insgesamt 14 neue putative Slp1 Interaktionspartner in Thrombozyten ermittelt werden. Unter den identifizierten Proteinen befand sich beispielsweise das kleine G-Protein Rab8, dessen Bindung an Slp1 bereits in transfizierten HeLa Zellen beschrieben war (Hattula et al. 2006). In der vorliegenden Arbeit wurde jedoch die Bindung von Rab8 an Slp1 erstmalig in Thrombozyten nachgewiesen.

Slp1 und Rap1GAP2 sind an der Sekretion der dichten Granula in Thrombozyten beteiligt

Um die funktionale Bedeutung der Interaktion zwischen Rap1GAP2 und Slp1 zu analysieren, sollte die Interaktion (i) im Hinblick auf die Rap1GAP2-Funktion in Rap1-vermittelter Zelladhäsion und (ii) im Hinblick auf die Slp1-Funktion in Rab27-vermittelter Sekretion untersucht werden (Bos et al. 2001, Johnson et al. 2005, Shirakawa et al. 2004). Es konnte kein Einfluss der Interaktion zwischen Rap1GAP2 und Slp1 auf die Adhäsion von transfizierten HeLa Zellen festgestellt werden. Zudem zeigten *in-vitro* GAP Assays, dass die Bindung von Slp1 an Rap1GAP2 die katalytische GAP-Aktivität von Rap1GAP2 nicht

beeinflusst. Demgegenüber deuteten Sekretionsversuche in transfizierten LNCaP Zellen darauf hin, dass Rap1GAP2 einen positiven Effekt auf die Sekretion von prostataspezifischem Antigen hat. Um dieses Ergebnis im endogenen System der Thrombozyten zu bestätigen, wurde ein Assay entwickelt, bei dem die Sekretion von Serotonin (5-Hydroxytryptamin, 5HT) aus dichten Granula der Thrombozyten fluorometrisch gemessen wurde. Da Thrombozyten kernlose Zellen sind, eignen sie sich nicht zur Transfektion. Um dennoch Proteine oder Peptide in das Innere von Thrombozyten zu bringen, wurden Thrombozyten mit dem bakteriellen Toxin Streptolysin-O permeabilisiert. Die nachfolgende Zugabe von rekombinantem Slp1-Protein hemmte konzentrationsabhängig sowohl die Ca^{2+}- als auch die GTPγS-induzierte Sekretion der dichten Granula. Die Zugabe von rekombinantem Rap1GAP2-Protein dagegen verstärkte die Sekretion. Der Rap1GAP2 Effekt konnte zusätzlich durch Experimente mit kurzen synthetischen Rap1GAP2-Peptiden bestätigt werden. Durch Deletion des Slp1-bindenden -*TKXT*- Motivs sowohl im Rap1GAP2-Protein als auch im Rap1GAP2-Peptid wurde die sekretionsfördernde Wirkung von Rap1GAP2 in Thrombozyten vollständig aufgehoben. Die Zugabe von rekombinantem Rap1 zu permeabilisierten Thrombozyten hatte keinen Einfluss auf die Sekretion. Zusammenfassend weisen diese Ergebnisse darauf hin, dass sowohl Slp1 als auch Rap1GAP2 an der Sekretion der dichten Granula in Thrombozyten beteiligt sind. Der Einfluss von Rap1GAP2 auf die Sekretion war dabei nicht auf die GTPase-aktivierende Wirkung von Rap1GAP2 gegenüber Rap1, sondern vielmehr auf die -*TKXT*- vermittelte Bindung von Rap1GAP2 an Slp1 zurückzuführen. Der genaue molekulare Mechanismus sowohl des Rap1GAP2 als auch des Slp1 Effekts auf die Sekretion der dichten Granula in Thrombozyten bleibt jedoch in zukünftigen Studien zu klären.

4. Fazit

Die Ergebnisse der vorliegenden Arbeit zeigen, dass das Rab27-bindende Protein Slp1 ein neuer direkter Interaktionspartner des GTPase-aktivierenden Proteins Rap1GAP2 in Thrombozyten ist. Die Expression von Slp1 wurde in Thrombozyten nachgewiesen. Damit ist Slp1 neben Munc13-4 das zweite bisher bekannte Rab27-bindende Protein in diesen Zellen. Der Nachweis der Interaktion von Slp1 mit GTP-gebundenen Rab27 legte eine Funktion von Slp1 als Rab27-Effektorprotein nahe und es konnte in dieser Arbeit gezeigt werden, dass Slp1 die Sekretion der dichten Granula in Thrombozyten beeinflusst.

Darüber hinaus zeigen die Ergebnisse der vorliegenden Arbeit, dass Rap1GAP2, zusätzlich zu seiner bereits bekannten Funktion bei der Thrombozytenaggregation durch die Regulation des kleinen G-Proteins Rap1, auch an der Sekretion der dichten Granula in Thrombozyten beteiligt ist. Der Rap1GAP2 Effekt auf die Sekretion in Thrombozyten beruht auf der -*TKXT*-

vermittelten Wechselwirkung mit Slp1, welche Teil eines komplexen Netzwerks von Protein-Protein-Interaktionen in Thrombozyten ist. Rap1GAP2 könnte somit eine zentrale Rolle bei der Koordination der wichtigen Funktionen Aggregation und Sekretion in Thrombozyten spielen.

DANKSAGUNG

An dieser Stelle möchte ich mich bei all jenen bedanken, die mich in den letzten Jahren begleitet und unterstützt und damit maßgeblich zum Gelingen dieser Arbeit beigetragen haben.

Mein ganz besonderer Dank gilt meinem Doktorvater PD Dr. Albert P. Smolenski, der mich als Doktorandin in seine Arbeitsgruppe aufgenommen und durch die Bereitstellung des Themas diese Arbeit ermöglicht hat. Ich danke ihm für das in mich gesetzte Vertrauen und seine stets freundliche, offene und verständnisvolle Art.

Ich danke Prof. Dr. Theo Dingermann für die freundliche Bereitschaft, die Betreuung dieser Arbeit im Fachbereich Chemische und Pharmazeutische Wissenschaften zu übernehmen.

Prof. Dr. Werner Müller-Esterl danke ich für die großzügige Unterstützung insbesondere in der Endphase meiner Promotion sowie die Möglichkeit in einem international-wissenschaftlichen Umfeld zu forschen.

Herzlich bedanken möchte ich mich desweiteren bei Dr. Meike Hoffmeister, die mir stets zur Seite stand und mich sowohl fachlich als auch menschlich unterstützt hat. Ich danke ihr für ihre stete Hilfsbereitschaft und die oft dringend notwendigen aufmunternden Worte.

Ich danke allen gegenwärtigen und ehemaligen Mitgliedern des Instituts für Biochemie II für die freundliche Zusammenarbeit und außerordentliche Kollegialität. Insbesondere gilt mein Dank allen freiwilligen Blutspendern und -abnehmern, die durch ihre selbstlose Hilfsbereitschaft alle Blutplättchenexperimente in dieser Arbeit ermöglicht haben. Der Arbeitsgruppe Prof. Dr. Werner Müller-Esterl danke ich für die freundliche und offene Aufnahme in ihre Mitte und die täglich angenehme und heitere Arbeitsatmosphäre. Dr. Antje Banning danke ich für die Endkorrektur dieser Arbeit.

Mein persönlicher Dank gilt meinen Freunden und Verwandten, die, auch wenn sie nicht alle in meiner Nähe sind, stets an mich glauben und mich unterstützen. Insbesondere danke ich meinen Eltern Tatjana und Viktor Neumüller für ihre grenzenlose Liebe und Zuneigung und das stets offene Ohr für die Sorgen und Ängste ihrer Tochter. Ich danke meinem Bruder Viktor Neumüller, der stets bestrebt ist, meinen Blick auf das Wesentliche zu lenken. Nicht zuletzt bedanke ich mich aber auch bei meinem Ehemann Malkhaz Merabishvili, der mich liebt und jederzeit für mich einsteht.

LEBENSLAUF

Persönliche Daten

Olga Neumüller
Deutschordenstrasse 58a
60528 Frankfurt am Main

Geburtsdatum	02. April 1980
Geburtsort	Balchasch, Kasachstan
Staatsangehörigkeit	deutsch
Familienstand	verheiratet seit 2005

Schulbildung

1987 – 1990	Grundschule, Balchasch, Kasachstan
1990 – 1992	Orientierungsstufe, Wathlingen, Deutschland
1992 – 1999	Hölty Gymnasium, Celle Abschluss: Allgemeine Hochschulreife

Hochschulbildung

Okt. 1999 – März 2004	Pharmaziestudium, Johannes Gutenberg Universität, Mainz
April 2002	1. Staatsexamen
März 2004	2. Staatsexamen
Mai 2004 – Okt. 2004	Pharmaziepraktikantin: Sanofi Aventis Pharma, DI&A Functional Genomics, Frankfurt am Main
Nov. 2004 – April 2005	Pharmaziepraktikantin: Süd Apotheke, Frankfurt am Main
Mai 2005	3. Staatsexamen Abschluss: Approbierte Apothekerin
seit Aug. 2005	Promotion am Institut für Biochemie II, Universitätsklinikum der Johann Wolfgang Goethe Universität, Frankfurt am Main Betreuer: PD Dr. Albert P. Smolenski
Juni 2006	Posterpreis der wissenschaftlichen Zeitschrift *Molecular Cell,* FEBS Special Meeting, Dubrovnik, Kroatien

EIDESSTATTLICHE ERKLÄRUNG

Hiermit erkläre ich an Eides statt, dass ich die vorliegende Dissertation selbständig und nur mit den angegebenen Hilfsmitteln angefertigt und dass ich noch keinen Promotionsversuch unternommen habe.

Frankfurt am Main, 23.11.2008 .....

Olga Neumüller